The University Of Sheffield.

Using Zebrafish Embryos to Identify Genes Involved in Atherosclerosis

George Alexander Bowley

A thesis submitted in partial fulfilment of the requirements for the degree of Doctor of Philosophy

The University of Sheffield
Faculty of Medicine, Dentistry and Health
Department of Infection, Immunity and Cardiovascular Disease

January 2022

Table of Contents

List of Abbreviations

AMPK – 5’ adenosine-monophosphate activated protein kinase
AKT – Protein kinase B
ABC – ATP binding cassette
ABCG1 – ATP binding cassette subfamily G member one
BMP2 – Bone morphogenic protein two
BP – Blood pressure
CRISPR – Clustered regularly interspaced palindromic repeats
Cas9 – CRISPR associated protein nine
CVD – Cardiovascular disease
dpf – Days post fertilisation
Dll4 – Delta like canonical notch ligand four
DA – Dorsal aorta
DLAV – Dorsal longitudinal anastomotic vessel
MCP1 – Monocyte chemotactic protein one
eNOS – Endothelial nitric oxide synthase
ER – Endoplasmic reticulum
ERK5 – Extracellular signalling regulated kinase five
EC – Endothelial cell
EdU – 5-Ethynyl-2’-deoxyuridine
FZD5 – Frizzled five
GADD45 – Growth arrest and DNA-damage-inducible protein 45
GATA4 – GATA binding protein four
HTS – High throughput screening
hpf – Hours post fertilisation
HDL – High density lipoprotein
HSS – High shear stress
HUVEC – Human umbilical vein endothelial cell
ICAM1 – Intercellular adhesion molecule one
IL-8 – Interleukin eight
ISV – Intersegmental vessel
Jag-1 – Jagged one
LSS – Low shear stress
LDL – Low density lipoprotein
MI – Myocardial infarction
MO – Morpholino
MEK – Mitogen activated protein kinase kinase

mTOR – Mammalian target of rapamycin
NFκB – Nuclear factor kappa-light chain enhancer of activated B cells
NOS – Nitric oxide synthase
OSS – Oscillatory shear stress
oxLDL – Oxidised low density lipoprotein
PI3K – Phosphoinositide three kinase
PPARγ – Peroxisome proliferator activated receptor gamma
p21Cip1 – Cyclin dependent kinase inhibitor one
SMC – Smooth muscle cell
SR-β1 – scavenger receptor beta 1
TNNT2a – Troponin T type 2a
VEGF – Vascular endothelial growth factor
VCAM1 – Vascular cell adhesion molecule one
VEGFR2 – Vascular endothelial growth factor receptor two
qPCR – Quantitative PCR

Acknowledgements

I would like to express a special thank you to my supervisors Prof. Paul Evans, Dr. Jovana Serbanovic-Canic and Prof. Tim Chico for their invaluable support and guidance throughout my PhD. I would also like to thank Aaron Savage and Yan Chen for their technical advice on molecular cloning during my first year, Karen Plant for helping me get started at the Firth Court lab, the aquarium team for looking after my fish, and the LMF team for providing critical support for my imaging work.

Thank you to Dr. Imo Höfer (Utrecht), and Prof. Sheila Francis (Sheffield) for providing human carotid endarterectomy samples for study.

Thank you to the NC3Rs and the British Heart Foundation for funding this work.

Finally, I would like to extend a personal thank you to my parents Stewart and Samantha Bowley, and my late grandparents Margaret and Alan Bowley for their unending support and belief.

Abstract

Atherosclerosis preferentially occurs in regions of low shear stress (LSS) which leads to development of cardiovascular disease (CVD). LSS causes endothelial cell (EC) dysfunction, which leads to regional susceptibility to disease. Excessive EC proliferation is a characteristic of endothelial dysfunction that leads to leakiness of arteries to pro-atherogenic lipoproteins. Understanding the mechanisms linking LSS to increased EC proliferation could allow identification of therapeutic targets to prevent atherosclerosis. CVD researchers often use murine models, we hypothesised that zebrafish embryos are a partial replacement model for study of vascular responses to flow *in vivo*. If substantiated, zebrafish have the potential to replace mice in studies identifying genes involved in atherosclerosis.

Antibody-based cell labelling, light-sheet imaging, and confocal microscopy were compared for study of EC proliferation in zebrafish embryos. Of these methods, live confocal imaging of EGFP expressing EC in transgenic zebrafish was most effective and showed that EC proliferation was reduced in the absence of blood flow. Candidate regulators of EC proliferation were identified by analysing existing data on genes which were differentially expressed at high and low shear regions of the pig aorta. Expression of candidate EC-regulatory genes was validated by performing qPCR on cDNA derived from zebrafish ECs. Morpholinos were then designed against each of these target genes and confocal microscopy was used to study the effect of gene knock-down on EC proliferation in response to flow.

We showed that knock-down of *wnk1a* rescued the rate of proliferation under no-flow conditions ($p=0.0004$, two-tailed t-test), whereas knockdown of *fzd5*, *gsk3β*, *trpm7*, and *bmp2a* reduced the rate of EC proliferation in embryos with normal blood flow. We found that the mouse orthologue of *wnk1a* - Wnk1 was upregulated in LSS regions of the mouse aorta ($p=0.043$, two-tailed t-test). These results showed that the zebrafish embryo is a useful *in vivo* model of vascular responses to flow which can identify targets for further study in mammals. By studying our genes of interest in the zebrafish, we expect to reduce mouse usage by 50% over the next five years.

1.0 Introduction

1.1 Pathophysiology of Atherosclerosis

Atherosclerosis is a cardiovascular disease (CVD) characterised by the development of atheroma, comprising of cellular, lipid and protein components which accumulate within the intima of arteries (Gialeli et al., 2021; Stary et al., 1995). Growth of atheroma leads to deformation of the surrounding tissue and narrowing of the lumen, which obstructs blood flow and reduces oxygen perfusion to downstream tissues. In some instances, plaque rupture causes acute thrombosis which can precipitate acute coronary syndrome or stroke. Atherosclerosis is the leading cause of death in the UK, therefore understanding its molecular basis is of great medical importance.

Healthy arteries are composed of an internal, uniform layer of endothelial cells (ECs) bound to an intimal layer of collagen, elastin, and proteoglycan rich matrix called the tunica-intima. This layer is surrounded by the tunica-media, which contains smooth muscle cells (SMCs) and provides contractile force. The media is wrapped in an external layer of connective tissue called the adventitia (Mercadante AA, 2021) (Fig 1).

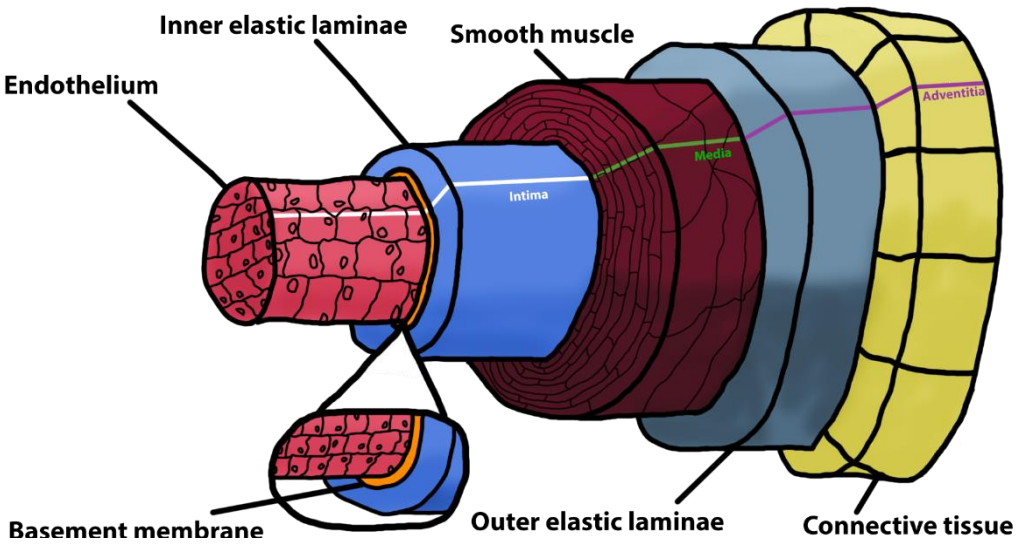

Figure 1: Diagram of normal arterial tissue structure. The innermost layer is the intima (White line), which is comprised of endothelium (Pink) connected to the inner elastic laminae (Blue) by a thin basement membrane (Orange). The intima is surrounded by the medial muscle layer (Crimson). The outer layer is the adventitia, an elastic (Grey) and connective tissue (Yellow) layer.

In healthy arteries blood flow through the lumen is unimpeded and the artery contributes to healthy circulation of blood throughout the body. Atherosclerosis develops in three phases over a period of several decades to progressively disturb the structure of the artery, and subsequently disturb these functions (Douglas & Channon, 2010). Atherosclerosis is initiated when lipoproteins become trapped in the vascular intima, marking the initiation of fatty streak development.

1.1.1 Fatty Streak Development

When endothelial tissue is damaged, aged, or dysfunctional (Fig. 2A), circulating low density lipoproteins enter the intima and are oxidised to form oxidised LDL. This initially occurs due to resident vascular cells (Navab et al., 1996). As a result of oxidation, oxLDL is trapped in the intima where it causes chronic activation of the innate immune system and initiates a prolonged state of EC activation (Fig. 2B) (Fukuchi et al., 2002; Li et al., 2018). Interestingly, some LDL's have been found circulating in the blood and causing generalised vascular inflammation, which shows that not all factors in development of atherosclerosis are localised at the site of disease onset (Estruch et al., 2013).

At the vessel surface, EC activation leads to immune cells recruitment (Fig. 2C) whilst in the intima, antigen presenting cells recognise oxLDL and present epitopes to nearby T-cells causing an adaptive immune response (Roy et al., 2022; Stemme et al., 1995). This two-pronged influx of immune cells results in further recruitment of monocytes, which further oxidise LDL, and differentiate to macrophages in the intima (Parhami et al., 1993; Park, 2021).

Macrophages have the capacity to scavenge lipoprotein breakdown products (cholesterol and cholesteryl esters) via ATP-binding cassette transporter and scavenger receptor beta 1 (SR-β1), (Chistiakov et al., 2016), however these clearance mechanisms are regulated by high-density lipoprotein (HDL) concentration. Thus, where HDL is low, or oxLDL is especially high, macrophages are unable to clear the trapped lipoproteins and accumulate phospholipid metabolites to become foam cells (Fig. 2D). Foam cells comprise the fatty streak and secrete IL-8 and monocyte chemotactic protein (MCP1), furthering the immune response (Han et al., 1998; Wang et al., 1996) these cells persist unless the HDL-C fraction is raised (Barter, 2005)

Originally, fatty streak development was studied using human plaque sections (Fukuchi et al., 2002; Stemme et al., 1995), the development of the ApoE $^{-/-}$ mouse line (Zhang et al., 1992) opened the door for widespread mechanistic research on atherosclerosis. Mouse models dominate study of plaque development and additional knockout lines with improved relevance to human disease have been developed (Oppi et al., 2019). Rabbit and zebrafish models have also been used, however zebrafish currently are not useful for studying plaque progression, whereas mouse and rabbit are (Back et al., 1995; Ma et al., 2012; Tang et al., 2021).

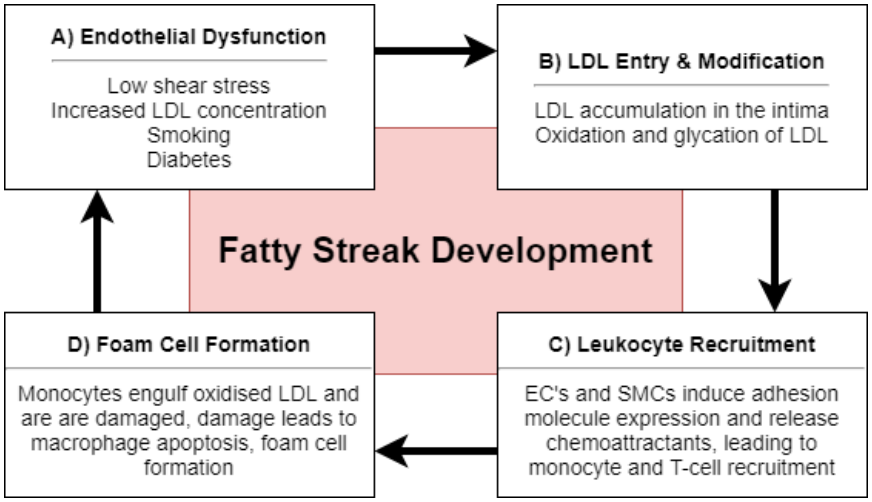

Figure 2: Diagram of the cycle of fatty streak development.

Collectively these processes form a feed forward loop which sustains break-down of endothelial barrier function and facilitates continued lipoprotein entry to the vessel intima.

1.1.2 Plaque Progression

The accumulation of foam cells in the artery leads to smooth muscle cell (SMC) proliferation and matrix secretion within diffuse regions of the intima (Fig. 3A), (Doran et al., 2008). Foam cells which have accumulated high levels of lipoprotein become apoptotic and phagocytosis driven clearance of these cells is inhibited (Schrijvers et al., 2005) leading to necrosis and release of lipid and cell debris which forms the plaque core (Fig. 3B-C). This core is surrounded by fibrin deposits which accumulate around damaged tissue. The degree of lipid accumulation, cell death, and fibrin deposition determines the ultimate structure and classification of the plaque. The proportion of macrophages and SMCs within the plaque determine the size of the necrotic core, and thickness of the fibrin capsule (Thorp & Tabas, 2009). Thus, the proportion of these cells also determines the degree of displacement of arterial tissues and the degree of vessel occlusion by narrowing of the lumen (Fig. 3D). The location and severity of plaque progression leads to a diverse range of atherosclerosis associated pathologies.

What is known about plaque progression comes from research on a combination of human endarterectomy/cadaver sections, mouse, and rabbit models. Mouse models are available for studying development of plaques including vulnerable plaques, plaque instability, and calcification (Chen et al., 2013; Goettsch et al., 2016; X. Wang et al., 2021). Rabbit models reflecting all of these features are also available (Havel et al., 1989) (Fan et al., 2001; Ji et al., 2015)

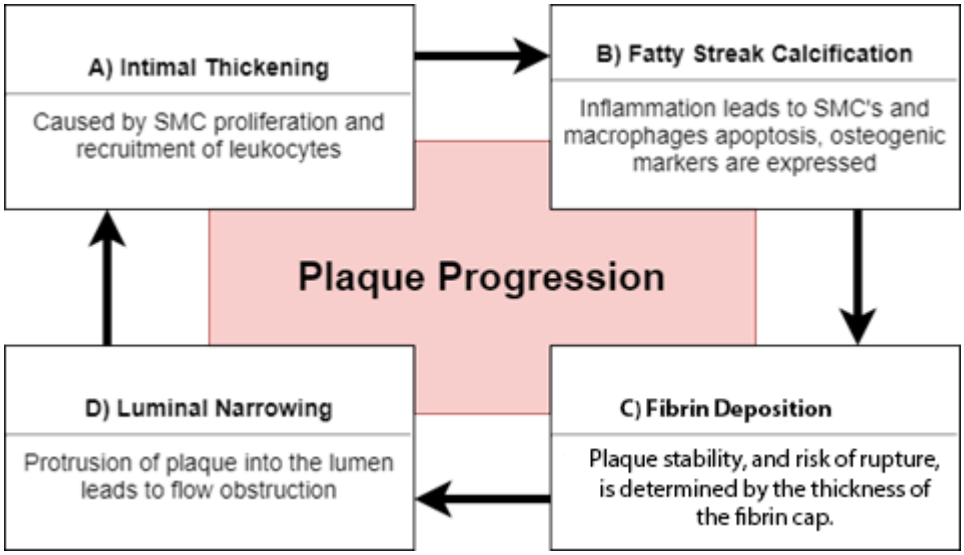

Figure 3: Diagram illustrating the process of plaque progression in atherosclerosis.

1.2 Clinical Manifestations of Atherosclerosis

Atheroma cause pathology via vessel occlusion and obstruction of blood supply to affected tissues. This can occur directly because of plaque stenosis or more frequently due to thrombosis which occurs when plaque content is exposed to the blood. Risk of morbidity or mortality is determined by the vulnerability of the plaque and the vulnerability of the patient.

Plaque vulnerability is determined by the thickness of the fibrous cap. Atheroma with thick fibrous caps are protected from rupture and thrombosis, whereas thin-cap atheroma are not (Osborn & Jaffer, 2013). Some thick-capped atheroma are also at risk of thrombosis when the endothelium becomes denuded, in a process called plaque erosion (Fahed & Jang, 2021). Thrombosis leads to sudden localised coagulation which results in obstruction of the artery, whereas rupture leads to release of thrombi into the circulation and causes obstruction of downstream vessels. Plaque thickness determines risk of rupture and therefore is a determinant of plaque vulnerability (Naghavi et al., 2003).

In those individuals at risk of plaque rupture and thrombosis, mortality is partially determined, by the clotting tendency of the blood. Mortality can be reduced by genetic disorders that reduce clotting as is the case for haemophilia (Tuinenburg et al., 2009), as well as by medications such as Aspirin (Ridker et al., 1991). Vulnerability can also be increased by disorders that increase clotting such as factor V Leiden or protein C deficiency (Eitzman et al., 2005; Spek et al., 1995). Therefore, the balance of coagulation in the blood is a key consideration in determining the vulnerability of the patient to the thrombotic consequences of atherosclerosis.

Whilst atherosclerosis is commonly associated with coronary heart disease and myocardial infarction there are several non-cardiac pathologies associated with the disease:

- Ischemic stroke – Mediated by release of thrombogenic material from atheroma of the carotid arteries (DeGraba, 2004).
- Loss of brain function – Mediated by chronic cerebral ischaemia caused by atherosclerotic occlusion of the carotid artery (Ihle-Hansen et al., 2021).
- Renal artery disease – Mediated by atherosclerotic occlusion of the renal artery.
- Peripheral artery claudication – Mediated by atherosclerotic occlusion of peripheral arteries, leads to loss of function.

The above pathologies can be categorised as obstruction mediated, as they are associated with disruption of blood flow.

Atherosclerosis also leads to pathologies which are mediated by disruption of the tissues themselves, such as where plaque driven disruption of the arterial wall weakens the tissue, causing aneurysms. Development of atheroma in the media is a key driver of this, as it leads to weakening of the elastic and smooth muscle tissue as is seen in abdominal aortic aneurysm occurring because of atherosclerosis (Golledge & Norman, 2010).

Importantly, in either case atherosclerosis does not produce noticeable pathology until it has progressed for many decades. Disease diagnosis likely occurs after a significant adverse

shock to the patient's health. At this point atheroma can be complex and calcified, which limits medicinal reversal of disease meaning the patient must now undergo treatments which carry significant risks (stent/bypass) and/or require lifestyle changes (anticoagulant therapy). A better way to minimise the impact of atherosclerosis is to identify ways to prevent or slow disease progression, hence studies investigating risk factors for the disease.

1.3 Risk Factors for Atherosclerosis

Risk of atherosclerosis is associated with:

- Age – Disease risk increases beyond 45 (men) and 55 (women).
- Weight – Being overweight increases risk.
- Genetics – Having parents diagnosed with the disease increases risk.
- Diet – Diets high in sodium, trans-fat, saturated fat, sugar and cholesterol increase risk.
- Sedentary lifestyle – Lack of physical exercise increases risk of disease.
- Blood pressure – Increased blood pressure is associated with risk of atherosclerosis (Agmon et al., 2000).
- Blood cholesterol – High LDL and low HDL increases disease risk.
- Smoking – Affects blood pressure, causes changes to cell metabolism that increase disease risk.

Summarised from (Rafieian-Kopaei et al., 2014).

High prevalence of these risk factors in the western world has led to an increase in cardiovascular disease cases in the west, compared to regions with healthier lifestyles (Oikonomou et al., 2018). For example, the UK has an ageing population (Storey, 2018) an obesity epidemic (Allender & Rayner, 2007), and high per capita consumption of alcohol and tobacco (Bhopal et al., 2004). Therefore, a significant number of people are at high risk of developing atherosclerosis, which is reflected in high per capita CVD incidence.

With this model of atherogenesis in mind, one could propose controlling disease by minimising modifiable risk factors. Indeed, it is still generally accepted that avoiding modifiable risk factors and maintaining low cholesterol, particularly low LDL:HDL ratio, confers protection from atherosclerosis. The mechanisms by which these risk factors precipitate increased risk of disease have been the subject of multi-decades of investigation by CVD researchers. It has become increasingly clear that risk of atherosclerosis is linked to the function and state of the endothelium.

1.4 The Roles of Endothelium in Atherosclerosis

Vascular endothelium is the interface between blood flow and the surrounding tissues. Endothelial tissue is not a simple barrier. It maintains haemostasis during injury and regulates the local immune response via regulation of junctional adherence proteins, and via immune cell recruitment (Galley & Webster, 2004).

In healthy individuals, the endothelium is a monolayer of uniformly aligned cells which are adhered to each other and the underlying intima by tight junctions (Dejana & Orsenigo,

2013). In this state, endothelium allows essential glucose, oxygen, and albumin to diffuse freely whilst restricting macromolecule access to the underlying tissue (Fig. 4).

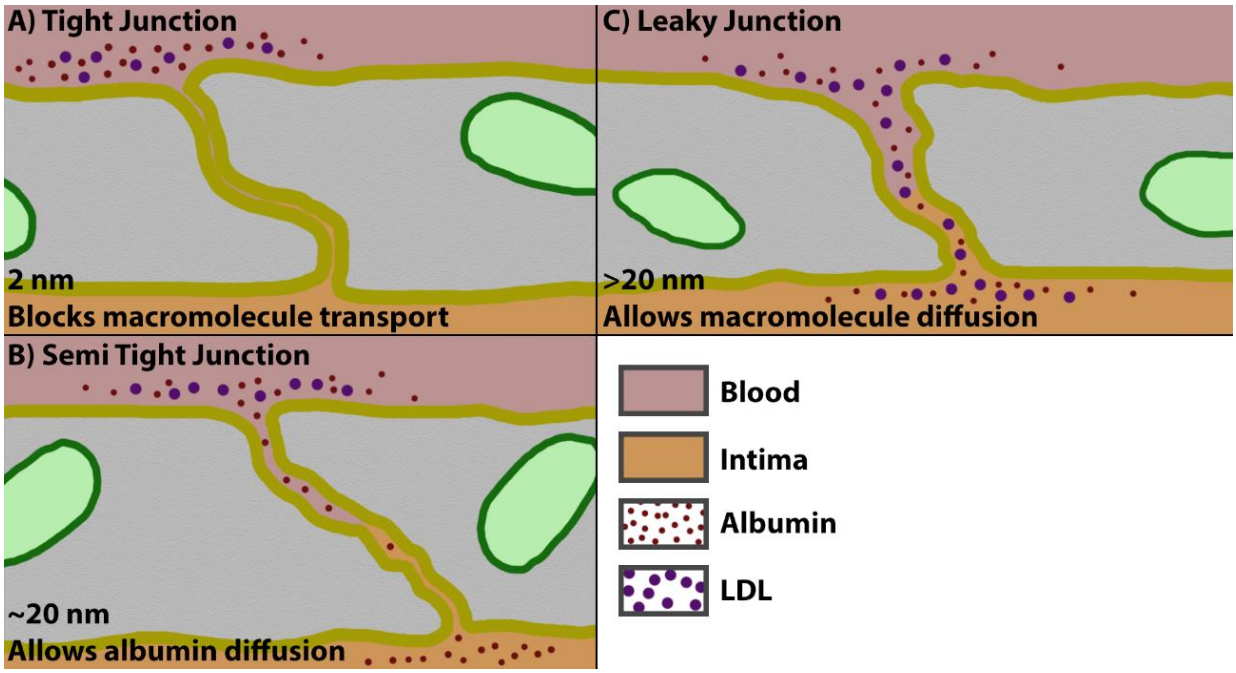

Figure 4: Diagram of the effect of endothelial junction size on molecular transport. Normal endothelial cells have a combination of A) Tight junctions (~2 nm) which prohibit macromolecule transport, and B) Semi tight junctions, which are larger (~20 nm) and allow albumin transport. Junctions which are larger than 20 nm are classed as leaky (C) and allow LDL transport into the intima.

Endothelial control of junction integrity is crucial to maintaining protection from atherosclerosis. If junction integrity is maintained, LDL is prevented from entering the intima and disease cannot occur. However, changes in endothelial cell behaviour significantly disrupt endothelial barrier function. The three key events that lead to this are apoptosis, inflammation, and proliferation.

1.4.1 Apoptosis in Atherosclerosis

Apoptosis is a form of programmed cell death characterised by controlled detachment and shrinkage of the cell membrane followed by packaging of cellular components into apoptotic bodies for phagocytosis by neighbouring cells. This process prevents inflammatory intracellular molecules from spilling into the surrounding tissue as would otherwise occur in injury associated cell death (necrosis).

In the healthy vasculature ECs exhibit very low levels of apoptosis, in atherosclerosis apoptosis is increased by environmental and immune factors.

Oxidised LDL: The presence of oxLDL in the endothelial microenvironment directly increases apoptosis via activation of MAP kinase, Jun kinase, and via Akt degradation (Chistiakov et al., 2016; Dimmeler et al., 1999; Salvayre et al., 2002). OxLDL also indirectly increases apoptosis by changing the oxidative state of the endothelium, resulting in increased ICAM-1 and MCP-1 expression which increases immune cell recruitment (Hubbard & Rothlein, 2000; Wolf & Ley, 2019). Recruited immune cells produce superoxide which increases EC apoptosis via angiotensin II (Dimmeler et al., 1997; Kojda & Harrison, 1999). Of these recruited immune cells, macrophages are transformed into foam cells by oxLDL, efferocytosis of foam cells is inhibited, thus foam cells accumulate, driving apoptosis and disease (Salvayre et al., 2002; Tajbakhsh et al., 2019).

TNF: Macrophages recruited to atherosclerotic tissue secrete TNF, which drives apoptosis of ECs via degradation of Bcl-2 and activation of caspase 3 (Dimmeler et al., 1999). Interestingly, anti-TNFα treatment increased plaque burden in mouse models of atherosclerosis, though this was thought to be sure to increased plasma lipid concentration (Oberoi et al., 2018).

Matrix Degradation: The extracellular matrix which anchors endothelial cells to the vessel is essential for maintaining cell survival. ECM promotes EC survival via increased Bcl-2 activity and via suppression of p53 regulated apoptosis (Mallat & Tedgui, 2000). Matrix is degraded during atherosclerosis by activation of FOXO3α, which induces VSMC apoptosis leading to secretion of MMP13 and breakdown of the ECM (Yu et al., 2018). immune cells which secrete matrix metalloproteases (MMPs), remodelling of the vascular matrix leads to increased endothelial cell apoptosis (Levkau et al., 2002). Interestingly there is some evidence for a mechanism to supress inflammation under basal levels of apoptosis via autocrine secretion of molecules which direct macrophages towards an anti-inflammatory state (Brissette et al., 2012) Nonetheless this system is overwhelmed in disease, where macrophages are pro-inflammatory, and inflammation is not resolved.

Increased apoptosis results in atherosclerosis loss of endothelial integrity, and loss of endothelial regulation of blood-intima transport (Fig. 4) which facilitates lipoprotein accumulation in the vasculature (Borén et al., 2020; Cancel & Tarbell, 2010). This perpetuates the production of pro apoptotic oxLDL and accelerates disease progression. Apoptosis of endothelial cells leads to progression of disease via increased EC secretion of pro-coagulant phosphatidylserine which increases tissue factor activity. EC apoptosis also leads to generation of pro-coagulant microparticles via externally expressed phosphatidylserine, which activates coagulation factor XII leading to local and systemic tendency towards coagulation (Mallat et al., 1999; Yang et al., 2017).

1.4.2 Inflammation in Atherosclerosis

Inflammatory mediators play a significant role in the initiation and progression of atherosclerosis. Initiation is driven by multiple inflammatory cytokines including IL-1β, IL-6 and TNF. These cytokines and other pro-inflammatory substances such as oxidised LDL induce activation of EC characterised by expression of adhesion molecules (e.g. E-selectin, VCAM-1, ICAM-1), chemokines (IL-8, MCP-1) and cytokines that co-ordinate the capture of leukocytes from the bloodstream to the arterial wall (Wolf & Ley, 2019).

This process leads to the recruitment of monocytes to the intima which subsequently differentiate into macrophages. These cells respond to subintimal oxLDL by priming and activation of the NLRP3 inflammasome, which leads to production of pro-IL-1β, pro-IL-18, and pro-caspase-1 (He et al., 2016). These pro-inflammatory cytokines subsequently perpetuate and amplify arterial inflammation. This is conducive to further infiltration and oxidation of lipoproteins which leads to progression of disease (Hulthe & Fagerberg, 2002). Recent studies suggest chronic inflammation is a significant cause of mortality and morbidity in late-stage atherosclerosis. Inhibition of IL-1β in the CANTOS clinical trial led to significantly reduced cardiovascular events without an associated reduction of serum LDL levels (Ridker et al., 2018). This suggests that inflammation is a significant driver of disease in humans.

During plaque development chronic inflammation is partially responsible for driving formation of the necrotic core, a feature of unstable rupture-prone plaques which confers heightened risk of morbidity and mortality in atheroma. Necrotic core growth is a consequence of inflammatory inhibition of efferocytosis of apoptotic macrophages within the lesion (Thorp et al., 2011; Thorp & Tabas, 2009). It can therefore be concluded that inflammation is a key initiator of atherosclerosis, and it also drives plaque progression towards dangerous rupture-prone forms.

1.4.3 Proliferation in Atherosclerosis

Endothelial cell proliferation is required for sprouting angiogenesis and repair of the vasculature following damage, therefore healthy maintenance of the vasculature requires endothelial cell proliferation. However, proliferation is a double-edged sword because it is required for vascular repair, but excessive EC proliferation in the arteries is associated with loss of EC alignment and increased junction gap, which leads to increased LDL transport to the intima (Cancel & Tarbell, 2011; Zhang et al., 2020).

Early studies on proliferation in the porcine aorta observed regional variation in endothelial permeability to Evans Blue solution, and that this increase in permeability was associated with increased endothelial cell turnover and a rounder, less polarized cell phenotype (Caplan & Schwartz, 1973). Later work in pigeons showed that lesions resulting from a high cholesterol diet exhibit higher levels of endothelial proliferation compared to healthy tissue and thus confirmed the association of proliferation with atherosclerosis (Taylor & Lewis, 1986). Whilst classically endothelial proliferation is pro-atherogenic, emerging evidence for an anti-atherogenic role for EC proliferation lends credence to the theory that EC proliferation is essential for coverage of 'gaps' in the endothelium left by apoptotic ECs (Zhang et al., 2016).

The relationship between proliferation, cell morphology and permeability were further revealed by subsequent studies which found the rate of EC proliferation is inversely proportional to EC alignment (DeStefano et al., 2017). Since junction permeability is proportional to EC alignment, increased EC proliferation is directly associated with increased junction permeability (Buchanan et al., 2014). In the arteries, this relationship suggests that proliferation leads to accumulation of LDL in the intima due to increased permeability and subsequently to an increased risk of atherosclerosis.

EC proliferation and downstream processes can occur in response to natural stimuli, i.e. the immune response, or due to atherogens such as cigarette smoke, and nicotine (Lee & Cooke, 2012; Michael Pittilo, 2000). Thus, the endothelium in individuals with sustained exposure to atherogenic factors undergoes increased proliferation and permeability. In response to acute injury, these changes may be beneficial as they facilitate immune system clearance of foreign material and enhanced tissue repair (Wu & Thiagarajan, 1996; Zhang et al., 2020). However, subsequent long term increases in endothelial permeability leads to accumulation of LDL and inflammatory cells in the arterial intima to drive atherosclerosis (Fig. 5).

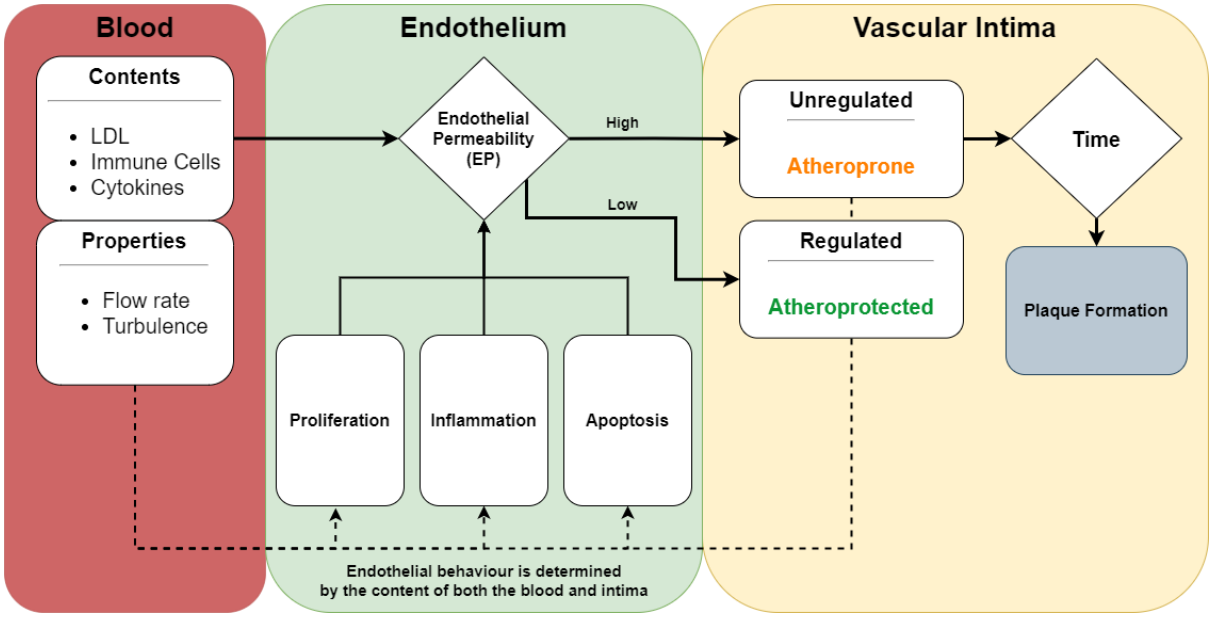

Figure 5: Flow chart illustrating the role of endothelium in control of endothelial membrane permeability. The contents and properties of the blood as well as the contents of the vascular intima determine whether the vessel is atheroprone or atheroprotected. If proliferation, inflammation, or apoptosis is triggered, this leads to increased endothelial permeability, which allows circulating LDL to enter the intima, where it further increases endothelial permeability.

Given that EC proliferation is essential for health, medically blocking it to prevent atherosclerosis would likely introduce severe health problems. So how can we prevent excessive proliferation driving disease but retain homeostatic repair processes? One school of thought is that investigation of the molecular mechanisms for why endothelium responds to flow could provide pharmacologically viable targets for prevention of atherosclerosis.

1.5 Extracellular Matrix in Atherosclerosis

The vascular extracellular matrix (ECM) is a complex 3D network composed of collagens, elastins, proteoglycans, glycoproteins, and hyaluronan. ECM is involved in regulation of cell fate and function and is thus key to normal function of vascular cells such as EC's, VSMC's, and immune cells (Karamanos et al., 2021).

The role of ECM in atherosclerosis is not as a scaffold on which atherogenic changes occur to residing cells, but as a dynamic player whose structure and function changes through progression of disease. Each component of the ECM has a different role within atherosclerosis (Gialeli et al., 2021):

Collagen: Collagens are abundant, isomeric proteins which contribute to the tensile strength of the arteries. Collagen is degraded during plaque development, then progressively deposited during plaque progression leading to accumulation of type I and II collagen fibres in plaques (Xu & Shi, 2014). Mouse studies show that the structural alignment of collagen fibres around the plaque cap determine the stability of the plaque, hence collagen is a valuable clinical marker for advanced atherosclerosis (Johnston et al., 2021).

Elastins: Elastin is a polymeric protein composed of multiple interlinked tropoelastins, each consisting of 36 alternating hydrophobic and hydrophilic domains (Vrhovski & Weiss, 1998). Elastin provides elasticity and flexibility to arteries in response to changes in blood flow and pressure exerted during the cardiac cycle. Whilst elastin is physically robust, age associated changes including calcification and lipid loading leads to progressive dysfunction of the arteries due to loss of elasticity. This leads to increased blood pressure, and altered haemodynamics (Fhayli et al., 2019).

Proteoglycans: Proteoglycans are a family of molecules composed of sulphated glycosaminoglycans attached to a protein core. The composition of the protein core determines the nature of the proteoglycan molecule; thus proteoglycans encompass heparins, keratans, hyaluronans, chondritins and dermatans (Karamanos et al., 2021). Within current models of atherosclerosis, atherogenic proteoglycans are retained within the arterial intima, leading to disease. These molecules include versican, biglycan, decorin, and perlecan and can act as immunomodulators, driving inflammation and susceptibility to disease (Gialeli et al., 2021).

1.6 Fluid Mechanics and Atherosclerosis

Blood flow is determined by arterial geometry, which naturally generates regional variation in the properties of flow. Uniform flow occurs in linear, unobstructed regions of the arteries and is defined as where all fluid layers flow in the same direction and do not mix. As a result, uniform blood flow is high near the arterial wall, which results in application of high

frictional force, and high shear stress (HSS) to the endothelium (Fig. 6A). At branches or bends flow is disturbed, which leads to crossing and reversal of fluid layers and can generate pockets of slowly circulating or static blood flow that exert low shear stress (LSS) on the vessel wall (Fig. 6B, (Roux et al., 2020)).

This nature of the relationship between blood flow and shear stress was quantified in Poiseuille's equation where shear stress is directly proportional to blood flow velocity and viscosity, and inversely proportional to the vessel radius. This equation and modern computing have enabled *in silico* modelling of shear stress in study of the relationship between flow and atherosclerosis (Koo et al., 2013; Serbanovic-Canic et al., 2017) and is the basis for early work that showed association of atherosclerosis to LSS, and protection from atherosclerosis to HSS (Caro et al., 1969; Moore et al., 1994).

Interestingly, low and oscillatory shear stress (OSS) does not comprehensively predict sites which are at risk of plaque formation. Others have shown that transverse shear stress, occurring where layers flow in a direction perpendicular to the mean, contributes to previously unexplained regions of plaque formation by application of corkscrew like force to the vessel wall (Peiffer et al., 2013).

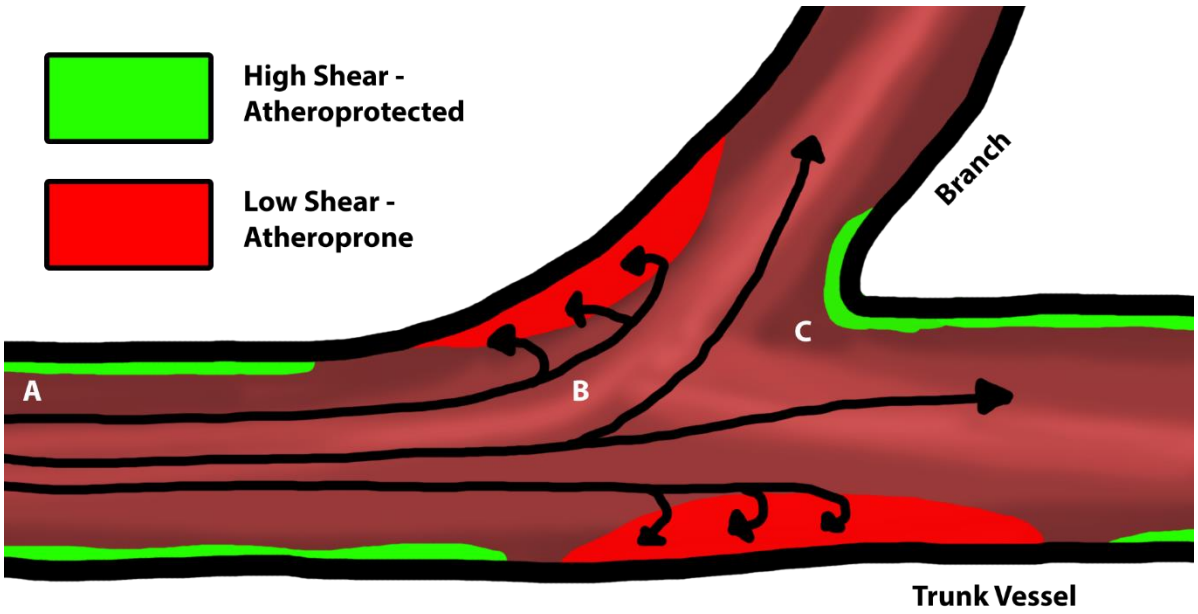

Figure 6: Diagram of blood flow patterns within a branched artery. Within the trunk, linear regions lead to unidirectional flow and high shear stress exerted on the vessel wall (A). At branches, changes in arterial geometry lead to disturbed flow near the branch site, these regions exert low shear stress on the vessel wall (B). Regions of high shear stress also occur at the branch point (C).

These observations are fundamental in connecting the role of blood flow, risk factors and time (or age) in atherogenesis. Blood flow, via its effect on endothelial permeability, inflammation, and thrombotic potential, determines disease risk for a specific region based upon its structure. Diet and blood cholesterol determine the proportion of LDL in the blood, and therefore determine the risk of LDL accumulation in those susceptible regions, i.e. regions of disturbed flow. Finally, disease progression occurs over years to decades, so in order to develop atherosclerosis one requires multiple factors including disturbed flow, systemic risk factors e.g. hyperlipidaemia, and time.

Disturbances in blood flow are caused by the structure of the vasculature and lead to regional endothelial dysfunction and susceptibility to atherosclerosis. If mechanisms linking disturbed flow with endothelial dysfunction were identified, these could be pharmacologically targeted to reduce risk of disease.

So, what is responsible for detection and response to flow? Endothelium, the tissue in contact with blood, is shown to detect and responds to changes in blood flow via a complex array of signalling components expressed on the apical membrane of each cell (Givens & Tzima, 2016). Shear stress causes deformation of this membrane based on the direction of flow relative to the cell (Ballermann et al., 1998). Early models proposed that under flow, ‘shear stress receptors’, a general term for any membrane component which acts in mechanotransduction, trigger a cellular response (Ishida et al., 1997). Studies have since uncovered a range of surface components with roles in detection of shear stress (Fig. 7).

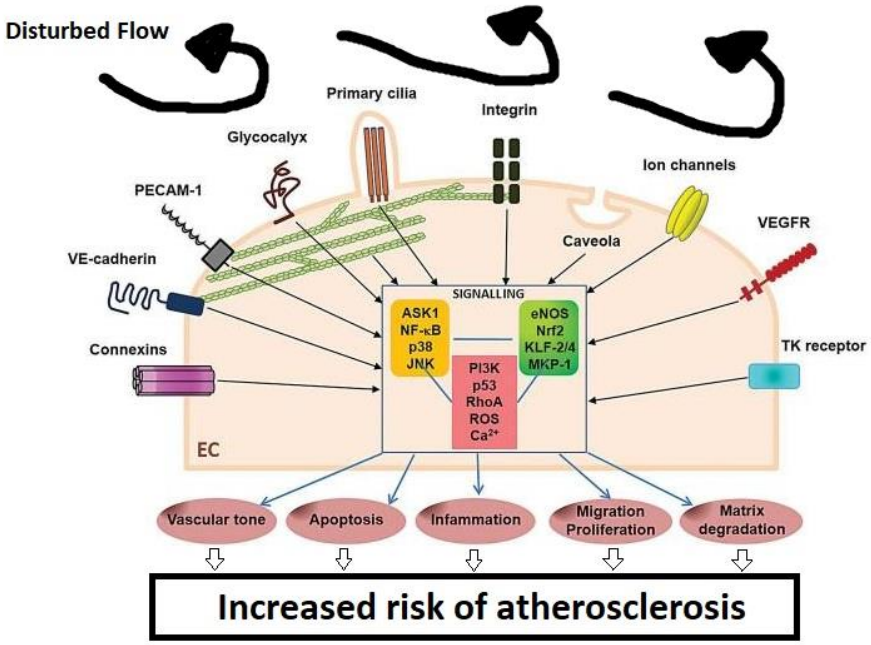

Figure 7: Diagram of mediators of endothelial detection and response to shear stress. Blood flow leads to movement of the apical surface. This is detected by surface components which activate interconnected signalling pathways which cause inflammation, apoptosis, changes in vascular tone, migration, proliferation, and matrix degradation. These changes collectively increased risk of apoptosis. Adapted from Kwak et al, (2014).

Under disturbed flow these surface components lead to increased endothelial cell apoptosis, inflammation and proliferation and increased risk of atherosclerosis via the pathways introduced in section 1.4:

1.6.1 Apoptosis in Response to Flow

Study of apoptosis using *in vivo* and *in vitro* models, as well as human clinical sections (Tricot et al., 2000) shows endothelial cells are protected from apoptosis under unidirectional flow and are pro-apoptotic under disturbed flow (Bartling et al., 2000; Heo et al., 2011; Serbanovic-Canic et al., 2017; Zhang et al., 2013).

Protection from apoptosis under HSS occurs via phosphorylation of Akt (Dimmeler et al., 1999), increased cadherin-13 expression (Serbanovic-Canic et al., 2017), and nitric oxide production (Braam et al., 2005).

Several mechanisms are thought to be involved in increased apoptosis under LSS. Some observed increased misfolding of proteins and accumulation of misfolded proteins in the endoplasmic reticulum (ER) of endothelial cells (Kim & Woo, 2018). This leads to increased ER stress and triggers the unfolded protein response which primes ECs to undergo JNK1 mediated activation of apoptosis in response to hypercholesterolaemia (Amini et al., 2014; Chaudhury et al., 2010). Serbanovic-Canic et al (2017) observed increased expression of PERP under LSS. As PERP stabilises p53, increased PERP under LSS could lead to apoptosis by increased levels of p53. Additionally, Mahmoud et al (2014) found LSS induces developmental pro-apoptotic genes GATA-4, FZD5, BMP2 in atheroprone ECs (Mahmoud et al., 2014). Upregulation of these genes leads to apoptosis via activation of protein kinase C, p53-sumoylation and mitochondrial activation of apoptosis (Chaudhury et al., 2010; Heo et al., 2011).

1.6.2 Inflammation in Response to Flow

As described previously, inflammation is involved in initiation and progression of atherosclerosis. Flow regulation of a range of pathways is responsible for chronic inflammation at atheroprone sites (Fig. 8).

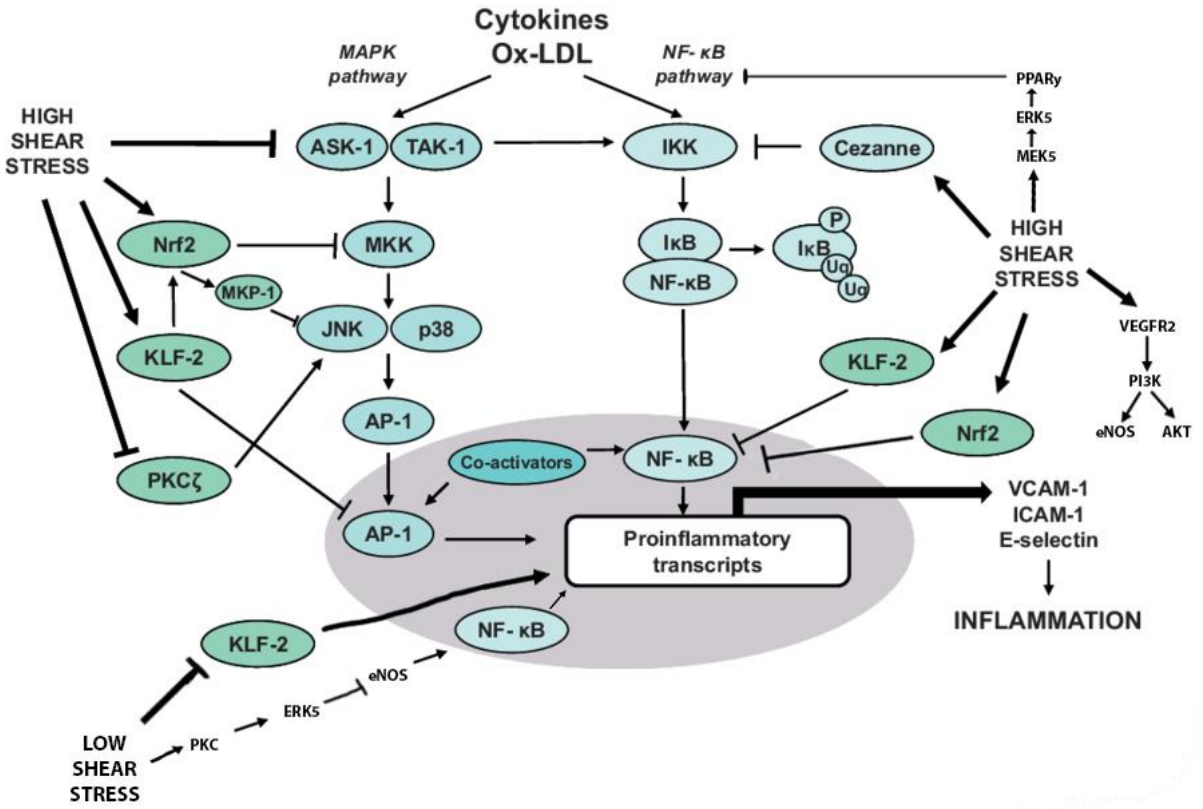

Figure 8: Diagram illustrating shear regulated inflammatory pathways. High shear stress (HSS – Green) is atheroprotective via Nrf2, PRKCZ and KLF2 mediated inhibition of JNK/p38 and NF-kB respectively. Low shear stress disinhibits inflammation and upregulates PRKCD which leads to inflammation via p38. Adapted from Warboys et al (2011).

High shear stress is anti-inflammatory as it induces KLF2 expression via the MAPK pathway (Parmar et al., 2006), KLF2 then inhibits JNK which reduces expression of proinflammatory AP-1 transcription factors. KLF2 also enhances Nrf2 activity which reduces AP-1 expression by supressing upstream activators of p38 and enhancing MKP-1 mediated negative regulation of p38 and JNK (Zakkar et al., 2009). Nrf2 activity also attenuates NF-kB, which attenuates the inflammatory response. Therefore, unidirectional flow leads to reduced VCAM-1 expression which limits leukocyte adhesion and infiltration to site.

HSS also modulates inflammation via suppression of NFκB. This occurs as a result of upregulation of eNOS under HSS, which increases NO production and inhibits upstream regulators of NFκB (Yurdagul et al., 2013). Under HSS, VEGFR2 undergoes ligand independent activation, and recruit phosphoinositide 3 (PI3K) kinase to activate eNOS and Akt which are anti-inflammatory (Jin et al., 2003). HSS also activates protein kinase C zeta (PKCZ), which inhibits JNK (Magid & Davies, 2005). High shear regions are also protected from inflammation via flow induced activation of MEK5, which is upstream activator of ERK5 (Zhou et al., 1995). Activated MEK5 phosphorylates the kinase domain of ERK5, which facilitates binding of ERK5's peroxisome proliferator activated receptor (PPARγ) binding site with the PPARγ hinge helix domain. This activates PPARγ which inhibits NFκB and downstream inflammatory mediators VCAM1 and E-selectin.

Disturbed flow results in loss of this anti-inflammatory state, and activation of pro-inflammatory processes (Heo et al., 2011). In regions of disturbed flow protein kinase C is activated, which phosphorylates ERK5 and downregulates eNOS production. Uncoupling of eNOS leads to production of superoxide which accumulates and activates NFκB. NFκB is also activated by inhibition of KLF2 under disturbed flow. Activation of NFκB leads to IL-8, VCAM-1 and E-selectin expression which causes inflammation and facilitates immune cell infiltration (Liu et al., 2017).

1.6.3 Proliferation in Response to Flow

The relationship between endothelial proliferation and flow is complex and can vary according to the direction of flow applied, the magnitude of shear stress, and the duration and time point chosen to measure the rate of proliferation.

The main types of flow used in these studies are static, unidirectional, and oscillatory. Both *in vitro* and *in vivo* studies show that oscillatory shear stress leads to the greatest overall rate of EC proliferation, but there are differing interpretations for how unidirectional and static conditions compare (Chakraborty et al., 2012; Dardik et al., 2005; DeStefano et al., 2017; Dolan et al., 2011).

Responses to unidirectional flow: In HUVECS, the rate of endothelial cell proliferation under steady unidirectional flow increases with shear stress magnitude (4 to 16 dyne/cm^2; (DeStefano et al., 2017). EC proliferation in bovine aortic endothelial cells (BAECS) exhibits a similar response to flow however the shear forces applied in the study were much greater (35 and 284 dynes/cm^2. (Dolan et al., 2011). Therefore, proliferation of venous and arterial EC in response to shear stress differs according to the shear conditions that they have been exposed to (shear stress set point).

Whilst the rate of steady unidirectional flow affects EC proliferation, disturbed flow leads to a greater pro-proliferative effect. There are multiple proposed mechanisms for the effect of disturbed flow on the endothelial cell cycle. Early studies observed p53 undergoes sustained upregulation under HSS and arrests the cell cycle via increased GADD45 and p21 expression (Akimoto et al., 2000; Lin et al., 2000). This inhibits cyclin dependant kinase and prevents phosphorylation of retinoblastoma protein, leading to cell cycle arrest. Similarly, Guo et al (2007) demonstrated that flow dependent activation of AMPK leads to cell cycle arrest via the Akt/mTOR pathway, it is intuitive that LSS would reverse this block on the cell cycle. Indeed, disturbed flow increases EC proliferation, currently understood mechanisms for this include Smad5 mediated processing of microRNAs targeting CREB binding protein and p53 (W. L. Wang et al., 2021), and shear regulated nuclear localisation (and thus activation) of YAP/TAZ which leads to transcriptional upregulation of proliferation linked genes (Wang et al., 2016).

Notch was also shown to have a role in endothelial cell proliferation in response to flow. (Noseda et al., 2004) demonstrated that Notch inhibits p21Cip1, preventing cellular response to mitotic stimuli. Later work by (Mack et al., 2017) suggests this is achieved by contact activation of Notch1 in response to binding of Jag1 at the basement membrane. Thus, reduced cell adhesion to the basement membrane under disturbed flow causes Notch1 intracellular domain (NICD) cleavage and disinhibition of p21Cip1, which allows cell cycle progression. NICD cleavage is also associated with EC activation.

These studies on endothelial responses to flow used a combination of *in vivo* and *in vitro* models to test their hypotheses. Whilst the hypothesis driven approach is useful when asking specific questions based on prior knowledge, it is not optimal for designing experiments which seek to identify novel genes involved in endothelial cell responses to flow. The Evans group has previously demonstrated the merit of applying unbiased, systems biology approaches to identify novel flow regulated genes involved in atherosclerosis using zebrafish embryos which will be described below (Serbanovic-Canic et al., 2017).

1.7 Zebrafish Embryos in Vascular Biology Research

The zebrafish (*Danio rerio*) embryo is a rapidly developing, optically transparent organism which can be genetically modified using a wide range of techniques. Zebrafish develop a functional circulatory system in 26 hours and are not classed as a protected species by the UK Home Office until 5.2 days post fertilisation. In addition to their use in fundamental developmental biology research, zebrafish embryos are also used to model cardiovascular disease (G. Bowley, E. Kugler, et al., 2021). This has gained momentum over the past three decades since scrutiny of use of mammals in research has led to a continued push for reduction and replacement which zebrafish embryo models allow.

An important asset of zebrafish research is the size and scope of its rapidly developing experimental toolbox. Proven methods for reporter line production (Moro et al., 2013), random or site directed mutagenesis (Poulain, 2017), and fine control over gene expression (Ekker, 2000) are available. Use of these tools alongside imaging techniques such as two-photon and light-sheet microscopy enables visualisation and control of development at a

level that is simply not possible in mammals. This level of manipulation and visualisation of the vascular system has led to significant advancements in vascular biology (G. Bowley, E. Kugler, et al., 2021).

Development of the zebrafish vasculature commences at 12 hours post fertilisation (hpf) when cells in the lateral plate mesoderm specify as angioblasts and migrate towards the midline. The first wave of migrating cells are arterial precursors whereas the following wave occurring three hours later are venous (Carroll & North, 2014). Both precursor populations accumulate ventral to the notochord, where they differentiate into the dorsal aorta (DA) and posterior cardinal vein (PCV) to form separate cords by 20 hpf. ECs contributing to vasculogenesis are derived from the primary angioblast populations and the somites, endothelial cells then migrate between the arterial and venous cords (Herbert et al., 2009). At 26 hpf EC junction formation begins, followed by tubulogenesis which creates the primitive circulatory system composed of the heart, DA and PCV. Initiation of the heartbeat marks the onset of function of the embryonic circulatory system.

Following establishment of the initial loop, sprouting angiogenesis occurs dorsally from the DA at ~22 hpf. Sprouts pass through the notochord, then the neural tubule guided by the boundaries of the somites, to form the aortic intersegmental vessels (aISV). Upon completion of primary angiogenesis, the leading tip cells undergo anastomosis and form the dorsal longitudinal anastomotic vessel (DLAV). At 36 hpf vascular endothelial cells sprout dorsally from the PCV towards the aISV, at 54 hpf these sprouts anastomose with the aISV to form venous intersegmental vessels (vISVs). Vascular endothelial growth factor (VEGF) signalling in sprouting endothelial cells results in alternate formation of vascular and lymphatic sprouts along the segmental plane, this is necessary for ISV circulation.

1.8 The Effect of Blood Flow on Endothelial Cell Behaviour in Zebrafish Embryos

The cardiovascular system of zebrafish embryos can be manipulated to enable study of endothelial cell behaviour under different flow conditions. Blood flow can be determined by microscopy or quantified precisely by capturing images for analysis. Flow can be stopped using tricaine (MS222) incubation or *tnnt2a* morpholino (MO) induced knockdown. It is even possible to manually modulate the heartbeat with a laser in certain transgenic embryos (Arrenberg et al., 2010).

Zebrafish embryos are routinely anaesthetised in 150 mg/L tricaine to reduce movement in imaging experiments. For studying EC responses to flow, increasing the tricaine concentration to 750 mg/L leads to total cessation of blood flow, this allows the investigator to control the point at which blood flow is stopped. Alternatively, injection of *tnnt2a* morpholino into fertilised embryos leads to knockdown of troponin T type 2a and complete loss of heartbeat *ab initio*. The advantage of the morpholino approach is it does not lead to haemostatic changes, however loss of flow throughout embryo development leads to abnormalities in arteriovenous identity and vessel pruning which are not seen in wildtype embryos (Kochhan et al., 2013; Renz et al., 2015).

Considering the remarkable level of conservation in vertebrate vascular development along with the range of tools available for use in zebrafish, it is surprising that compared to other

model organisms, comparatively little research on the effect of flow on the basic cellular processes of migration, apoptosis and proliferation has been done in zebrafish. Our group studied the effect of blood flow on apoptosis in the zebrafish embryo and found that absence of blood flow leads to increased endothelial cell apoptosis (Serbanovic-Canic et al., 2017), others have studied the effect of blood flow on endothelial cell migration and extrusion (Campinho et al., 2020; Weijts et al., 2018), yet specific analysis of zebrafish endothelial cell proliferation in response to flow does not currently exist.

Interestingly, researchers at the University of Sheffield observed a significant decrease in endothelial nuclei in *tnnt2a* morphants compared to controls, this observation confirms that blood flow affects EC behaviour in zebrafish (Kugler et al., 2021; Watson et al., 2013). However, because this was based on a simple nuclei count, it is not possible to attribute the change solely to changes in proliferation as it could have occurred because of migration or apoptosis. Data from Serbanovic-Canic et al (2017) suggest apoptosis could be partially responsible, as seen in the significant increase in apoptosis in tnnt2a morphant embryos at 30 hpf, which was followed by a marked reduction in EC number by 48 hpf.

These questions highlight the importance of identifying the precise role of endothelial cell proliferation in response to flow. It is therefore important to develop a novel assay for endothelial proliferation in zebrafish, and specifically determine the degree to which flow affects this process. Development of such an assay will allow us to screen for genes which mediate endothelial cell proliferation in response to flow, and therefore potentially identify genes involved in atherogenic endothelial proliferation found in low shear sites.

1.9 Novel Approaches for Study of Flow Regulated Genes Involved in Atherosclerosis

Flow is linked to atherosclerosis by a vast and complex set of molecular pathways which change endothelial cell behaviour. Identifying the genes involved using a hypothesis driven study requires *a priori* knowledge of the system in question. This effectively means the study design is limited to ‘known unknowns’ and prohibits identification of completely novel pathways involved in disease.

The introduction of high throughput screening techniques gives researchers the ability to test the effect of flow by reading the entire endothelial transcriptome, this yields a dataset which describes expression of many thousands of genes under different flow conditions. These data can then be used as the basis for further studies to determine the function of genes in relation to atherosclerosis.

These approaches offer scientific benefits and also have the potential to significantly reduce use of animals in cardiovascular disease research. Mice are the most widely used model in CVD studies (Oh & Ishikawa, 2018) and procedures on mice are often non-recoverable which leads to sacrifice of a large proportion of study animals. When combined with *in vitro* screening, screening-led studies can reduce animal use both by identifying candidate genes in an accurate and efficient way, and by eliminating or reducing the severity of procedures used in functional studies.

Our group used a high throughput screen to identify putative regulators of endothelial cell apoptosis under low shear stress (Serbanovic-Canic et al., 2017). An open-ended functional screen was then used to identify which genes which were involved in apoptosis *in vivo*. This study was made possible by screening of candidate genes which generates an unbiased dataset which can be reused and repurposed in future work (Fig. 9).

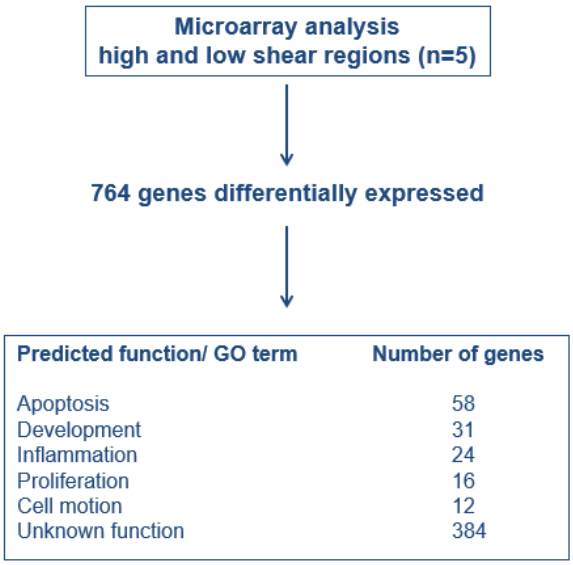

Figure 9: Microarray analysis of endothelial cells from high and low shear regions of porcine aorta led to identification of genes which were differentially expressed under high and low shear conditions (Serbanovic-Canic et al., 2017).

Similar approaches have been used elsewhere to identify novel flow regulated genes that regulate inflammation (Doran et al., 2021). However, unbiased gene screening has not been applied to identify flow-sensitive regulators of EC proliferation which is a central process in atherogenesis. The study presented in this thesis will apply the system previously demonstrated by our group to identify novel flow regulated genes involved in endothelial cell proliferation using zebrafish larvae as the model organism.

2.0 Hypothesis and Aims

I hypothesise that zebrafish embryos can be a viable alternative to mammalian models used to study vascular proliferative responses to flow. If viable, this model has the potential to replace mice and decrease costs for analysis of genes or compounds for atheroprotective effects.

Aim 1 – Establish a zebrafish embryo model of EC proliferation in response to flow.

Aim 2 – Establish a system for screening candidate genes for effects on EC proliferation in the zebrafish embryo.

Aim 3 – Validate expression of genes identified through this screening approach in mouse and human.

3.0 Materials and Methods

3.1 Materials

3.1.1 Transgenic Zebrafish Lines

The following transgenic lines were used, for lines obtained from collaborators at the University of Sheffield the originating group is given in brackets:

Transgenic line	Expression pattern
Tg fli1a:EGFP ^{y1} (Lawson & Weinstein, 2002)	Endothelial promoter driven green fluorophore.
Tg gata1:dsRed ^{sd2} (Traver et al., 2003)	Erythroid promoter driven red fluorophore.
Tg fli1a:LifeAct-mClover ^{sh467} (Savage et al., 2019)	Endothelially expressed green fluorophore localised to filamentous actin. Visualises actin cytoskeleton.
Tg fli1a:nls-mCherry ^{sh550} (Chen et al., 2021)	Endothelially expressed red fluorophore localised to the nucleus. Visualises endothelial nuclei.
Tg fli1a:nls-EGFP ^{sh549} (Chen et al., 2021)	Endothelially expressed green fluorophore localised to the nucleus. Visualises endothelial nuclei.
Tg Ubi:dCas9-cryaa:CFP (Noël group, unpublished)	Ubiquitously expressed dCas9 protein. Blue fluorescent protein expressed under the crystalline promoter
Tg Ubi:fucci ^{w141} (Bouldin & Kimelman, 2014)	Ubiquitiously expressed fluorescence ubiquitin cell cycle indicator.

3.1.2 E3 Medium

Zebrafish larvae were kept until 5.2 days post fertilisation in E3 medium. E3 medium is composed of 5 mM NaCl, 0.17 mM KCL, 0.33 mM MgSO4 and 0.33 mM CaCl2.

3.1.3 Morpholinos

The following morpholinos were used in this study:

Gene of interest	Morpholino sequence (5'-3')	Dose (ng)	Publication
tnnt2a	CATGTTTGCTCTGATCTGACACGCA	1.0	(Serbanovic-Canic et al., 2017)
non targeting control	CCTCTTACCTCAGTTATTTATA	1.5	(Serbanovic-Canic et al., 2017)
wnk1a	ACTTGACCATCTTGTCGTTGAGATT	1.75	(Lai et al., 2014)
gsk3b	GTTCTGGGCCGACCGGACATTTTTC	1.75	(Lee et al., 2007)

fzd5	GATGCTCGTCTGCAGGTTTCCTCAT	3.5	(Cavodeassi et al., 2005)
sema6a	TGCTGATATCCTGCACTCACCTCAC	2.0	(Ebert et al., 2014)
trpm7	ATCCAGGACTTCTGGGACATTCT	1.75	(Sah et al., 2013)
bmp2a	TGGACGAGACCATGATGATCTCTGC	3.125	(Quillien et al., 2011)
angptl4	TCAGCAATGATAAACTGACTTACCA	2.5	(Serbanovic-Canic et al., 2017)

3.1.4 CRISPRi

During this study CRISPR interference was used for genetic knockdown. Guide RNAs (gRNAs) were designed using CHOPCHOP (Valen et al, 2019) to target ±50 bp of the transcription start site (TSS). This method was used to design four unique gRNAs for each target gene.

3.1.4.1 dCas9 Endonuclease

The dCas9 non-cleaving Cas9 endonuclease was expressed in transgenic zebrafish (ubi:dCas9-cryaa:CFP) kindly provided by the Noël group. Plasmid derived dCas9-mRNA was also tested using pcs2-dCas9 provided by the Wilkinson group.

3.1.4.2 Guide RNAs used for CRISPRi Experiments

CRISPRi target	**gRNA sequence (5'-3')**
wnk1a – TSS 1	ATTTAACAAATCGAGAAGCC
wnk1a – TSS 2	TTTTCAGGGAATTGGACGCA
wnk1a – TSS 3	TTTCGTGATCGACAATAACC
wnk1a – TSS 4	AGTTATCGGCGAATAACCAA
gsk3b – TSS 1	GTAACGCACTTTACGTCGAT
gsk3b – TSS 2	AGATGAGCGCGAGCACAGCC
gsk3b – TSS 3	AACGGTGAGCAGAATCCCCA
gsk3b – TSS 4	ACAGAGAGTCGAGGATCCGT

3.1.5 qPCR Primer Design

Primers were designed so that the forward and reverse primers bound to separate exons. This was done for compatibility with the SYBR Green kit and to minimise amplification of genomic DNA.

3.1.6 Primers Used in this Study

Quantitative PCR (qPCR) primers (F, forward; R, reverse) were used to determine expression of genes of interest in whole zebrafish larvae and zebrafish endothelial cells. qRT-PCR was further used to determine whether gRNA injection into ubi-dCas9 zebrafish embryos resulted in knockdown of the target gene. The following primers were used:

Target gene	Sequence (5'-3')
wnk1a F	TGAAGCCTGGCAGTTTTGAC
wnk1a R	TCCTTGATGCAGTACCTCTCA
trpm7 F	TCAGTAAGCAGGAGAGGAGC
trpm7 R	GACTTCCCCAGCAGCAGAT
tnfsf10 F	TCAATGTCCAGTCGATATCAGAA
tnfsf10 R	TGAGGGAAGAACACGAGAGAC
thbs4a F	GCACCATGTCCTGAGGGTTA
thbs4a R	CATGGGTTGAACTGGCACTC
thbs4b F	CTGAAGGGGTGGAGTGTGG
thbs4b R	AGGGGTTAAACTGGCACTCA
serpinc1 F	AGAGCAGCTGACGAAAATGG
serpinc1 R	AGTTGGGACCTTCAGCATCA
sema6a F	CTCTGAACGGCCGTGTCT
sema6a R	TGATCCTTCAGCACTCGACC
kng1 F	CGTTTTGTTGGTGCGGTTTT
kng1 R	AGATCCTGAGAGCCTTATCTGC
igf1 F	AGACAGGCAAATCTCCACGA
igf1 R	ATAGGTTTCTTTGGTGTCCTGG
gsk3b F	GGTGGAGATCATCAAGGTGTT
gsk3b R	TCTGCGGGAATTTGAACTCG
fzd5 F	CCCCCACAAAAATGTGATCGGG
fzd5 R	TGCGCTCATCCTGGGAAAAGTA
bmp2a F	GCAGACCCAGAGCTCACTTA
bmp2a R	TGTAGATTCATCATGGTGGAAGC
bmp2b F	CCGAGGAGCACTATGGGAAA
bmp2b R	AGTGCCTCGAAAGCCTCTTC
angptl4 F	AACAGAACATCCGCATCAGG
angptl4 R	TCAGAGACAGTCGCTCGTTT
b-actin F	AGCCATCCTTCTTGGGTATG
b-actin R	TGATCTCCTTCTGCATCCTG
rps29 F	TTTGCTCAAACCGTCACGGA
rps29 R	ACTCGTTTAATCCAGCTTGACG

3.1.7 Buffers and Solutions

The following buffers and solutions were used throughout the study:

Solution	Composition
Phosphate Buffered Saline (PBS)	150 mM phosphate buffer, 0.85% NaCL
PBS Tween (PBST)	1x PBS, 0.1% Tween-20
PBST DMSO (PDT)	1x PBST, 1% DMSO
4% PFA	2 ml paraformaldehyde per 50 ml 1x PBS
1% β-mercaptoethanol	0.5 ml β-mercaptoethanol per 50 ml MQ
Tricaine (MS222)	4g tricaine methanesulfonate in 1 L dH2O pH 7-7.5

Proteinase K	10 mg/ml of proteinase K in glycerol
TE Buffer	10 mM Tris-HCL, pH 8.0, 1 mM EDTA
E3	5 mM NaCl, 0.17 mM KCl, 0.33 mM CaCl2, 0.33 mM MgSO4
EdU Solution	EdU 500 uM, 15% DMSO, 85% E3
Permeabilization Solution	Saponin reagent diluted to 1x in PDT
TAE Buffer (50x)	2 M Tris-acetate, 50 mM EDTA
Lysis Buffer	1% β-mercaptoethanol, Buffer RLT

3.1.8 Antibodies

The following antibodies were used in this study:

Antibody	Host species	Target species	Manufacturer
Anti-PCNA	Rabbit	Zebrafish	GeneTex (GTX124496)
Anti-WNK1	Rabbit	Mouse, Human	Abcam (ab137687)
Anti-vWF	Mouse	Human	BD (AB_2216594)
Anti-CD144	Rat	Mouse, Human	BD (AB_2244723)
IgG	Rabbit	Mouse, Human	Abcam (ab37415)
IgG-AF568	Goat	Zebrafish, Mouse, Human	ThermoFisher (AB_143157)
IgG-AF488	Goat	Zebrafish, Mouse, Human	ThermoFisher (AB_2534074)
IgG-AF488	Goat	Zebrafish, Mouse, Human	ThermoFisher (AB_2534069)

3.1.9 Mice

Mice used in this study were wildtype male C57BL6/J Charles River strain aged 12 weeks. These mice were studied under the PPL of Sheila Francis (P5395C858)

3.1.10 Human Tissue

Anonymized human coronary plaque sections were kindly provided by Prof. Dr Imo Hoefer - Atheroexpress Biobank, Utrecht. Anonymized human stable and unstable carotid plaque sections were kindly provided by Prof. Sheila Francis.

3.2 Methodology

3.2.1 Zebrafish Maintenance and Husbandry

Zebrafish care and experimental procedures were carried out under Project Licence 70/8588 issued by the UK Home Office and local ethical committee approval was obtained. Adult zebrafish were kept at a constant temperature of 28±1°C and at pH 7.5±0.5. They were subjected to a light/dark cycle of 14 hours of light and 10 hours of darkness. Adult zebrafish were fed a diet of artemia and dry Zebrafeed™. For mating, pairs of male and female zebrafish were placed into mating tanks and separated by a divider to allow accurate timing

of fertilisation. For experiments where this was not required, a box for embryo collection with a mesh insert and marbles on top was placed in the fish tank to harvest progeny

The AB and Nacre wild type lines were used in this study. Nacre zebrafish lack melanocytes and are thus more transparent than conventional wildtype lines, this makes Nacre highly suitable for light microscopy (Lister et al., 1999).

3.2.2 Zebrafish Welfare

Adults: For all experiments described, embryos were produced by pair mating eight male and eight female adults of the same transgenic line. This was done to minimize the chance that zero pairs produced embryos, and to minimise confounders by limiting the genetic diversity of the embryos. Adults do not suffer pain or distress from pair mating and were returned to their home tanks immediately after producing embryos, home tanks contain environmental enrichments such as fake jellyfish and fake seaweed. No adults suffered adverse events because of this work.

Embryos: No embryos used in this study exceeded 5.2 dpf. For all experiments described, embryo collection stopped after 60 embryos were obtained. For PCNA and EdU experiments, embryos were treated then screened for the endothelial marker (*Tg fli1:EGFP* for PCNA, and *Tg fli1a:nls-mCherry* for EdU) then three embryos were randomly selected for imaging. For time-lapse imaging experiments, embryos were screened for *Tg flia:nls-mCherry* and *Tg fli1a:LifeAct-mClover*, then three embryos were randomly selected for imaging. Embryos not selected for imaging were humanely destroyed using bleach.

3.2.3 Dechorionating Zebrafish Embryos

Embryos were dechorionated 24h before experimentation (to a minimum of 24 hpf). Dechorionation was done by inserting closed forceps to pierce the chorion, then opening them to free the embryo.

3.2.4 Mounting Zebrafish Embryos for Timelapse Imaging

For the ZEISS Z-1 lightsheet microscope, embryos were suspended in liquid low melt agarose (0.8-1.2%) and drawn into a capillary. Embryos were suspended in the microscope once the agarose had set.

For confocal microscopy embryos were added to low melt agarose (0.8-1.2%), then drawn into a Pasteur pipette, and decanted into an Ibidi µ-Dish (35mm, cat #81156). Thin tip forceps were then used to push the embryo to a side mounted position.

3.2.5 Zebrafish Embryo Microinjection

For microinjection, a glass slide was placed into a petri dish and braced against the edge of the dish. The dish was tilted, and embryos were decanted so as to lay in a row against the edge of the slide.

For needle preparation glass capillaries (WPI cat #TW100F-4) were pulled into needles using a Sutter P1000. Ejection volume was calculated using a graticule (Breckland Scientific) and pico pump (H. Saur).

3.2.6 Molecular Biology

3.2.6.1 Whole Zebrafish RNA Isolation

To obtain RNA from whole embryos, ~60 embryos were dechorionated and placed into a sterile 1.5 ml Eppendorf tube, excess E3 medium was removed. Lysis buffer was added, and embryos were pipetted until destroyed. Embryo lysate was pipetted into a QIASHREDDER column (Qiagen) and purified lysate collected by centrifugation. RNA was then isolated using a RNeasy kit (Qiagen) following manufacturer protocol. RNA stocks were stored neat at -80 ºC or diluted for immediate use in cDNA synthesis.

3.2.6.2 Zebrafish Endothelial Cell Isolation

To obtain zebrafish endothelial cells, ~60 embryos containing endothelially expressed GFP (fli1a:EGFP-gata4:dsRed) were collected and incubated to 72 hpf. Embryos were then transferred to Tryp-LE solution and gently agitated at 37 ºC until liquified.

Liquified embryo solution was sorted for GFP positive and GFP negative cells by FACS. The resulting solutions were centrifuged at 400 g for 5 minutes to obtain a pellet.

3.2.6.3 Zebrafish Endothelial RNA Isolation

To obtain RNA from zebrafish endothelial cells, cells were isolated as above then mixed into 1% β-mercaptoethanol / buffer RLT solution. RNA was isolated using a RNeasy kit (Qiagen) following manufacturer protocol. RNA stocks were stored neat at -80 ºC or diluted for immediate use in cDNA synthesis.

3.2.6.4 cDNA Preparation

RNA concentration was determined using a NanoDrop spectrophotometer (Thermo Scientific). To obtain cDNA, iScript kits (Bio-Rad) were used in which 1 µL reverse transcriptase and 4 µL of 5x iScript reaction mix was made up to 20 µL with 1 µg of RNA. Samples were incubated in a thermocycler programmed following the manufacturer protocol (Bio-Rad).

3.2.6.5 qPCR

qPCR was used to quantify relative expression of genes within a cDNA sample. qPCR was performed using SYBR-Green master mix (Bio-Rad) according to the manufacturers protocol. A 384 well plate was set up with 5.0 ul SYBR-green master mix, 0.6 ul 10 mM primer mix, and
4.4 ul of cDNA per well. Samples were set up in triplicate and expression data was analysed in GraphPad Prism.

3.2.6.6 Bacterial Transformation

TOP-10 *E. coli* cells (Thermo Fisher) were thawed on ice for 15 minutes before addition of 2 µL of plasmid. The reaction mix was incubated on ice for 30 minutes followed by a 30 second heat shock at 42 ºC. The reaction mix was again incubated on ice for 5 minutes, then 500 µL of LB broth was added and the mix was shaken at 37 ºC for 1 hr. Culture was plated

onto LB plates containing the relevant antibiotic and incubated at 37 ºC overnight. Single colonies were then picked and grown in LB broth containing the relevant antibiotic. 6 ml of colony culture was used per miniprep, 25 ml of colony culture was used per midiprep.

Plasmid DNA was isolated from cultures using QIAprep Spin Mini Kit (QIAGEN) for minipreps or QIAprep Midi Kit (QIAGEN) for midipreps per manufacturer protocol.

3.2.6.7 Restriction Enzyme Digestion

Restriction enzymes used were obtained from Thermo Fisher or New England Biolabs (NEB). Each microgram of DNA was digested using 10 units of enzyme in a 1x dilution of the specified buffer.

3.2.6.8 Gel Electrophoresis

0.8% agarose gels were made by adding 0.4g of agarose powder to 50 ml of 1x TAE buffer. 2 µL of dilute ethidium bromide was added for visualisation of gel bands. Samples were loaded in 1x loading dye alongside NEB 1 kb DNA ladder. Gel electrophoresis was performed at 140v until bands were resolved.

3.2.6.9 Gel Extraction and DNA Purification

Resolved gels were examined to identify bands containing the desired genetic material. Bands were excised and transferred to a 2 ml tube. A QIAquick Gel Extraction Kit (QIAGEN) was used to extract sample from agarose gel following manufacturer protocol.

3.2.6.10 DNA Ligation

DNA ligations were set up in a 1:1, 1:3 and 3:1 ratio of vector to insert. Ligation reactions were performed using 4 µL of 10x T4 DNA ligase buffer and 1 µL of T4 DNA ligase (NEB) made up to 20 µL with vector and insert DNA. Ligations were performed at room temperature for 10 minutes.

3.2.6.11 Multisite Gateway Cloning

Multisite gateway cloning was performed using three entry vectors and a destination vector (Kindly provided by Dr Rob Wilkinson). All vectors were diluted to 20 fmol and 1 µL of each vector added to a reaction mix. LR Clonase (ThermoFisher) was thawed for 5 minutes and vortexed, 2 µL of LR Clonase and 4 µL of dH2O was added to the reaction mix. The reaction mix was incubated at 25 ºC for 16 hours before the reaction was stopped by addition of 1 µL proteinase K and incubation at 37 ºC.

3.2.7 Genetic Manipulation

3.2.7.1 Morpholino Knockdown

Morpholino knockdown was performed by microinjection into zebrafish embryos at the single cell stage. Morpholinos used are listed in 3.1.3. This study used the published *wnk1a* morpholino (Lai et al, 2014), *gsk3b* morpholino (Lee et al, 2007), and *fzd5* morpholino (Cavodeassi et al, 2005).

3.2.7.2 CRISPR Interference

For CRISPR interference guide RNAs were acquired as single part sgRNAs from Sigma. In this approach tracrRNA and crRNA come as a single unit. dCas9 was expressed in the transgenic line ubi:dCas9-cryaa:CFP. CRISPR interference was performed by microinjection of gRNAs into transgenic embryos at the single cell stage. gRNAs were injected at 500pg per embryo.

3.2.8 Cell Labelling and Immunostaining

3.2.8.1 Whole Mount Immunostaining

Tg fli1:EGFP embryos were fixed in 4% paraformaldehyde (PFA) at 30 hpf to allow screening for proliferation in the main trunk vascular beds, then whole mount immunostaining was performed using anti-PCNA antibody (GeneTex, RRID: AB_11161916. Diluted 1:50) and AlexaFluor-568 mouse anti rabbit secondary antibody (ThermoFisher, RRID: AB_143165. Diluted 1:200). Colocalization of PCNA and fli1-EGFP was used to define proliferating ECs. Embryos not treated with PCNA antibody were imaged during protocol optimization to ensure the specificity of PCNA antibody. Detection of cell proliferation was defined as where a nucleus is both positive for PCNA and for fli1-EGFP.

3.2.8.2 EdU Labelling

The Click-iT™ EdU Cell Proliferation Kit (Thermo Fisher) was used to label DNA of proliferating cells with AlexaFluor-488. The protocol was modified for zebrafish as follows:

Zebrafish larvae with *Tg fli1a:nls-mCherry* were collected at 30 hpf and incubated in EdU solution (EdU 500 uM, 15% DMSO, 85% E3) at 28°C for 1 h. Larvae were fixed in 4% PFA overnight then washed and transferred to permeabilization solution (supplied in kit) for 1 h. Permeabilised larvae were then treated according to manufacturer protocol. Proliferating ECs were defined as cells positive for fli1a:nls-mCherry and EdU.

3.2.8.3 *En Face* Immunostaining

Mouse aortas were dissected from WT mice aged 12 weeks and fixed in 2% PFA for 30 minutes. The aorta was cleaned of adventitia then cut into sections. Blocking and permeabilization was done overnight by incubating sections in 20% goat serum in 0.5% triton-X100 at 4°C. The first arch was treated with Rabbit anti-Wnk1 antibody, and the second arch with Rabbit IgG, both samples were also treated with Rat anti-CD144 antibody. Following overnight incubation in primary antibody, samples were washed and treated with secondary antibodies Goat anti-Rabbit AF568 and Goat anti-Rat AF488. Following incubation, excess antibody was washed off and nuclei were visualised using TOPRO-3 iodide. n=3 animals were used.

3.2.8.4 Standard Immunohistochemistry

Human plaque slides were first dewaxed by Xylene/Ethanol treatment, then antigen retrieval was performed using boiling citrate buffer (0.01M) pH 6.0. Following this, permeabilization was done using 0.01% triton-X100 solution in PBS. Non-specific binding was blocked by treating the slides with 1% BSA in PBS for one hour. Slides were then treated

with primary antibodies for WNK1, rabbit IgG and vWF, then incubated at 4°C overnight. Residual primary antibody was washed away using PBS, and secondary antibodies were added for one hour before washing again and treating with DAPI.

3.2.9 Microscopy

3.2.9.1 Brightfield Microscopy

Standard light microscopy was used to screen out dead or undeveloped embryos, and to identify tnnt2a morphant embryos that lack a heartbeat. The morphant phenotype (no heartbeat) was observed in all (100%) of embryos injected with MO-*tnnt2a*.

3.2.9.2 Fluorescent Microscopy

Fluorescent microscopy was used to identify and select embryos containing *Tg fli1a:nls-mCherry* or *Tg fli1:EGFP* after they were non-terminally anaesthetised using E3 medium. Fluorescence screening was done using a ZEISS Axio Zoom V16 at 28 hpf. Zeiss filter set 63 (HE mRFP, cat no 489063-0000-000) was used. Camera mode was used and pixel binning set to 5×5 to maximise sensitivity to the fluorophore. Screened embryos were washed in E3 media without tricaine, then transferred into fresh E3 prior to further imaging.

3.2.9.3 Confocal Microscopy

Zebrafish - For confocal imaging, embryos were non-terminally anaesthetised using tricaine and mounted in 1–2% agarose over which standard E3 medium was placed. Still images were taken using a Nikon A1 confocal microscope at 1024×1024 resolution (0.62 µm per pixel), z-stacks were taken in 8-µm increments. Time lapses were taken using a Zeiss LSM880 in Airyscan mode. Images were captured at 1848×1848 resolution (0.47 µm per pixel), z-stacks were taken in 3.43-µm increments. Images were analysed using NIS Elements or ZEN respectively. Composite images were generated by performing maximum intensity projection of the stack data, no other processing was performed. For both microscopes, excitation was done by a 488 nm and 568 nm laser.

Mouse – For each animal, the IgG control sample was imaged first to calibrate the Nikon A1 confocal. 568 laser power was reduced until signal was barely visible. The first arch was then imaged, regions of high and low shear stress were identified by looking for expression of endothelial marker (CD144 – AF488), regions of high shear show high EC alignment whereas regions of low shear show low EC alignment. Three distinct regions of low and high shear were imaged for each animal. Wnk1 expression was quantified as an average of the three regions for high and low shear stress.

Human – For each sample, the IgG control was used to calibrate the Lecia Thunder Imager. 568 laser power was reduced until WNK1 signal was barely visible. The whole slide was then imaged. Regions of endothelium were identified by using an endothelial marker (vWF – AF488). WNK1 expression was quantified in the endothelium of each sample.

3.2.9.4 Light Sheet Microscopy

For light sheet microscopy8, 10, non-terminally anaesthetised embryos were immobilised using 1% agarose and mounted in a glass capillary. Embryos were suspended in melted agarose (37°C, 0.8–1.2% w/v) then drawn up into a glass capillary using a plunger. Agarose suspended embryos were then pushed through the capillary and suspended into the imaging chamber containing E3 and tricaine. Images were captured at 1920×1920 resolution (0.23 µm per pixel), z-stacks were taken in 1-µm increments. Images were captured every 15 minutes for 4 h using ZEISS Z1 light sheet microscope and processed using ZEN software. Post-acquisition, maximum intensity projection was used to produce a single image for each time point. EC proliferation was defined as where fli1a:nls-mCherry nuclei visibly divide over the course of the time lapse. Experimental embryos were then euthanised using bleach.

3.2.10 Quantification and Statistical Analysis

3.2.10.1 Quantification of Endothelial Cell Proliferation

Endothelial cell proliferation was quantified from 58 hpf to 72 hpf. Proliferation events were defined as where the fluorescently labelled nucleus divides. Seven intersegmental vessels (ISVs) were monitored over the entire time lapse. The number of endothelial cell proliferation events in each embryo was expressed as a fraction of the total number of endothelial nuclei in the seven monitored ISVs at the start of the time lapse.

3.2.10.3 Quantification of ISV Blood Flow

To quantify blood flow in the ISVs, a ZEISS Axiozoom V16 was used to image *Tg (gata4:dsRed)* expression in live zebrafish embryos at 72 hpf. Images were captured at 240 fps. For analysis, images were converted to binary using ImageJ threshold tool, then TrackMate (Tinevez et al., 2017) was used to measure the velocity of the erythrocyte signal. Erythrocyte velocity was taken for five embryos per morphant, then compared by two-way ANOVA.

3.2.10.2 Statistical Analysis

Statistical analysis is described in each figure legend. For the screening study, a minimum of n=8 embryos were used per group, group sizes differ due to deaths or embryo movement during imaging. Analysis was done using GraphPad PRISM (RRID:SCR_002798), an open-source alternative to this is JASP (RRID:SCR_015823).

4.0 Optimising a Method to Quantify Endothelial Cell Proliferation in Zebrafish Embryos

Excessive EC proliferation is a core component of EC dysfunction, and a key factor in flow dependent susceptibility to disease. This group previously studied apoptosis, another component of EC dysfunction in zebrafish (Serbanovic-Canic et al., 2017) and others have studied the effect of flow on gene expression in zebrafish endothelial cells (Watson et al., 2013) but no study of flow responsive EC proliferation has been reported in zebrafish. Development of an approach for this would bring a host of practical benefits such as reduced experimental time and cost, as well as partial replacement of the use of mice with non-regulated zebrafish embryos, thus reducing use of animals in atherosclerosis research.

In this chapter I present a series of studies to assess whether using zebrafish embryos as a model of EC proliferation in response to flow is viable. This was published in Bowley et al, (2021). I hypothesised that loss of blood flow would result in changes in EC proliferation compared to control embryos and I tested the following four methods for assessing EC proliferation in the developing zebrafish embryos:

1) Whole-mount immunostaining using PCNA antibody
2) Proliferating cells labelling using 5-Ethynyl-2´-deoxyuridine (EdU)
3) Imaging transgenic lines with cell cycle reporter genes
4) Time-lapse imaging of transgenic lines with reporter genes for EC nuclei

4.1 Whole Mount Immunostaining for PCNA

Initial experiments used whole mount immunostaining for proliferating cell nuclear antigen (PCNA) as a method for quantifying EC proliferation. Use of this in zebrafish tissue sections had been published previously (Leung et al., 2005) but whole mount immunostaining was preferable in this case because of the need to analyse whole vessels and different vascular beds. Embryos *of Tg fli1a-EGFP* were studied at 30 hpf and 48 hpf to see if detection of proliferation changed as the embryo develops (Fig. 10).

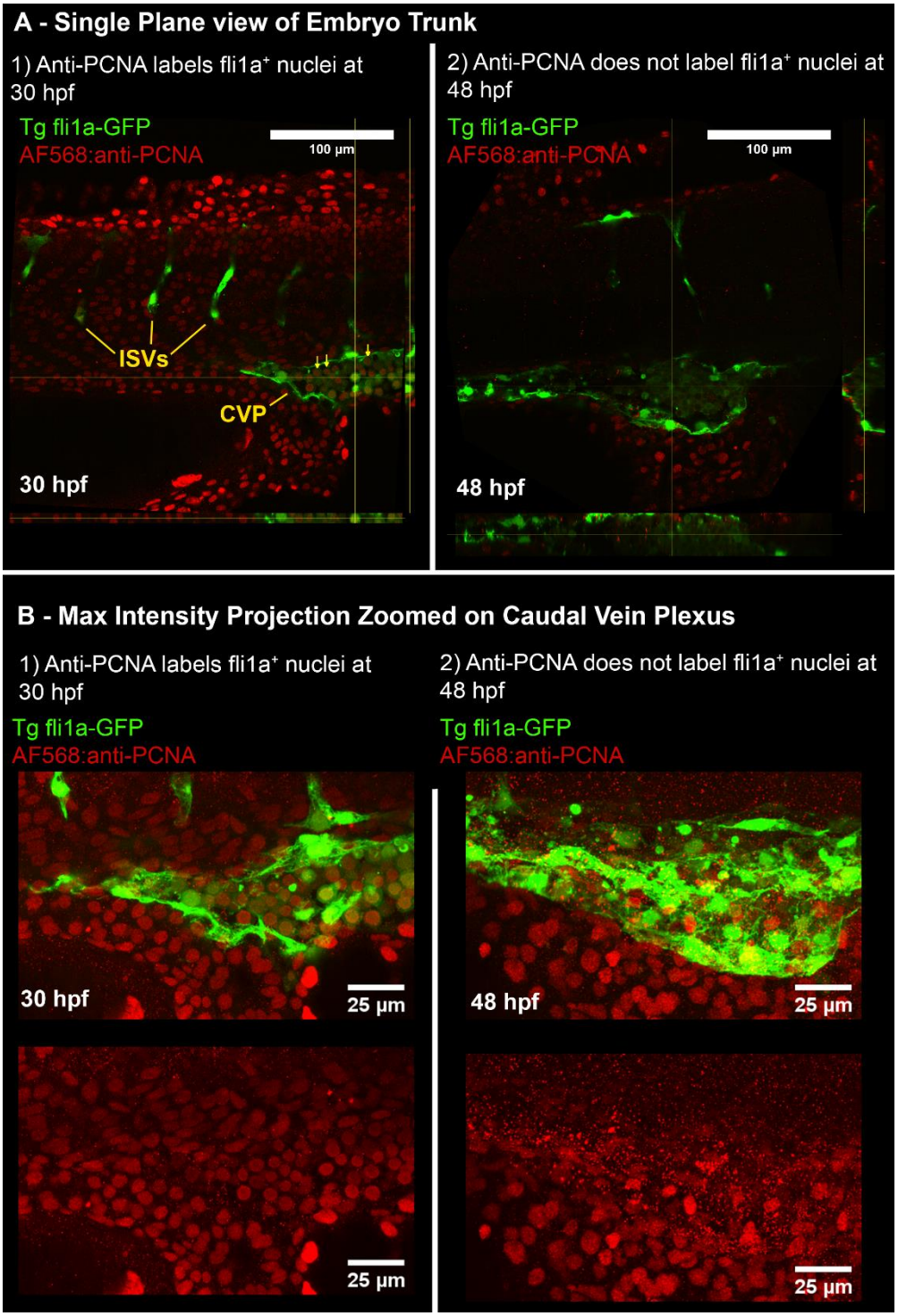

Figure 10: Whole mount immunostaining of zebrafish larvae for PCNA. A - Confocal imaging was used to generate a z-stack of *fli1a-GFP* and PCNA expression in the trunk. Embryos were imaged from the side, anterior left, dorsal up. Orthogonal views are presented alongside the image. The caudal vein plexus (CVP) and intersegmental vessels (ISVs) were imaged to determine whether endothelial cell proliferation was detected in these vascular beds. At 30 hpf anti-PCNA was colocalised with *fli1a* positive cells (labelled with yellow arrows). At 48 hpf, anti-PCNA was not colocalised with *fli1a* positive cells. B – Max intensity projection reveals PCNA immunostaining labels nuclei within the caudal vein plexus (CVP) at 30 hpf, but not at 48 hpf.

Analysis of the caudal vein plexus (CVP) at 30 hpf showed colocalization of many PCNA positive and fli1a positive cells, however no colocalization was observed at later time points. This suggested detection of proliferation was limited to the earlier time point. It was suspected that either the growth of the developing embryo restricted antibody penetration after 30 hpf, leading to no detection of proliferation after this point, or PCNA detected a population of EC progenitors in the CVP that are not present at 48 hpf. Literature supported the former theory (Leung et al., 2005), hence to avoid spending time optimizing antibody penetration, a molecular labelling approach was sought.

4.2 EdU Labelling of Proliferating Cells

EdU is a soluble molecule which can be added to zebrafish embryo media (E3) in combination with a permeabilising agent (DMSO) to allow it to diffuse into embryonic cells. When intracellular, during cell proliferation EdU is incorporated into newly synthesised DNA. After fixation EdU is labelled with a fluorescent azide to allow visualisation of cells which have undergone proliferation. The rationale for use of EdU was that this molecular method would detect proliferation over a window of time, rather than at the point the embryo was fixed as was the case for the previous approach. This was predicted to allow capture of a larger number of proliferation events, and avoid problems with deep tissue penetration seen when immunostaining for PCNA.

Previously EdU labelling for up to 4 hours was demonstrated in zebrafish embryos (Kugler et al., 2021), therefore this method was used to attempt to quantify EC proliferation (Fig. 11).

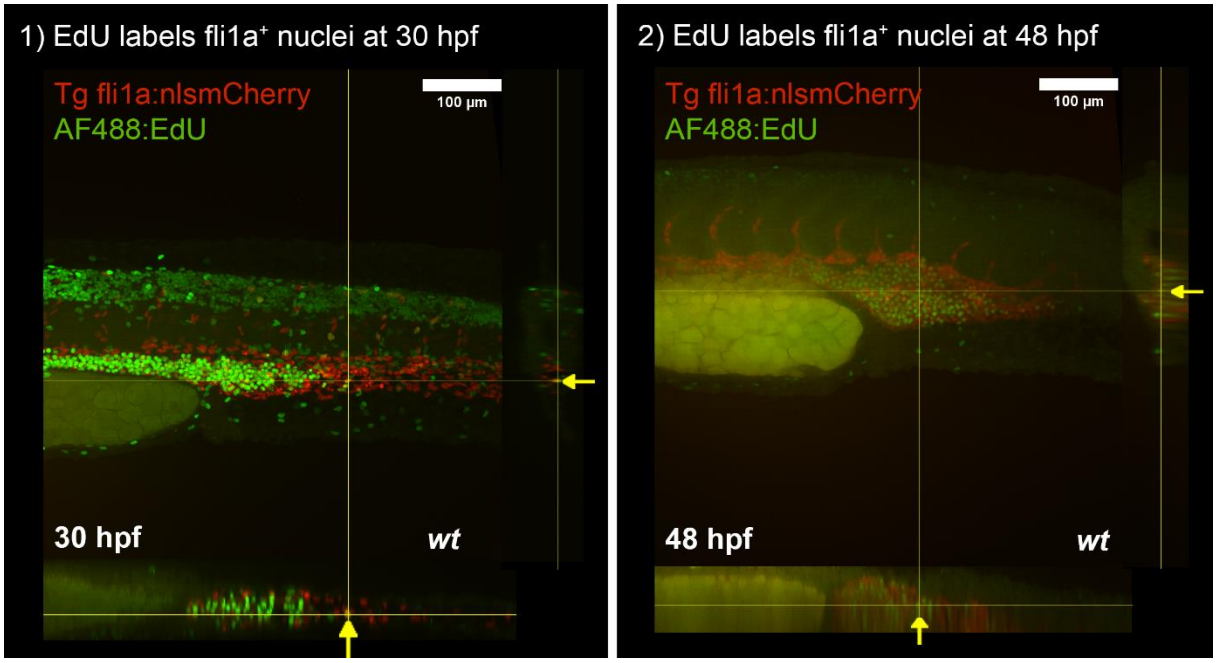

Figure 11: EdU labelling of zebrafish larvae. Proliferating ECs of *Tg fli1a:nls-mCherry* embryos were labelled using EdU and visualised using EdU-binding fluorescent azide. Embryos were imaged from the side, anterior left, dorsal up. Examples of proliferating endothelial nuclei are marked with the orthogonal viewer (yellow cross). Proliferating nuclei can be seen at the points indicated (yellow arrows) Orthogonal views are presented for the X and Y axes.

EdU labelled endothelial cells in the deep tissues as confirmed by analysis of the images at 30 hpf and 48 hpf, which represented an improvement over immunostaining. EdU also appeared to capture a greater number of putative proliferating endothelial cells Thus, confirming my suspicion that the limited window for detection of EC proliferation via immunostaining had limited detection using the previous approach. Whilst these data confirmed that EdU labelling can detect endothelial cell proliferation, as shown, quantification of these data was complicated by the high number of proliferating non-EC in the region. Manual examination of individual z-slices did not identify more than one or two proliferating EC nuclei per embryo which is a small fraction of all those labelled EdU-positive. Since the objective was to develop a method to statistically compare EC proliferation under different treatment conditions, and screen genes for involvement in proliferation under flow and no-flow conditions, this approach was too laborious for large screening experiments since it did not detect enough proliferating EC nuclei to allow a robust statistical comparison between groups. To increase the numbers of EdU-positive EC detected I increased the EdU incubation period to detect proliferation over a longer timeframe, but this approach was unsuitable as application of DMSO, the essential cell permeabilizer, for longer periods resulted in cardiac arrest and death (not shown).

Therefore, to meet the objectives, a change in approach was required.

4.3 Generation of Transgenic Zebrafish Containing an Endothelially Expressed Cell Cycle Indicator

Zebrafish FUCCI (Fluorescence ubiquitin cell cycle indicator) was investigated as a method to allow visualisation and quantification of endothelial cell proliferation. FUCCI ubiquitously expresses two fusion proteins which are then differentially degraded during the cell cycle to visualise cycle phase at the cellular level. *Geminin:mCerulean* is degraded during G1 and *Cdt1:mCherry* is degraded during mitosis (M), this leads to Cerulean expression during S, G2 and M, and mCherry expression during G1 (Bouldin & Kimelman, 2014). (Fig. 12).

This was desirable as it would allow proliferation to be quantified in live embryos using fluorescence microscopy without any further treatments as was required for previous approaches. However, to quantify EC proliferation using FUCCI an endothelial marker must also be present therefore I attempted to re-engineer FUCCI to express the cell cycle markers under the endothelial promoter (*fli1a*) rather than the ubiquitous promoter, the new transgenic was named fli1a cell cycle indicator (FLICCI).

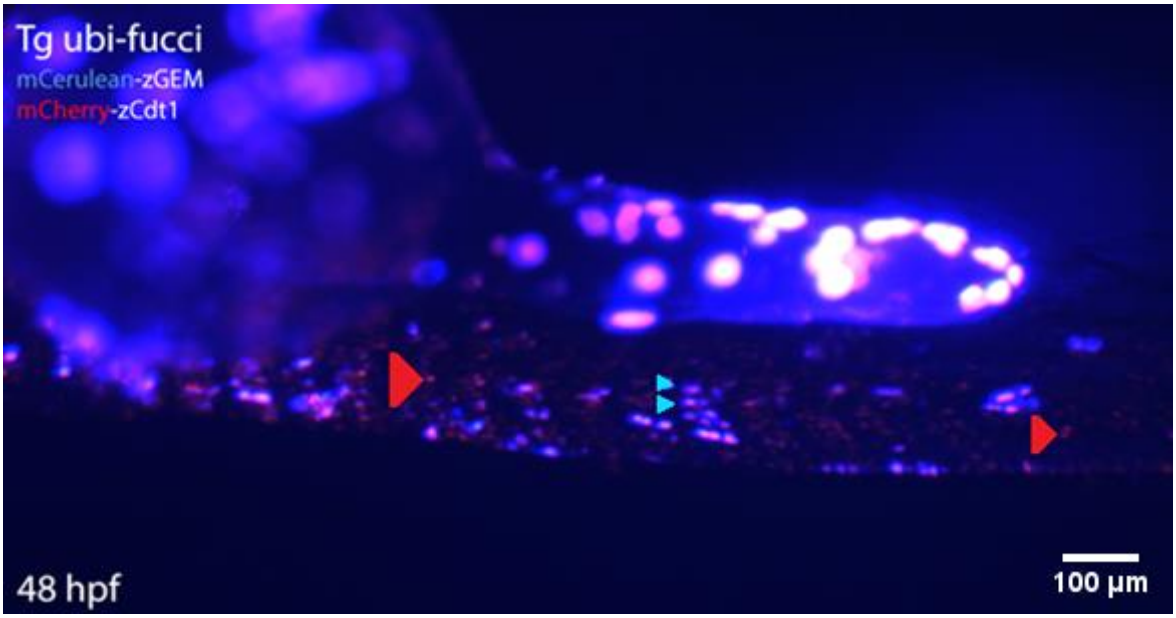

Figure 12: FUCCI expression in the zebrafish embryo. Representative image of transgenic zebrafish embryo expressing ubi-fucci. Embryo was imaged from the side, anterior left, ventral up. Examples of cells in G0 are marked with red arrowheads. Examples of cells in mitosis are marked with blue arrowheads. Double positive cells are undergoing G to S transition.

To produce a FLICCI transgene, the zebrafish endothelial promoter (*fli1a*) was positioned upstream of the cell cycle indicator components thus enabling endothelial specific production of each of these proteins. To develop this transgene, I used a modified version of the Thermo-Fisher Multisite Gateway protocol. This protocol clones three entry vectors containing the 5’ promoter, middle and 3’ tail elements into a destination vector containing the system for transgenesis (Fig. 13).

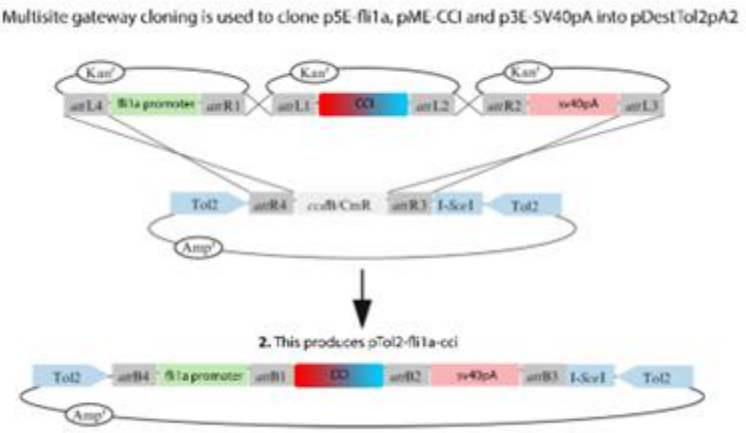

Figure 13: Multisite gateway cloning protocol. Diagram of planned multisite gateway procedure showing 5' entry *fli1a* promoter, middle entry CCI, and 3' entry sv40 polyA tail plasmids being cloned into the pDestTol2P2A vector to produce pTol2-fli1a-CCI.

As the endothelial fli1a promoter, poly-A tail, and zebrafish Tol2 destination vectors were already in hand, production of FLICCI required creation of a novel middle entry vector containing the cell cycle indicator (pME-CCI). I successfully produced pME-CCI by directionally cloning part of the donated FUCCI plasmid into an existing pME-MCS2 vector using a protocol previously used in the lab. Synthesis of pME-CCI was validated by digesting putative clones with BsaB1, which cuts within the CCI cassette, but not within the MCS2 plasmid, this confirmed successful cloning of pME-CCI (Figure 14).

pME-CCI Synthesis

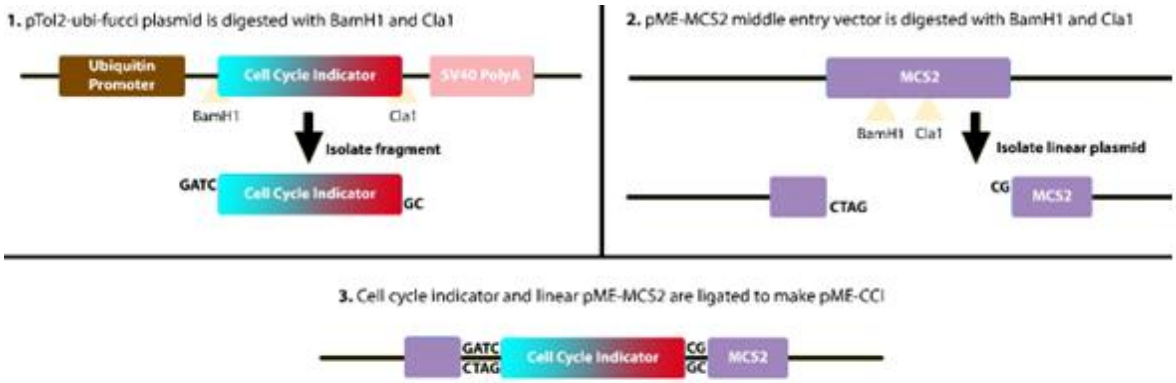

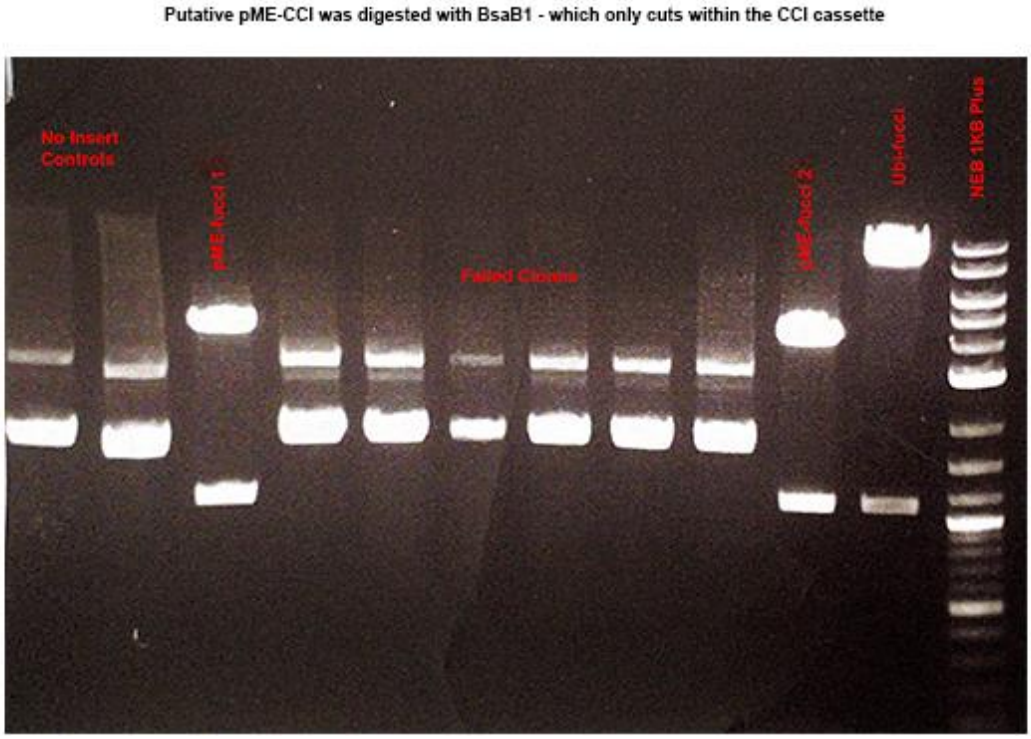

Figure 14: Directional cloning protocol for generation of pME-CCI. Diagram illustrating generation of pME-CCI plasmid by directional cloning. (1) Donor cassette is taken from purified digestion product of pTol2-ubi-fucci. (2) pME-MCS2 is linearized with identical restriction enzymes to produce a complementary ligation site. (3) T4 ligation is performed to produce pME-CCI plasmid.

After validating production of pME-CCI by restriction digests, multisite gateway cloning was used to produce the desired FLICCI construct. This produced multiple colonies from which putative FLICCI was isolated. Analysis of these plasmids by restriction digests was attempted, the restriction enzymes Hpa1, Sbf1 and Pml1 were used to target each insert. Hpa1 was predicted to cut twice within the promoter (fli1a), Sbf1 and Pml1 were expected to cut once within the CCI and polyA tail respectively. Despite troubleshooting, restriction digests were not consistent with the predicted band pattern (Fig. 15).

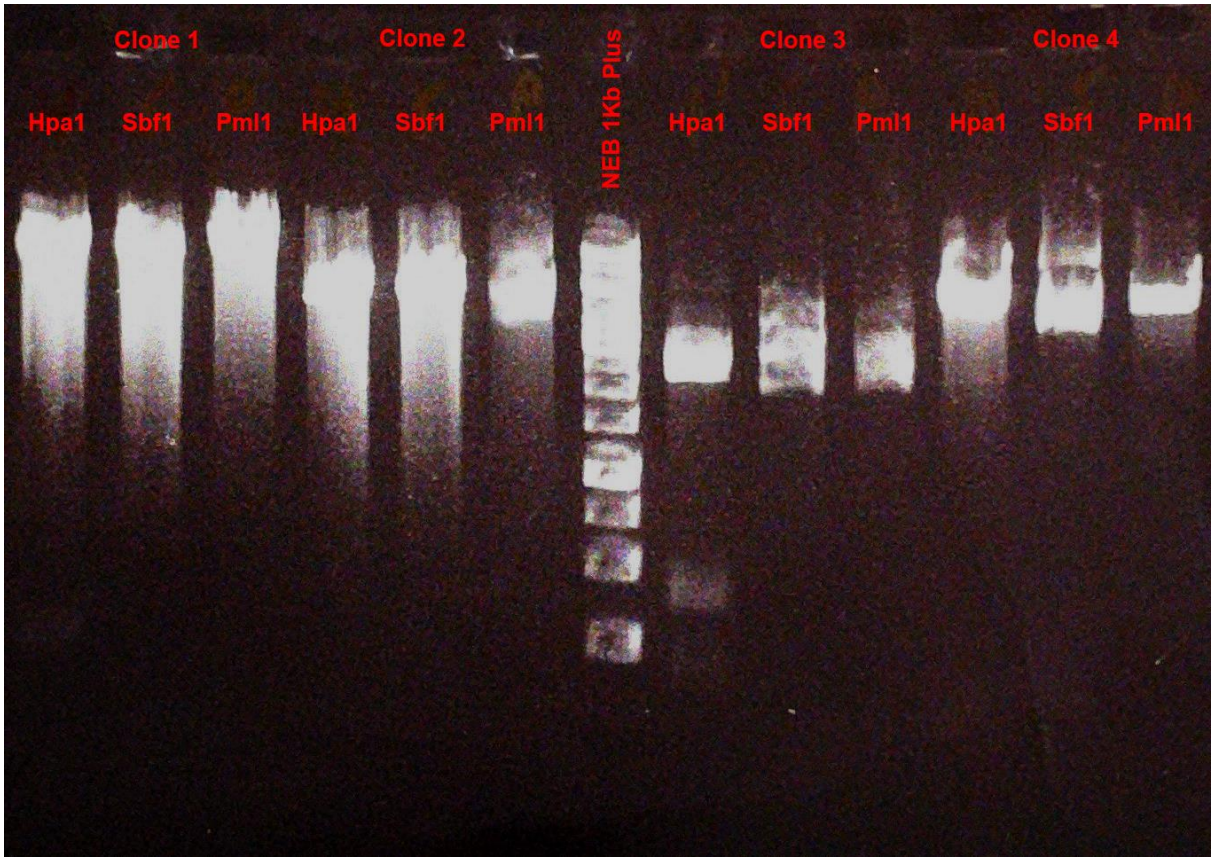

Figure 15: Restriction digests of putative FLICCI showed abnormal cloning had occurred using the multisite gateway protocol. Four putative FLICCI clones were isolated and digested using Hpa1, Sbf1, and Pml1. Hpa1 was expected to produce three bands, whilst Sbf1 and Pml1 were expected to produce one band. No clones showed expected banding patterns, and clones three and four showed banding consistent with concatenation, or multiple insertion of the promoter and CCI vectors.

Sanger sequencing was used to attempt to confirm the sequence of putative FLICCI, but results suggested that abnormal cloning had occurred. Finally attempts to validate putative FLICCI plasmids *in vivo* by observing embryos injected with putative FLICCI did not result in FLICCI expression. Therefore, it was concluded that cloning had failed (see discussion for possible reasons), troubleshooting did not resolve these problems therefore a simpler transgenic system was sought.

4.4 Time-lapse Imaging of Endothelial Nuclei in the Intersegmental Vessels

Previous data (Fig. 11) suggested that EC proliferation occurs at a low rate in the developing vasculature, therefore a method for observation of endothelial cells over a longer timeframe was desired to increase the number of events observed.

To do this, two transgenic lines were used. One contained endothelial nuclear mCherry (*Tg fli1a:nls-mCherry*), another contained endothelially expressed f-Actin:GFP (*Tg fli1a:LifeAct-mClover*). These lines were crossed, and their progeny screened to obtain embryos with both transgenes. These embryos were then studied by light sheet microscopy to identify EC proliferation in the ISVs (Fig. 15).

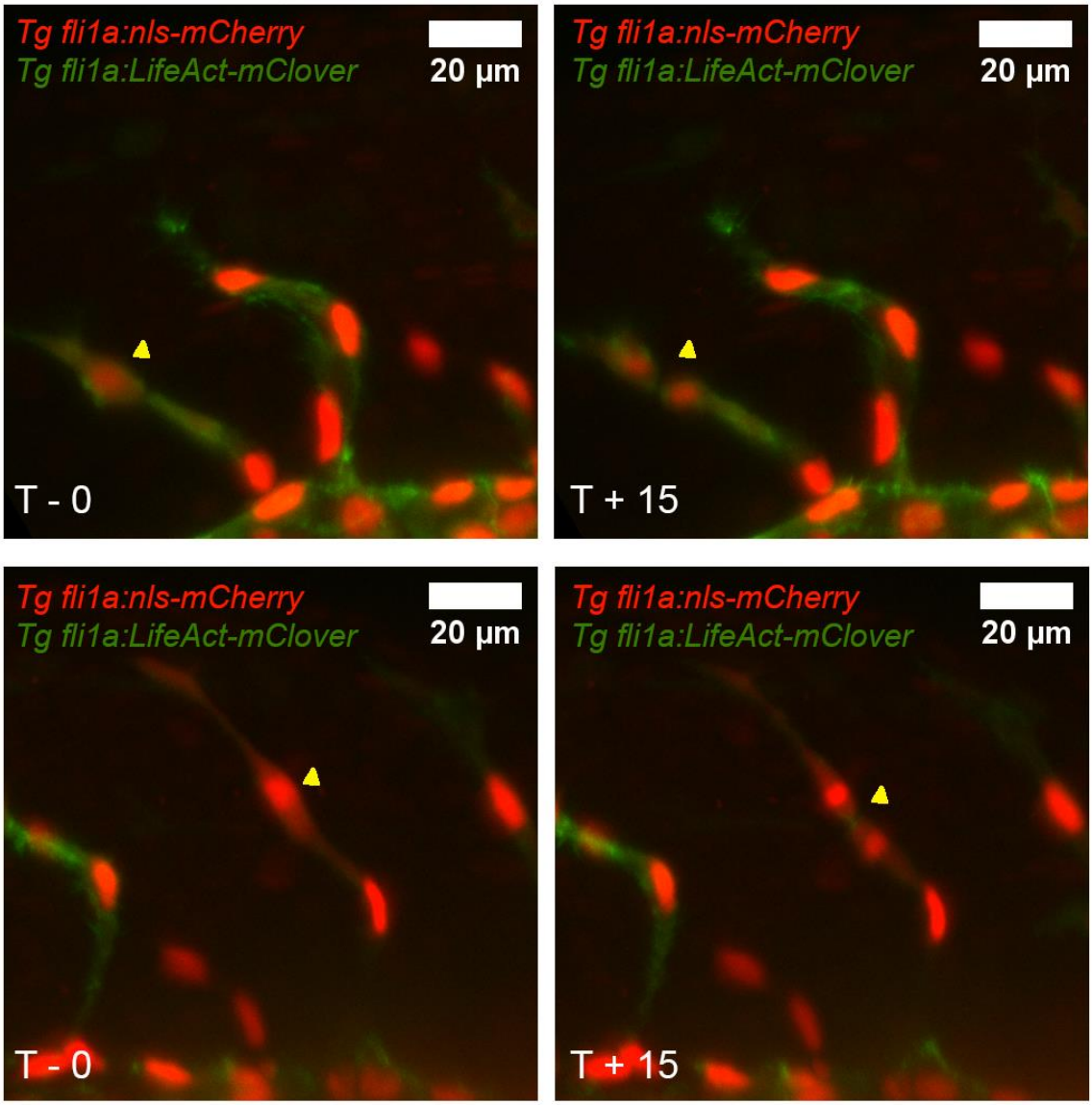

Figure 16: Endothelial cell proliferation can be directly observed in the intersegmental vessels. The trunk was studied from 26 to 30 hpf in 15-minute intervals using a light sheet microscope. Endothelial nuclei were labelled using the transgenic marker *Tg fli1a:nls-mCherry* (red) whilst endothelial F-actin was labelled using *Tg fli1a:lifeAct-mClover* (green). EC proliferation was defined as where one nucleus visibly divides into two (yellow arrows).

EC proliferation was visible in the intersegmental vessels (ISVs) and accurate quantification was feasible over an extended period. The dorsal aorta (DA) and posterior cardinal vein (PCV) were not quantified as the three-dimensional density and overlapping nature of EC nuclei in these regions makes manual analysis of proliferation extremely difficult. In the ISVs, EC nuclei are trivial to count and track, and proliferation occurs along the vessel axis which means that proliferation along the imaging axis (z) cannot be missed, this would be an issue in other vascular beds.

Having identified that time-lapse imaging was suitable for quantification of EC-proliferation in the ISVs, I next sought to determine how EC proliferation was affected by flow. To study this, the Zeiss LSM880 Confocal was used to simultaneously screen groups of WT, tricaine treated, and *tnnt2a* morphant embryos to compare EC proliferation under flow and no-flow conditions, images resolved EC nuclei at quality comparable with light-sheet (Fig. 17B), but allowed many more embryos to be studied simultaneously (n=15), improving the utility of this approach.

Four WT, five *tnnt2a-MO,* and six high dose tricaine (MS222) treated embryos were imaged from 54 hpf to 70 hpf and quantification of endothelial cell proliferation was performed by selecting seven ISVs and counting the total number of nuclei, then calculating the fraction of proliferating nuclei over the time-lapse (Fig. 16-17). Flow and no-flow embryos were treated with a standard immobilising dose of tricaine routinely used in zebrafish imaging (0.4%). It was observed that endothelial cell proliferation was significantly reduced in no-flow conditions both as a result of tricaine treatment (blood flow abolished immediately prior to time-lapse imaging), and as a result of *tnnt2a* knockdown (blood flow never initiated). A concomitant reduction in the number of EC nuclei in no-flow embryos was also observed (Fig. 18).

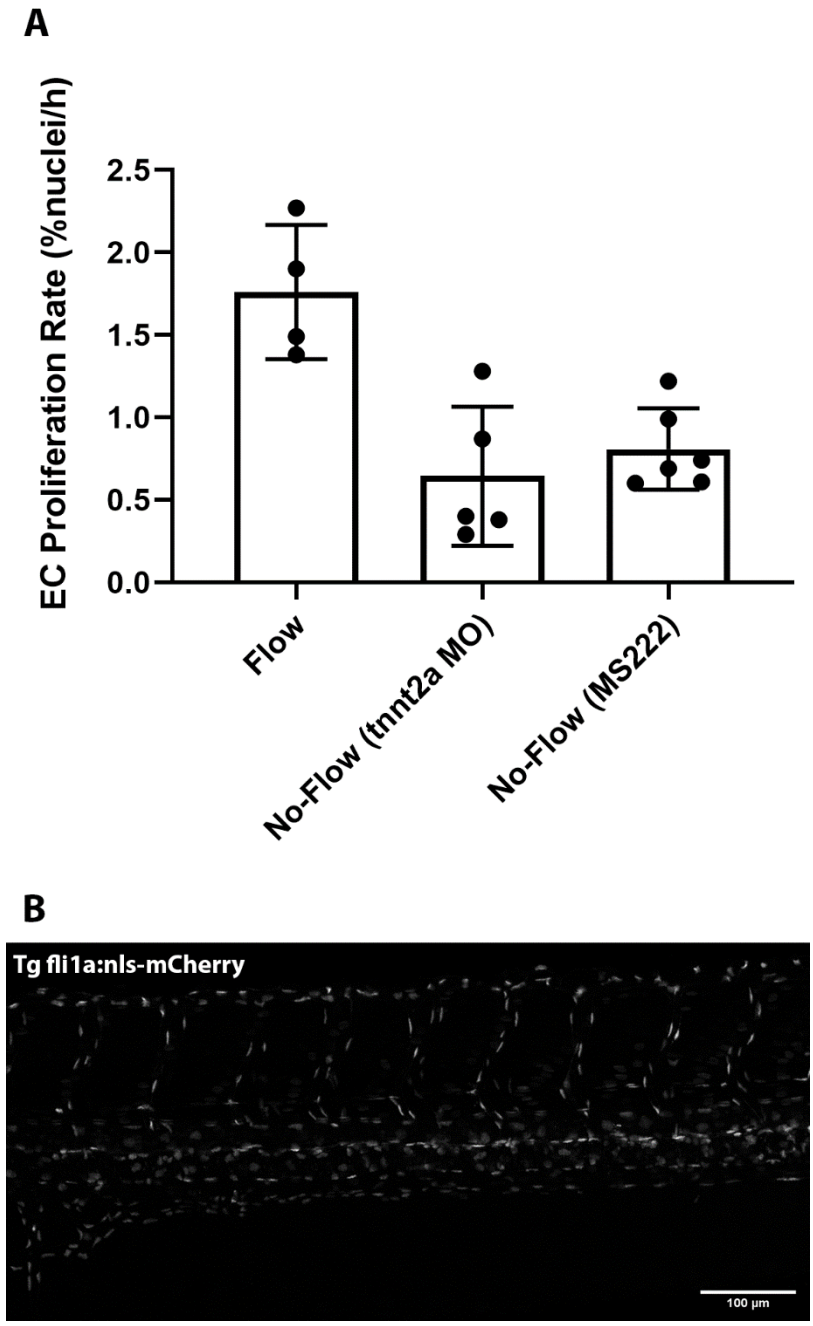

Figure 17: Endothelial cell proliferation is reduced in high dose MS222 treated and *tnnt2a MO* treated embryos. A - The intersegmental vessels of four wildtype, five *tnnt2a* morphant, and six tricaine (MS222) treated embryos were imaged from 54 to 70 hpf. The rate of endothelial cell proliferation in the ISV's was quantified as a percentage of nuclei dividing per hour. B – representative image of fli1a:nls-mCherry expression in a zebrafish embryo at 54 hpf.

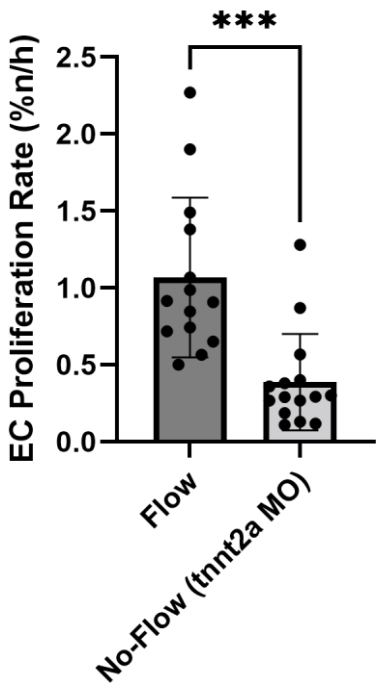

Figure 18: Endothelial cell proliferation is significantly reduced in embryos without blood flow. The intersegmental vessels of four wildtype, five *tnnt2a* morphant, and six tricaine (MS222) treated embryos were imaged from 54 to 70 hpf. The rate of endothelial cell proliferation in the ISV's was quantified as a percentage of nuclei dividing per hour. Comparisons were done using an unpaired t-test, *** denotes significant results ($p<0.001$).

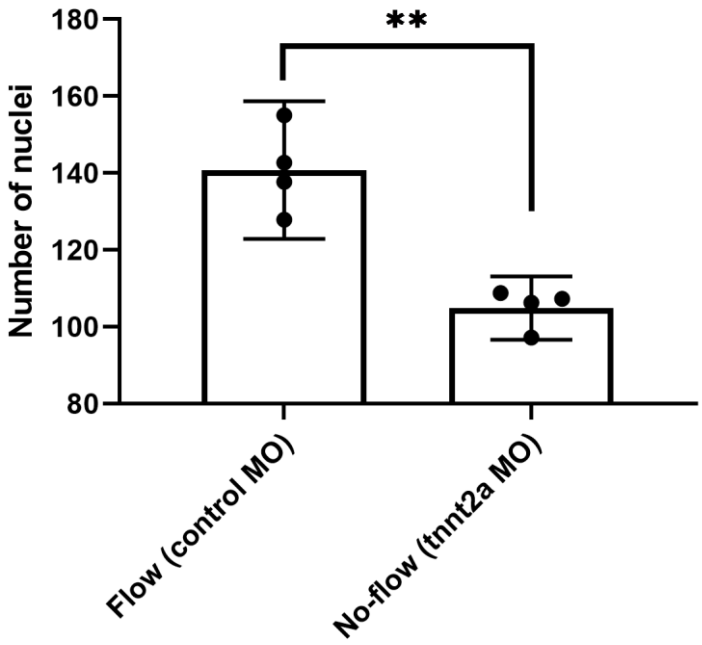

Figure 19: Endothelial nuclei number were significantly reduced in embryos without blood flow. The intersegmental vessels of four wildtype, and five *tnnt2a* morphant embryos were imaged at 70 hpf and the number of EC nuclei quantified. Comparison was done using an unpaired t-test, ** denotes significant results ($p<0.01$).

4.5 Discussion

These data show that it was possible to quantify endothelial cell proliferation in zebrafish by using time-lapse confocal imaging of nuclei localised fluorescent proteins expressed under the *fli1a* promoter.

Using this approach, it was demonstrated that endothelial cell proliferation was flow responsive in the zebrafish embryo and indicated that proliferation in the ISVs was positively regulated by flow.

4.5.1 Why Cloning of FLICCI Was Not Successful

To briefly address the unsuccessful cloning approach, failure to produce a functional FLICCI plasmid was likely the result of duplication of the promoter and/or CCI elements during the cloning process. Troubleshooting included experimenting with different LR reaction entry clones concentrations and replacing the LR clonase enzyme. Further troubleshooting of this approach was not considered due to time and cost constraints, and since time lapse nuclear imaging had since been proven as a straightforward and effective method for quantifying EC proliferation, FLICCI was ultimately dropped (Bowley et al., 2021).

For future studies, FLICCI offers significant advantages for study of complex vascular beds such as the DA, PCV and cerebral vessels as it would allow the researcher to monitor the cell cycle over time, rather than scan the time-lapse for nuclear division. This would greatly enhance the depth of information one can access by timelapse imaging EC nuclei for proliferation.

Another confounding factor in cloning that may have contributed to failure was detection of mutations in the *attl4* site in the p5E-fli1a vector used to produce FLICCI. Mutations here could have caused abnormal integration of *fli1a* into the destination vector, and non-functional product. Sequencing the p5E vector at the time could have led to earlier detection of this problem but this was not pursued as successful use of p5E-*fli1a* by other groups at the University of Sheffield led to the assumption that the vector was functional.

4.5.2 Endothelial Cell Proliferation is Reduced Under Static Blood Flow in the Intersegmental Vessels

Comparing EC proliferation in flow (WT) and no-flow (*tnnt2a-MO*/tricaine treated) embryos revealed that the rate of EC proliferation and the number of EC nuclei was significantly reduced in the absence of flow. These observations are supported by previous studies in zebrafish (Kugler et al., 2021; Watson et al., 2013) as well as *in vitro* studies which found EC proliferation was increased under sustained high shear stress (DeStefano et al., 2017; Schwartz et al., 1999). The main considerations for interpreting these results are the influences of different types of shear stress on EC's, how these stresses are represented in the zebrafish embryo, and differences inherent to *in vivo* and *in vitro* approaches.

The ISV vascular bed was chosen because it allowed accurate imaging and quantitation of EC proliferation using transgenic zebrafish. Unlike the cerebral vasculature or the DA and PCV, ISVs are unobstructed by nearby vessels; hence for side mounted embryos ISV nuclei are

clearly visible, as they are the only EC nuclei between the DA and DLAV. This meant that ISV nuclei could be identified accurately using a single transgene, which reduced breeding complexity and increased imaging speed relative to more complex regions. Analysis of the ISV was carried out by side mounting of embryos which was simpler than using other orientations and enabled rapid mounting of multiple embryos and study of multiple groups at a time. The method could be applied to quantify EC proliferation in other vascular beds; however, the ISVs represent the optimal choice in terms of the simplicity of the anatomy.

The decision to image embryos older than 54 hpf was made because blood flow is not always present in the ISVs prior to this point, and it was essential to compare EC proliferation under flow and no-flow conditions. Other vascular beds such as the DA and PCV are exposed to blood flow from ~26 hpf meaning similar experiments in these vessels could be completed faster, however similar study of these vessels is complicated by a vast increase in the density of EC nuclei which would make manual counting extremely difficult. If quantification of nuclear division could be automated, similar studies of these regions would be useful to see whether EC proliferation and the response to flow are between different vascular beds.

4.5.3 Advantages of Time-Lapse Nuclear Imaging Compared to Other Methods for Study of Endothelial Cell Proliferation

Endothelial cell proliferation has been studied using a wide range of approaches. Understanding how these data fit in with other publications requires careful consideration of the impact of different methods and models used in each approach.

The first hurdle to contextualising these data is being able to compare proliferation rates between publications. Whilst some publications report proliferation as a rate it is common, especially in studies which use immunostaining or cell labelling, to see proliferation reported as a count. In these cases, it is difficult or impossible to determine the rate of proliferation which complicates comparison of results.

Both *in vitro* and mouse studies report that endothelial cells remain mostly quiescent under normal conditions (Ezaki et al., 2001; Poduri et al., 2017). Given that the basal rate of EC proliferation is low, it was not surprising that my studies of embryos imaged using EdU detected few events in 400 to 500 endothelial nuclei over a one-hour incubation time. Thus, the inefficacy of EdU labelling was a consequence of proliferation events simply being too rare to be seen in high numbers. Switching to time-lapse imaging of transgenic zebrafish with fluorescent EC nuclei greatly improved detection of EC proliferation, in part because vascular beds could be analysed over extended periods and demonstrated the importance of choosing the correct approach.

By looking for division of labelled nuclei one could argue this approach might mistake emergence of multinucleate ECs for EC proliferation. Whilst multinucleate ECs are a well described marker of atherosclerosis for which *in vitro* models exist (Tokunaga et al., 1998; Wu et al., 1999), classical models rely on treatment of cultured cells with LDL, and modern models (pre-print data) rely on treatment with insulin. Hence it is unlikely that conditions for multinucleate EC formation are met naturally during embryo development, however if

target gene knock down led to multinucleate EC production, the apparent increase in proliferation (compared to controls) would be cause to classify said gene as a 'hit' and result in serendipitous further study of the gene. Emergence of multinucleated ECs could be excluded by incorporating an additional transgenic which visualised cell membranes to allow differentiation of cell division from multinucleation.

The approach described in this study, and similar approaches *in vitro* allow calculation of the proliferation rate at high temporal resolution. Data storage limitations aside, light sheet and Airyscan microscopes can achieve time-lapse imaging with an imaging interval measured in minutes, whereas cell labelling, antibody and tritiated thymidine-based approaches must label proliferation for upwards of twelve hours to detect a significant number of events. These approaches can thus only determine the overall rate of proliferation, whereas the novel approach described can report the proliferation rate continuously. Thus, our described method for measuring EC proliferation allows continuous measurement and is thus capable of detecting transient changes in proliferation rate.

Transient changes in proliferation are well described in endothelial cells subjected to changes in shear stress. Indeed, oscillatory shear, where the endothelial cell is constantly subjected to shear from both directions, leads to a greater rate of proliferation than steady state static conditions (Chakraborty et al., 2012). Similarly, endothelial cells cultured to confluence in static conditions exhibit significantly increased proliferation for a period of hours after initiation of unidirectional flow, which then returns to a basal level over a period of days (DeStefano et al., 2017). These observations support the idea that methods for study of endothelial cell responses to flow must be capable of imaging at high temporal resolution to capture these changes, or potentially significant flow responsive behaviour may be missed.

4.5.4 Advantages of Zebrafish Compared to Other Models for Study of Endothelial Cell Proliferation

A wide range of models are used to study the role of shear on EC proliferation, differences between these models can complicate comparison of results. Differences emerge because of variation in blood/fluid flow, shear stress, genetics, and tissue complexity within each model (Table 1).

Table 1: Summary table comparing models of EC responses to flow.

	Mice	Zebrafish Embryo	HUVECS
Imaging subject	Tissue sections	Whole embryo Specific regions	Cells
Live imaging	Yes	Yes	Yes
Methods for viewing proliferation	Transgenic markers Immunohistochemistry Cell labelling Intravital microscopy	Transgenic markers Immunohistochemistry Cell labelling	Transgenic markers Immunohistochemistry Cell labelling
Biological relevance	High	High	Lower
Relative cost	High	Moderate	Low
ASPA protected	Yes	No	No
Models EC response to disturbed flow	Yes	To be confirmed	Yes

Blood flow generates a range of spatiotemporal forces which are defined in shear stress research as steady unidirectional flow, steady static flow, directional oscillatory flow, and disturbed flow, each of which apply different forces to the vasculature. Thus, the degree to which these forces are modelled and the capacity of the model system to respond influences the observed endothelial response.

Current *in vitro* models use a combination of parallel plate, orbital shaker or microfluidic systems to expose endothelial cells to flow (Buchanan et al., 2014; Mahmoud et al., 2014). These models have been used to generate useful data on gene expression and cell behaviour under well-defined shear conditions but lack the capacity to replicate three dimensional forces (stretch, torsion) present *in vivo*. Biological relevance is similarly limited by the homogenous cell populations used in *in vitro* studies, which whilst constantly improving do not fully replicate the relationship between cells and the ECM, cells and other tissues, or cells and the immune system (Mannino et al., 2015). Functional studies seeking to identify genes involved in endothelial responses to shear are better suited to *in vivo* models where the effect of shear in a whole system can be investigated in a physiological context.

These experimental design considerations lead to something of a dilemma. Researchers can choose to design a study with high fidelity live imaging and fine control of shear stress, at the cost of being limited to reductionist models that do not necessarily represent the endothelial response *in vivo*. Or they can adopt a wholistic model such as the mouse and generate more biologically relevant data with scope for live imaging via intravital microscopy (Vaghela et al., 2021), however this approach loses precise control of shear stress conditions relative to *in vitro* models, and introduce animal welfare considerations to the research, particularly if invasive imaging approaches are used (Camacho et al., 2016).

Use of the described zebrafish approach offers advantages that had previously been mutually exclusive, high-fidelity imaging, biological relevance, and control of shear stress, whilst also removing the need to cull protected species, and offering an animal reduction approach to generate samples for investigation. This feature set makes the approach very appealing to wider adoption in the field.

4.5.5 Endothelial Cell Proliferation in Zebrafish Embryos Compared to Other Models

As previously stated, EC proliferation is differentially affected by different flow and shear conditions. In order to use zebrafish to screen for genes involved in EC proliferation in response to flow, it is important to first define what type of flow results in EC proliferation, so that this flow pattern can be replicated in zebrafish.

I observed an EC proliferation rate of 1.76% of cells per hour in wt embryos, compared to 0.64% of cells per hour in *tnnt2a* morphants, and 0.81% of cells per hour in MS222 treated embryos. Thus, the rate of EC proliferation in static conditions is lower than the rate of proliferation under flow. A comparable study *in vitro* supports these data. DeStefano et al (2017) observed that initiation of unidirectional flow over HUVECS cultured under static conditions led to a brief large increase in the proliferation rate which then fell over time to reach a steady state. They observed that the EC proliferation rate is greater in steady state unidirectional than steady state static conditions, which is aligned with my observations of steady state zebrafish endothelial cells (zECs).

This indicates that endothelial cell proliferation is increased when flow occurs over cells that are not 'acclimatised' to the direction of flow. Indeed, shear direction and EC polarity are known to influence EC behaviour, which DeStefano observed as the rate of EC proliferation was inversely proportional to the alignment of ECs. Thus, endothelial cell proliferation appears to increase when flow is against the plane of alignment. This is observed *in vivo* in the partial carotid ligation mouse model where EC proliferation is increased where flow is disturbed and thus tangential to EC alignment, and *in vitro* where oscillatory shear stress (OSS) and transition from static to unidirectional flow also increase EC proliferation (Dardik et al., 2005; Nam et al., 2009). Hence, I conclude that zebrafish embryos can be used to determine the mechanisms underlying EC responses to changes in flow.

Other researchers have analysed EC responses to chronic disturbed flow in mice (Table 1). For example, in mice, carotid ligation is used to cuff the carotid artery to produce a region of disturbed or stopped flow. Complete ligation of the artery is also atherogenic, but EC proliferation is not immediately increased, (Li et al., 2018; Nam et al., 2009; Poduri et al., 2017). This supports the idea that disturbed flow leads to a higher rate of endothelial cell proliferation than unidirectional or static flow. Indeed, this is supported by *in vitro* studies which observe increased EC proliferation under OSS compared to unidirectional or static conditions (Chakraborty et al., 2012; Dardik et al., 2005).

Whilst the static blood flow generated in *tnnt2a* morphants are not comparable to low shear stress flow seen in mammals, zebrafish ECs under static conditions display some similarities to ECs subject to low shear in mammals (Goetz et al., 2014; Packham et al., 2009; Parmar et al., 2006).

4.6 Conclusions and Future Work

I conclude that zebrafish embryos conserve the pattern of flow responsive endothelial cell proliferation seen in other models under steady state conditions. I therefore pursued the zebrafish embryo model to analyse the effect of morpholino based knock-down of my genes of interest to determine their role in endothelial cell proliferation in response to flow (Chapter 5).

Because my approach imaged zebrafish ECs (zECs) under steady state conditions, disturbed flow was not modelled. However, it may be possible to analyse zEC response to disturbed flow in future studies by imaging zECs during the transition from SSS to SSL conditions. If validated, this would allow screening of genes specifically involved in the zEC response to disturbed flow by using flow state transition as an analogue of disturbed flow/OSS. This would potentially extend the biological relevance of the model and allow screening of genes for their impact on proliferation in response to disturbed flow, in addition to their role in acute responses to flow.

To evaluate this model against cultured cells and the mouse, one could first study the expression of classical shear stress markers within the embryo vasculature. For example, it would be useful to quantify expression of markers such as IL-8, and TGFβ both in control-MO embryos and embryos treated with *tnnt2a*-MO. One could then quantify expression of these LSS/OSS markers in the ISVs and compare them across flow and no-flow conditions, and across vascular beds. Performing this experiment with an awareness of the type of flow found in the zebrafish vasculature (Roustaei et al., 2021) would allow us to define how completely zebrafish embryos recapitulate responses to flow *in vitro* or in mouse.

5.0 Screening Genes for Effects on Endothelial Cell Proliferation in Response to Flow

In previous work (Serbanovic-Canic et al., 2017) the group quantified differentially expressed genes within high and low shear regions of the porcine aortic endothelium and identified 764 shear responsive genes. Of these genes, 14 were putatively associated with cell proliferation based on pathway analysis. Rather than study all these genes in mouse, I asked whether it is possible to use zebrafish embryos to identify genes which clearly link shear stress to endothelial proliferation, and thus identify a narrower list of genes for mammalian study. This approach was previously demonstrated for apoptosis and expanding the applications of zebrafish to study EC proliferation, another key process in EC dysfunction, would further advance the utility of zebrafish models for study of atherosclerosis and reduce the use of mice in the field.

Having established a system for studying the effect of flow on EC proliferation in zebrafish embryos, we now wanted to use this system to study the effect of systematic knock-down of our genes of interest to screen them for effects on EC proliferation in response to flow. We originally intended to use CRISPR-Interference (CRISPRi) for this, as the technique theoretically allowed for both ubiquitous and endothelial cell specific knock-down of our target genes. However, we found that CRISPRi did not produce efficient knock down and therefore switched to using morpholino antisense oligonucleotides (MOs) (see Discussion).

In this chapter I describe:

1. Identification of zebrafish orthologues of previously identified proliferation linked genes and validation of gene expression in zebrafish ECs.
2. Validation that gene knock-down does not lead to changes in blood flow.
3. Screening of the effect of gene knock-down on the rate of EC proliferation in response to flow.

I hypothesized that zebrafish could be used to identify shear responsive genes with effects on EC proliferation.

5.1 Identifying and Validating Zebrafish Orthologues of Proliferation Linked Genes

I firstly took all significantly shear-regulated putative regulators of proliferation from existing data derived from the porcine aorta (Serbanovic-Canic et al., 2017) and identified zebrafish orthologues using Ensembl (Table 2).

Table 2: Proliferation linked porcine genes and their zebrafish orthologues.

Porcine Gene	Zebrafish Orthologue	% identity (protein)
WNK1	wnk1a, wnk1b	35.13, 15.15
TRPM7	trpm7	70.74
SEMA6A	sema6a	35.46
IGF1	igf1	56.63
GSK3β	gsk3β	84.56
FZD5	fzd5	68.94
ANGPTL4	angptl4	33.94
BMP2	bmp2a, bmp2b	63.2, 61.74
KNG1	kng1	14.29
TNFSF10	tnfsf10	39.93
THBS4	thbs4a, thbs4b	60.18, 66.21
SERPINC1	serpinc1	56.42

I then designed and validated qPCR primers for each zebrafish gene by using melt curves to assess their specificity, and then testing their efficiency in cDNA from whole embryos at 24 and 48 hpf (wnk1a shown, Fig 18). It was not possible to validate primers for detection of wnk1b as gene expression was very low, so this gene was excluded from the study.

WNK1a primer pair one			X	Log	Ct
			Neat	1	0	27.35
Forward	AAGAGCGTCATAGGTACCCC		10^-2	0.1754386	-0.756	29.89
Reverse	AAGGCATACACATCCACCGA		10^-4	0.0307787	-1.512	32.32
Slope	-2.941		10^-6	0.0053998	-2.268	33.95
Efficiency	118.815		10^-8	0.0009473	-3.023	Na

Primer pair two had efficiency closest to 100%, and were therefore selected for use.

WNK1a primer pair two			X	Log	Ct
			Neat	1	0	26.49
Forward	TGAAGCCTGGCAGTTTTGAC		10^-2	0.1754386	-0.756	28.83
Reverse	TCCTTGATGCAGTACCTCTCA		10^-4	0.0307787	-1.512	31.41
Slope	-3.277		10^-6	0.0053998	-2.268	33.65
Efficiency	101.903		10^-8	0.0009473	-3.023	36.47

Figure 20: Comparing the amplification efficiency of qPCR primers. Two pairs of primers for wnk1a were used to amplify wnk1a in zebrafish cDNA, cDNA was diluted in series and the efficiency of each primer pair was calculated. Primer pair two had the closest efficiency to 100%, so this pair was chosen for later work.

Having identified zebrafish orthologues and validated primers to measure their expression, I sought to quantify expression of each gene in zebrafish endothelial cells to determine whether the zebrafish orthologues are endothelially expressed. To do this I collected embryos with fluorescently labelled endothelial cells (*Tg fli1a:EGFP*), generated single cells from them, and performed fluorescence activated cell sorting (FACS) to isolate GFP positive cells (Fig. 19).

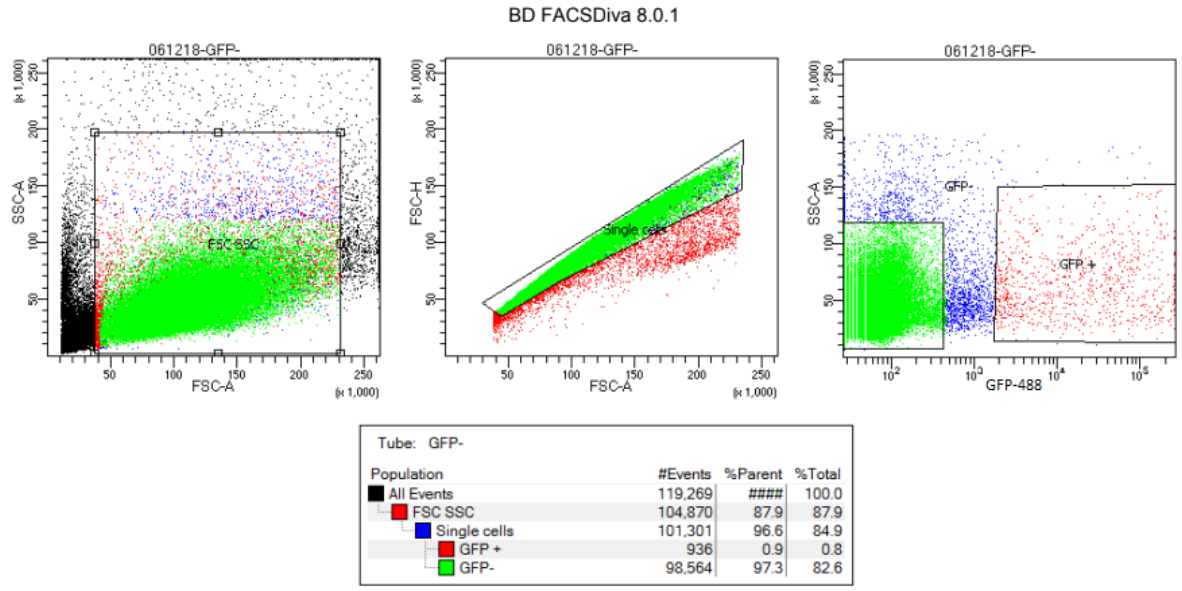

Figure 21: FACS of cellularised *Tg fli1a:EGFP* zebrafish at 48 hpf. Trypsin solution (TrypLE) was used to disassociate 100 zebrafish embryos containing *Tg fli1a:EGFP* into cell solution. FACS was used to select GFP positive cells (EC) and GFP negative cells (non-EC).

Initial FACS successfully isolated 936 GFP positive cells out of 101,301 total cells. To validate that the sorted cells were endothelial, I generated cDNA from each group and used qPCR to measure expression of the endothelial marker VE-cadherin in the GFP positive population relative to the GFP negative population. VE-cadherin was enriched 22-fold in GFP positive cells (ΔΔCt -4.04, -4.74. n=2) which confirmed the endothelial identity of the GFP positive cell population.

Having confirmed that this approach yielded endothelial cells I then determined which of the zebrafish orthologues (Table 1) are endothelially-expressed. To do this I measured expression of each gene in zebrafish endothelial cells, I calculated the level of expression of each gene of interest normalised against β-actin (housekeeping gene), as this gene was strongly and consistently expressed in zebrafish embryos (McCurley & Callard, 2008). I then selected for genes with a delta CT of less than 10, as this indicated the genes were expressed in zECs (Table 3). I also calculated expression of each gene relative to VE-cadherin in GFP+ cells (Fig. 20).

Table 3: Gene expression (Ct) of genes of interest across three experiments. Delta Ct was calculated by subtracting target gene Ct value from the corresponding β-actin Ct value. Lower values indicate the gene was more strongly expressed. Green values have a delta Ct of less than 10.

Gene	Delta Ct 1	Delta Ct 2	Delta Ct 3
wnk1a	8.63	8.24	8.42
trpm7	7.03	11.23	11.18
tnfsf10	12.07	11.54	11.57
thbs4a	11.03	16.11	17.55
thbs4b	NA	12.74	12.38
serpinc1	NA	12.97	13.42
sema6a	6.2	9.86	9.01
kng1	10.18	19.2	14.58
igf1	4.56	15.93	11.99
gsk3b	7.15	8.72	7.95
fzd5	4.36	10	9.73
bmp2a	4.5	14.35	14.6
bmp2b	14.59	13.64	12.65
angptl4	7.32	6.91	10.03

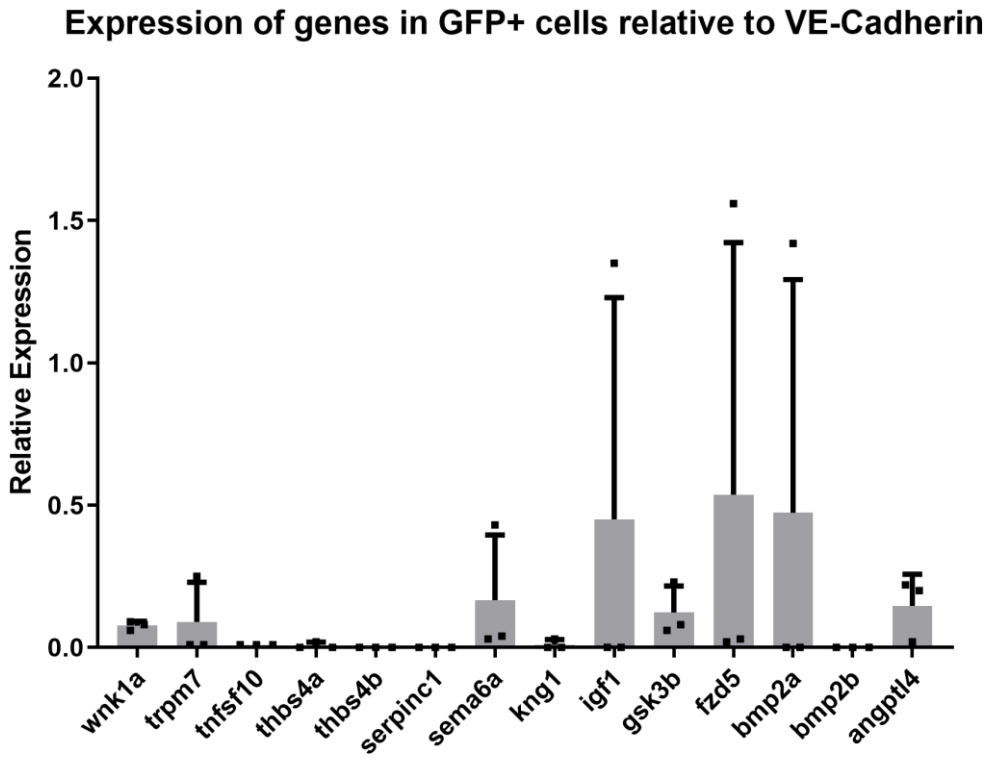

Figure 22: Quantification of expression of genes of interest in zebrafish endothelial cells relative to VE-cadherin. Gene expression was measured in transgenic *Tg fli1a: EGFP* zebrafish. Endothelial cell cDNA was derived from embryos at 48 hpf. Expression of each gene was determined using qPCR, with primers validated for efficiency (Fig. 18). Expression of each gene was measured relative to VE-cadherin in n=3 experiments, genes which were expressed zEC's in at least one experiment were selected for further study. Error bars are standard deviation.

The genes *wnk1a*, *trpm7*, *sema6a*, *igf1*, *gsk3β*, *fzd5*, *bmp2a* and *angptl4* (hereafter termed 'candidate genes') were expressed (delta Ct ≤ 10 in at least one experiment) in zebrafish endothelial cells. The remaining genes were excluded from further analysis as they were not expressed in ECs and were therefore unlikely to be involved in shear responsive EC proliferation.

5.2 Screening Genes for Effects on EC Proliferation in Response to Flow

I next screened candidate genes for the ability to regulate the rate of EC proliferation in response to flow. In this chapter I describe the use of CRISPRi and morpholino based knock-down approaches in the zebrafish embryo.

5.2.1 CRISPRi did not Efficiently Knock Down Genes of Interest

I initially planned to use CRISPRi to silence candidate genes. Initial testing of this system for knockdown of wnk1a and gsk3b involved design of four independent gRNAs targeting the transcription start site of each gene +/- 150 bases, all four guides were then co-injected into embryos expressing dCas9 protein, and the level of mRNA expression compared in embryos with and without dCas9 expression. Expression levels were compared at 78 hpf, as this is close to the age of embryos after imaging for proliferation. Initial experiments targeting *wnk1a* and *gsk3β* showed no clear reduction of *gsk3β* expression whereas *wnk1a* expression appeared partly reduced (Fig. 21).

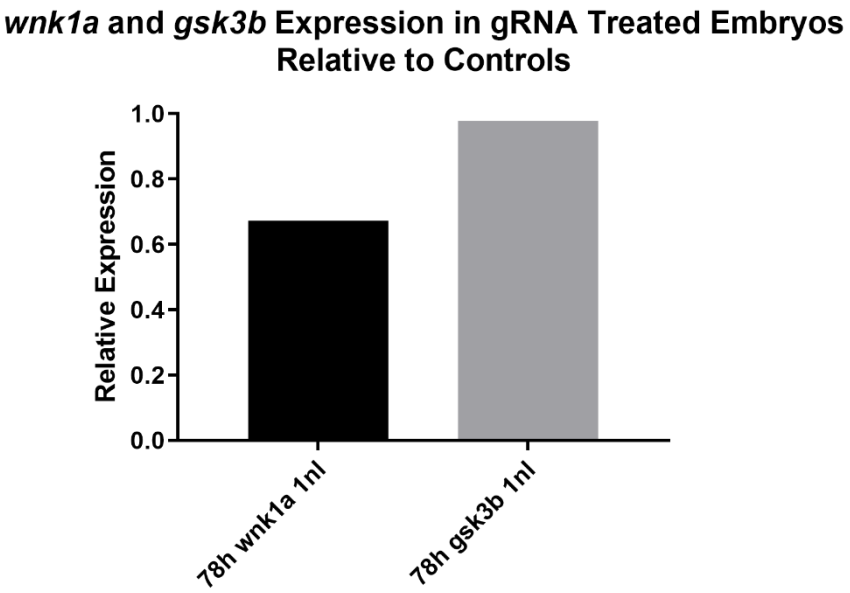

Figure 23: CRISPRi for *wnk1a* and *gsk3β.* *Tg ubi:dCas9-cryaa:CFP*$^{+/-}$ embryos were treated with an equimolar mixture of four gRNAs targeting *wnk1a.* Separately, *Tg ubi:dCas9-cryaa:CFP*$^{+/-}$ embryos were treated with and an equimolar mixture of four gRNAs targeting *gsk3β.* At 78 hpf, embryos were separated by *cryaa-CFP* expression, and RNA isolation performed on a minimum of 40 embryos per group. Expression of each target gene was measured in dCas9 positive (*cryaa* positive) embryos compared to dCas9 negative (*cryaa* negative) embryos.

As CRISPRi for *wnk1a* appeared to be more efficient, this was investigated further and knockdown was compared when embryos were injected with one or two nanolitres of gRNA, at 52 and 72 hpf (Fig.22). There was no clear effect of CRISPRi on expression of *wnk1a* under any tested conditions. Optimization of this approach by use of dCas9 protein, dCas9 mRNA, or further increased gRNA dosage did not result in increased knock-down efficiency (data not shown). As other groups in the department were having similar technical difficulties with this system it was decided that MOs would be used instead for gene screening.

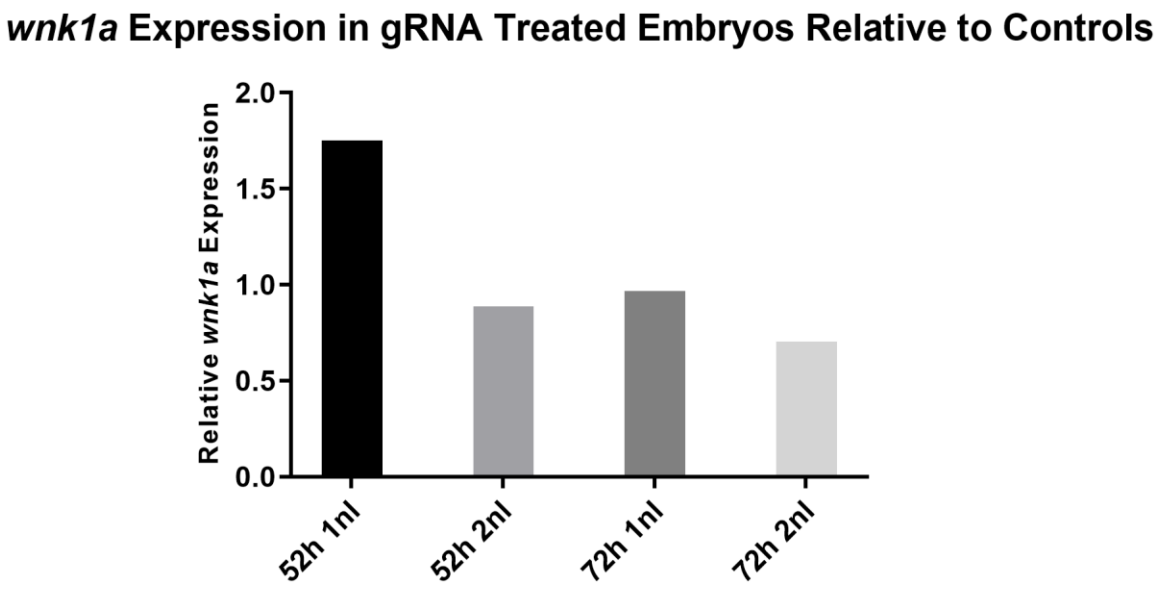

Figure 24: CRISPRi for *wnk1a* showed no effect of time or gRNA dosage. *Tg ubi:dCas9-cryaa:CFP*$^{+/-}$ embryos were separately treated with one or two nanolitres of an equimolar mixture of four gRNAs targeting *wnk1a.* At 52 hpf, and 72 hpf embryos were separated by *cryaa-CFP* expression and RNA isolation performed on a minimum of 40 embryos per group. Expression of each target gene was measured in dCas9 positive embryos compared to dCas9 negative embryos.

5.2.2 Morpholino Screening for Genes Involved in EC Proliferation in Response to Flow

To identify morpholinos for our candidate genes I searched the zebrafish information network (ZFIN) for published MOs targeting each gene. I excluded MOs for which published phenotypes included aberrant vasculogenesis and/or blood flow, as this would have prevented study of EC proliferation in response to flow. Published MOs fitting these criteria were identified for wnk1a, gsk3β, fzd5, sema6a, trpm7, and angptl4.

I initially used ZFIN to conduct a literature search where I ruled out morpholinos which led to gross embryo abnormalities. Most MOs had no published effect on overall embryo morphology. However, for *igf1* we previously showed the embryo phenotype was grossly abnormal (Serbanovic-Canic et al., 2017), hence knockdown of igf1 was not studied further. Preliminary testing was then done to determine whether the published dose of MO led to abnormal ISV development or absent blood flow, for genes where this was the case, MO dosage was halved (for final MO doses see methods). Absent blood flow led to a characteristic 'collapsed' appearance of ISV's (Fig. 23), supporting published data which shows reduced vessel diameter (Kugler et al., 2021).

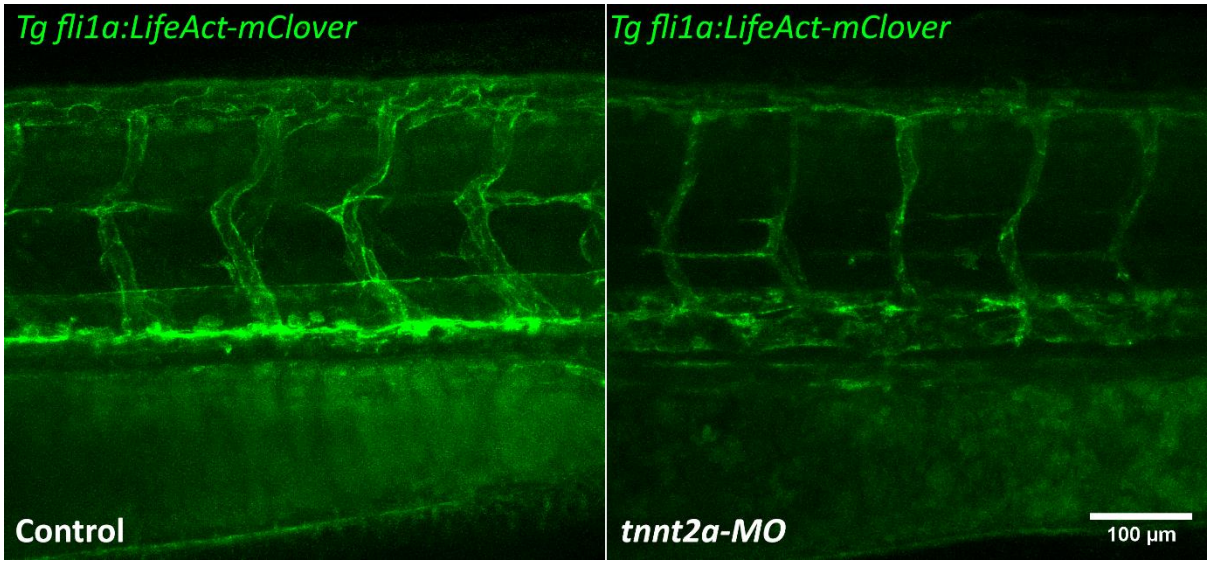

Figure 25: F-actin localisation was compared in embryos with and without blood flow. Embryos with blood flow were treated with control MO, embryos without blood flow were treated with *tnnt2a* MO. These are representative images of eight embryos (n=4 per group). Embryos were imaged from the side, anterior is left, dorsal is up.

Despite existing publications on our chosen MOs showing broadly normal vascular development (see methods), no analysis of whether morpholino dosage affects blood flow was available, so I then studied the effect of morpholino treatment on ISV blood flow, to determine whether there was an effect (Fig. 24). The rate of blood flow was quantified in the ISVs of embryos expressing *Tg (gata1:dsRed)* - a transgenic line which labels erythrocytes, at 72 hpf (Fig. 24).

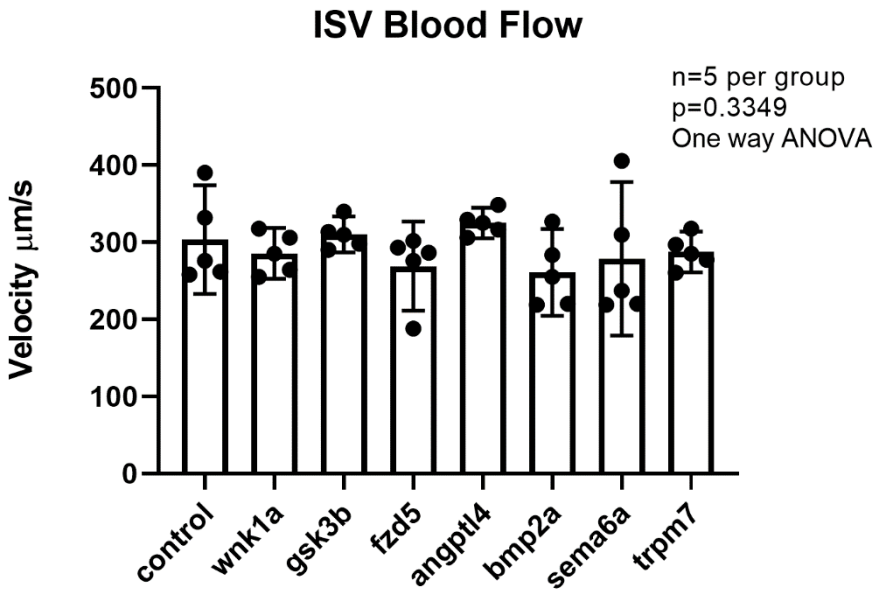

Figure 26: Knock-down of candidate genes does not affect blood flow in the ISVs. Blood flow was quantified in the ISVs of *Tg gata1:dsRed* morphants at 72 hpf. n=5 embryos per group. One-way ANOVA was performed, no morphant had significantly different blood flow to the controls. For morpholino dosage see methods.

Having confirmed that ISV blood flow was normal in all morphants, I then analysed the effect of gene knock down on the rate of EC proliferation in flow and no-flow embryos to identify genes which are required for shear responsive changes in the rate of proliferation. To do this, I used the method described in the previous chapter, where *Tg fli1a:nls-mCherry* embryos are treated with morpholino targeting the gene of interest (flow group), or both morpholino targeting the gene of interest as well as morpholino targeting *tnnt2a* (no flow group).

Embryos of these treatment groups for all genes of interest were studied using confocal microscopy. The rate of EC proliferation in the ISVs was quantified (Fig. 25).

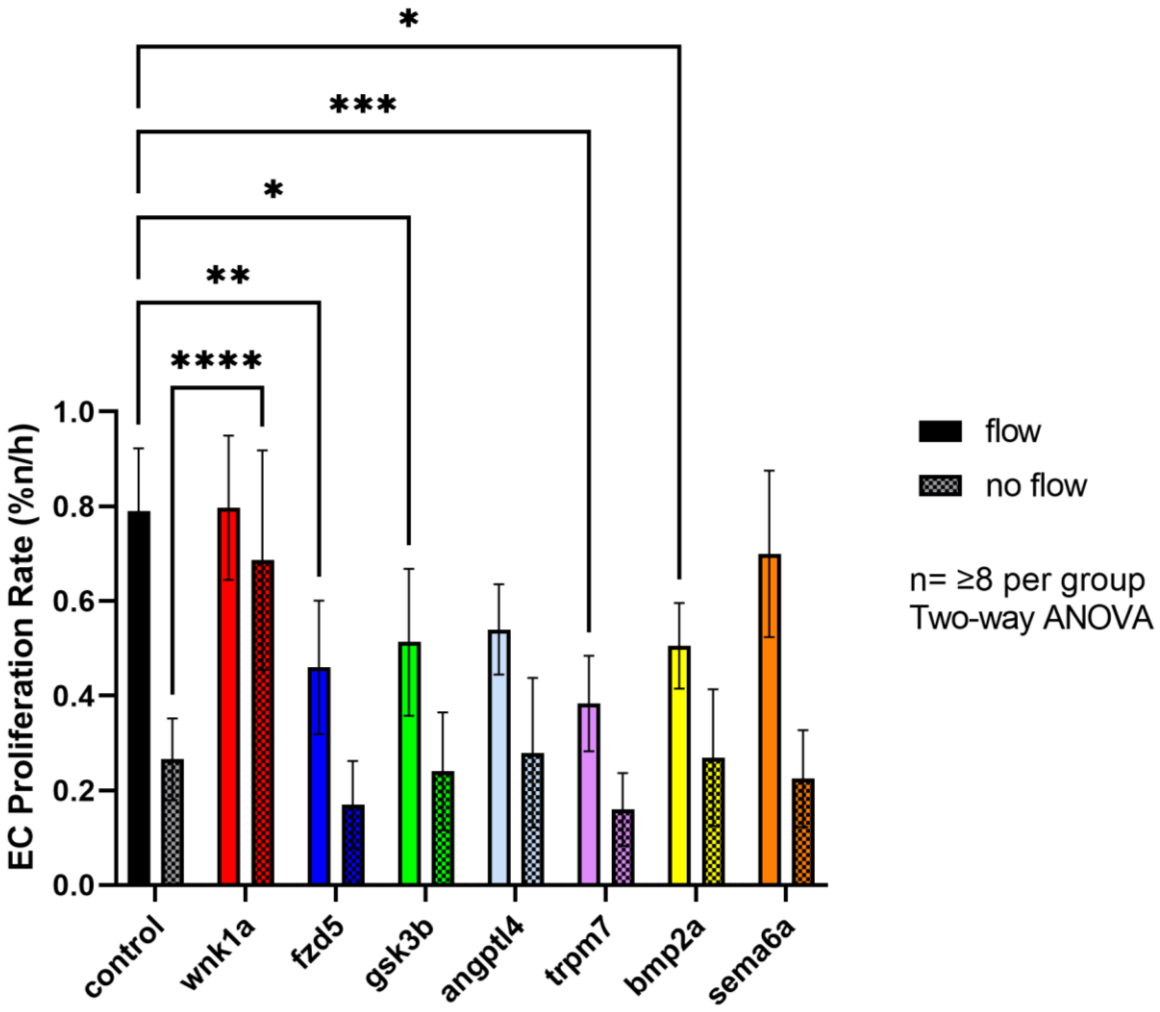

Figure 27: EC proliferation was quantified between 54 and 70 hpf in morphants for each candidate gene with and without blood flow. Embryos expressing *Tg fli1a:nls-mCherry* were injected with morpholino for the gene of interest (detailed in methods), for 'no-flow' embryos *tnnt2a* MO was also injected to stop the heartbeat from developing. For 'flow' embryos no further treatment was done. For each gene and flow condition, proliferation was calculated as described in the previous chapter (Fig. 15). Proliferation was calculated in a minimum of eight embryos per condition. Error bars are 95% confidence limits. Non-significant comparisons not shown.

As shown in the previous chapter, loss of blood flow led to reduced EC proliferation (Figure 16 control: flow versus no flow). Knockdown of *wnk1a* rescued this phenotype (p=0.0004, two tailed t-test), whereas knockdown of *fzd5*, *gsk3β*, *trpm7*, and *bmp2a* led to reduced EC proliferation under flow (p=<0.0241 Dunnett's multiple comparisons test). Knockdown of *angptl4* and *sema6a* did not affect the rate of proliferation under flow or no-flow conditions. Given that knockdown of *fzd5, gsk3β, trpm7,* and *bmp2a* led to reduced EC proliferation under flow, these results suggest these genes are required for proliferation in zebrafish ISVs under normal conditions. Conversely, w*nk1a, angptl4,* and *sema6a* had no effect on proliferation under flow and were thus not required for proliferation under normal conditions.

5.3 Discussion

These data demonstrate the feasibility of using zebrafish embryos to screen genes selected from existing datasets for effects on endothelial cell proliferation in response to flow. I show that zebrafish *wnk1a* is required for reduced EC proliferation under no-flow conditions, and that *fzd5, gsk3b, trpm7,* and *bmp2a* are required for normal EC proliferation under normal blood flow conditions.

5.3.1 Zebrafish *wnk1a* and Mammalian Wnk1 Encodes a Protein Serine/Threonine Kinase Involved in Several Key Processes

Wnk1 (zebrafish *wnk1a*), full name WNK lysine deficient protein kinase 1, is a serine threonine kinase which is expressed throughout zebrafish development, and essential in endothelial cells for viability of mouse embryos (White et al., 2017; Xie et al., 2010). Wnk1 is ubiquitously expressed and acts on the ERK5 pathway via MAP4K activation as well as a cell osmolarity regulator via Ste20-related proline-alanine-rich kinase (SPAK) and its effect on sodium chloride cotransporter (Chávez-Canales et al., 2014; Xu et al., 2005). Hence Wnk1 is implicated in endothelial proliferation, and control of cell/blood ion content and is thus involved in hypertension and perhaps atherosclerosis (Bergaya et al., 2011; Zhang et al., 2018).

5.3.2 CRISPRi Most Likely Failed Due to Low Knockdown Efficiency Beyond 28 hpf

The major objective of my research was to screen several genes for a potential role in proliferation and therefore a medium-throughput approach was required. The original plan was to use CRISPRi and I therefore tested this approach by designing CRISPRi to target two genes; *wnk1a* or *gsk3b.* However, despite using a protocol that was pre-validated locally, I did not generate efficient knockdowns of *wnk1a* or *gsk3b* using CRISPRi. Others at Sheffield have successfully applied this technique in zebrafish (Savage et al., 2019), however these groups used CRISPRi on embryos which were no older than 28 hpf, whereas I used CRISPRi on embryos between 48 and 72 hpf. This could indicate that the rate of CRISPR gRNA degradation is such that gRNA concentration remains sufficient for knockdown in the early embryo (~28 hpf) but not at or beyond 48 hpf. It has been suggested that the first generation CRISPRi approach (use of sp dCas9 to create steric hinderance) which is derived from the prokaryote *Streptococcus pyogenes* is less efficient against the larger eukaryotic RNA polymerase II (Qi et al., 2013), this fits with my suggestion that CRISPRi success varies

with embryo stage/size as it is possible that the concentration of gRNA was insufficient in the older/larger embryos that I studied. Using an increased initial gRNA concentration may remedy this problem, however this was not tested as the high unit cost of gRNA makes this approach uneconomical for analysis of multiple genes.

Gene knockdown by CRISPRi was studied using qPCR, whilst reduced expression was seen this effect was not significant or reproducible hence the effect of CRISPRi based gene knockdown on EC proliferation was not progressed any further.

5.3.3 Use of Antisense Approaches Compared to Mutants

I concluded that CRISPRi were unsuitable for medium-throughput screening of vascular genes at > 48 hpf. Alternative systems for tissue specific knockdown, such as *cre-lox,* are highly labour intensive and therefore, while they are excellent systems for in depth study of single genes of interest, they are unsuitable for screening of multiple genes. Moreover, cre-lox systems may trigger genetic compensation which might affect EC proliferation.

I chose morpholinos as a replacement system as they are a highly efficient and well understood means of achieving gene knock down in zebrafish larvae. Both morpholino and CRISPRi systems avoid genetic compensation, which is triggered in zebrafish with deleterious mutations (El-Brolosy et al., 2019). This is a particularly important consideration in zebrafish as the species was subject to teleost-specific genome duplication (Meyer & Schartl, 1999). Because of this many zebrafish genes have a number of paralogues and thus have partial functional redundancy, as is the case for example with *stag1a* and *stag1b* (Ketharnathan et al., 2020). Unfortunately, using morpholinos meant losing the ability to do tissue specific gene knockdown, which would have been possible using CRISPRi (Savage et al., 2019).

Use of morpholinos has been viewed as controversial as some studies showed low correlation of morphant and mutant phenotypes (Kok et al., 2015). In detail, phenotypes seen in morphants were more severe, which some believe are due to off target effects. One major off target effect is upregulation of p53. Whilst upregulation of p53 is seen in morphants this is not MO specific and is rather an effect of antisense technologies in general, as p53 upregulation is also seen in siRNA treatment (Robu et al., 2007). Upregulation of p53 is dependent on the dose of morpholino, in a study of *egfl7* there was no upregulation of p53 at MO doses below 1 ng whereas at doses above 2 ng p53 upregulation becomes significant (a five-fold increase) and continues to rise above this level (Rossi et al., 2015).

As p53 supresses proliferation, in my experiments one might argue that MO treatment *per se* might be responsible for the general reduction in proliferation observed in morphant embryos with blood flow compared to controls (Fig. 25), however this was not the case for *wnk1a, angptl4,* or *sema6a* all of which were delivered at doses greater than 1 ng with no decrease in proliferation. These data suggest that altered proliferation in response to silencing of *wnk1a,* is more likely due to gene knock-down, and not due to off target effects. Further work should now be carried out to further test the function of *wnk1a* including the use of inducible genetic deletion strategies in zebrafish and mice.

5.3.4 Rationale for Deviating from the Published Dose of Morpholinos

All morpholinos used in this study are published, and their effects validated (see methods for references). When initially testing the effect of each MO, for all MOs I observed reduced survival, as well as instances of altered blood flow or vascular development. This was expected as in many publications the dose was set at the level which produced abnormality, and often led to a large proportion of embryos dying. This presented two issues: (1) Gross abnormalities often led to abnormal ISV development or absent blood flow. (2) Embryos would sometimes die during imaging, thereby ruining the experiment. Thus, the decision was made to reduce MO dose to avoid flow and vessel development abnormalities, and excess deaths.

It was considered that reduced MO dose would reduce the effect of gene knock-down, however for genes where knockdown led to vascular defects or absent blood flow, partial knockdown was the only way to study effects on EC proliferation in response to flow. Publications show MO dose effects are varied depending on the target gene, with some exhibiting linear dose dependent effects on protein expression, and similar functional studies showing exponential reduction in enzyme function (Chu et al., 2013; Johnson et al., 2013). In detail, well validated MOs can yield very high knockdown efficiency (>80%) in a dose range of only 0.9 to 1.8 ng (Kamachi et al., 2008). With this considered, reduction of MO dose was deemed to be an appropriate approach, but one requiring careful interpretation of the data since knockdown was partial not full.

5.3.5 Knock-Down of *wnk1a* Increased the Rate of EC Proliferation Under No-Flow Conditions

Screening showed that knockdown of *wnk1a* in embryos with no blood flow led to increased EC proliferation compared to no-flow controls (*tnnt2a* morphants. Fig. 25), hence wnk1a is required for reduced EC proliferation when blood flow was absent. The potential effects of morpholino induced p53 activation on EC proliferation can be discounted, as this would *reduce* the rate of proliferation (while Wnk1 silencing had the opposite effect). Likewise altered blood flow could not contribute as blood flow was completely stopped by the absence of the heartbeat. Additionally, the effects of morpholino injection were controlled against a non-targeting control morpholino, hence it is likely that this effect is due to *wnk1a* knockdown alone.

Since the sole paralogue of *wnk1a,* wnk1b, was not knocked down in this study, it can be concluded that knockdown of only *wnk1a* is sufficient to affect EC proliferation, and that *wnk1b* expression alone is not sufficient to maintain the effect of flow on EC proliferation. This conclusion is consistent with my observation that wnk1b expression was extremely low in whole zebrafish embryos (7-10 cycles lower than other genes of interest).

The involvement of *wnk1a* in endothelial cell proliferation is also supported by the presence of defective angiogenesis phenotypes in high dose *wnk1a* morphants. Lai et al (2014) observed severely defective vessel formation in embryos dosed with 5 ng of MO, I reduced the dose to 1.75 ng which preserved angiogenesis and led to development of normally functioning blood vessels (Fig. 24). Because of these considerations, I suggest that *wnk1a* is

essential for angiogenesis during early development, therefore total knockdown leads to severe angiogenic defects, and that after vessel development *wnk1a* continues to regulate vessel remodelling by modulating EC proliferation in response to blood flow.

Interestingly, the published phenotypes of *wnk1a* morphants are exclusively vascular which suggests that the effect of *wnk1a* on proliferation is specific to vascular cells. Indeed, if *wnk1a* affected proliferation in other cell types, then we would expect to see other abnormalities. Studies on *Wnk1*$^{-/-}$ mice also suggest an EC specific function for *Wnk1* as knockouts show abnormal angiogenesis and heart development which is rescued by EC specific expression of *Wnk1*. EC specific *Wnk1* expression also rescues survival during development (Xie et al., 2010). Similarly, abolition of *wnk1a*/Wnk1 in mouse and zebrafish leads to abnormal angiogenesis but not vasculogenesis which suggests that gene function is highly conserved in vertebrates. Collectively, these data suggest that the effects of *wnk1a* in zebrafish are EC mediated however an efficient EC specific CRISPRi approach would be needed to test this further.

Overall, I considered the *Wnk1a* data to be particularly compelling because *Wnk1a* knockdown ***rescued*** proliferation and because of the consistency of this phenotype with other observations. Therefore, Wnk1 was selected for further study in mammalian arteries (Chapter 6).

5.4 Conclusions and Future Work

This chapter demonstrates a method for functionally studying genes involved in EC proliferation in the zebrafish and shows that *wnk1a* is involved in EC proliferation in response to flow. If, as literature states, this gene is strongly evolutionarily conserved, we would expect to find the same result in mouse and further demonstrate the utility of zebrafish for screening mammalian genes. The mouse orthologue *Wnk1* was therefore analysed at high and low shear regions of the aorta to validate my findings in zebrafish and these data are presented in Chapter 6.

The main limitation of this screening approach is that MOs are not EC specific thus these data do not exclude the possibility that changes in expression of target genes in the whole organism led to the changes in EC proliferation shown, rather than endothelial expression of each gene of interest.

Future work should establish additional genetic modulation approaches based on genome integrated second generation CRISPRi and CRISPR-activation to validate the global knock-down phenotypes seen in morphants, determine the effect of endothelial specific knock down of 'hits', and open the door to studying upregulation of 'hits' in a global or tissue specific manner. One novel approach for tissue specific knock-down is to generate a transgenic which drives dCas9-KRAB (a second generation CRISPRi approach described by Long et al, (2015)) *and* gRNA expression under a tissue specific promoter. This approach was validated for generation of loss of function transgenics and shown to phenocopy existing approaches such as loss of *Tnfsf11* by *cre-lox* mediated gene deletion in mouse (MacLeod et al., 2019). Whilst not yet shown in zebrafish, zebrafish transgenesis is far simpler to achieve than in mouse, hence this approach is likely to work. If so, this would overcome the

problems associated with my CRISPRi approach by maintaining gRNA expression, and thus knock-down, over time. These suggestions represent ways to further improve the utility of zebrafish as a model for screening genes involved in EC proliferation, and to validate that the results seen are the result of endothelial expression of each target gene.

6.0 Validation of Shear Stress Regulation of WNK1

I previously described how screening zebrafish genes for roles in flow responsive proliferation of endothelial cells revealed that lysine deficient protein kinase 1a (*wnk1a*) was required for reduced proliferation under no-flow conditions. I next wanted to determine whether this gene is shear regulated in mammals, as this would help to demonstrate whether zebrafish accurately model the mammalian response. To do this, I analyzed mouse WNK1 in high and low shear regions of the aorta. We also wanted to determine whether expression of the human orthologue (WNK1) is associated with plaque severity in atherosclerosis. To do this we studied expression of WNK1 in human carotid endarterectomy plaque sections.

I hypothesized that WNK1 would be upregulated under low shear stress in mouse and associated with plaque severity in humans.

6.1 Endothelial WNK1 was Upregulated Under Low Shear Stress

To determine whether WNK1 was shear regulated in mammals the mouse was used. Mice are ideal for studying the effect of shear stress on endothelial gene expression as techniques such as *en face* can quantify expression of proteins of interest in high and low shear regions of the aorta using immunofluorescent histochemistry. WNK1 expression was quantified in endothelial cells from high and low shear regions of the aorta of wildtype mice (Fig. 26).

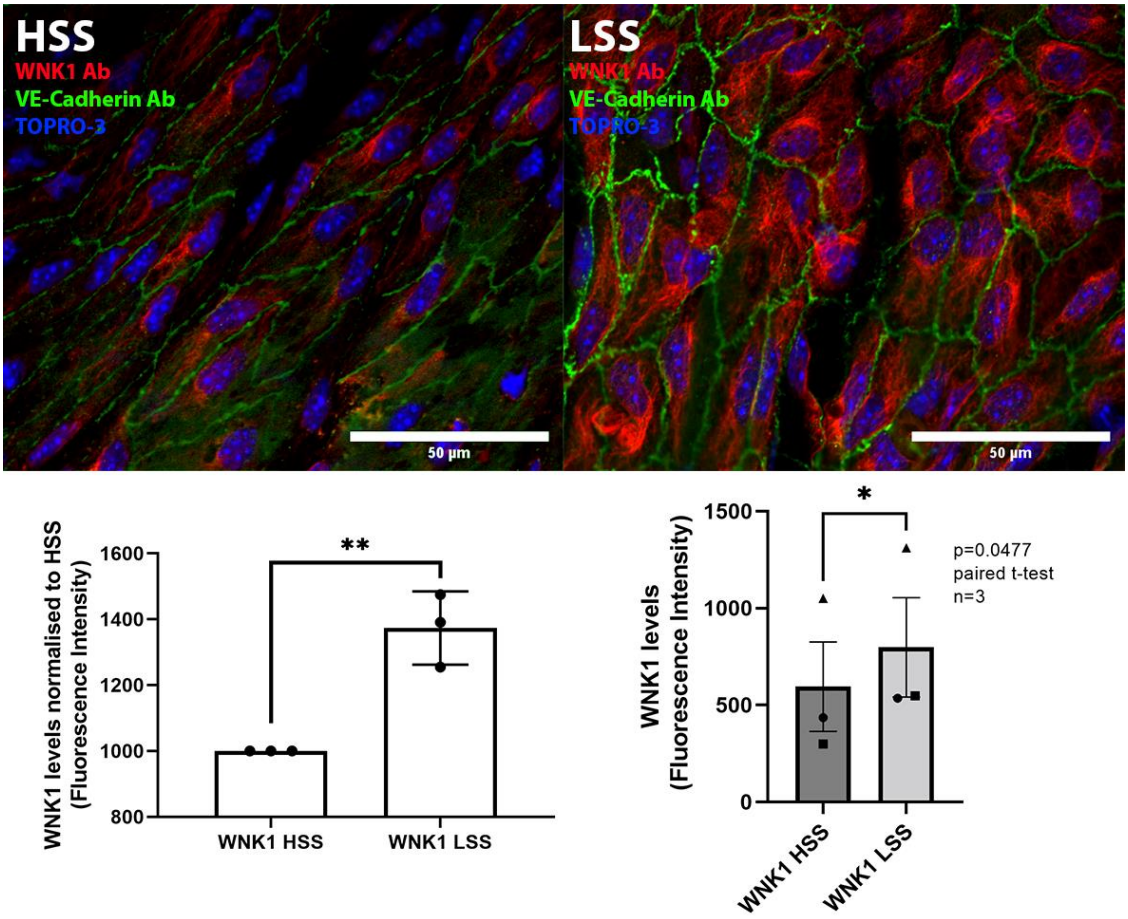

Figure 28: *Wnk1* is upregulated under low shear stress in the mouse endothelium. *Wnk1* was detected by staining whole mouse aortic arch samples with anti-WNK1 antibody, then a red (568 nm) fluorescent secondary antibody. Vascular endothelial cadherin (*VE-cadherin*) was detected by staining with anti-VE-cadherin antibody, then green (488 nm) fluorescent secondary antibody. TOPRO-3 was used as a counter stain for cell nuclei. *Wnk1* (Red), *VE-cadherin* (Green), TOPRO-3 (Blue). High shear areas were identified by looking for endothelial cell alignment (left image). Low shear areas were confirmed by detecting disorganised endothelium (right image). Representative images from one animal shown. WNK1 expression was quantified by analysing 568 nm mean fluorescence intensity in high and low shear areas. Fluorescence intensity was normalised to the high shear value for each animal (left graph). Non-normalised data is shown on the right graph.

WNK1 was significantly upregulated in regions of low shear stress, this justified study of WNK1 in human coronary plaque sections.

6.2 WNK1 was Expressed in Human Carotid Plaque Sections

Having confirmed shear stress association of *Wnk1* expression in the mouse aorta, I then sought to quantify expression of the human orthologue WNK1 in atherosclerotic plaque sections to determine whether expression was associated with plaque severity in atherosclerosis. Initially, graded human carotid endarterectomy sections from the AtheroExpress Biobank (AEB) were studied, and WNK1 antibody staining was compared against an IgG control to confirm antibody specificity in human tissue. Signal in the 568 nm (red) channel was strong in the WNK1-Ab treated sample, and very weak in the IgG control, indicating specific WNK1 staining in human plaque sections.

Due to limited numbers of AEB samples, and delays acquiring additional AEB tissues, the following experiments used human carotid endarterectomy tissues kindly shared by the Sheila Francis group. Study of WNK1 expression in ten patient samples revealed consistent strong WNK1 expression throughout, including in regions of endothelium which were defined as regions containing strong positivity for endothelial marker (Fig. 27A, 27B). However, despite optimization of staining, endothelial detachment was observed in eight out of ten samples (Fig. 27C), which prevented analysis of endothelial WNK1 expression levels. Only samples from ten patients were available for staining and therefore these data are considered preliminary.

Table 4: WNK1 staining in different regions of carotid endarterectomy samples.

Sample	WNK1 Staining		
	Endothelium	**Neointima**	**Media**
47A	N/A	Yes	Yes
49B	N/A	Yes	Yes
51C	N/A	Yes	Yes
52A	Yes	Yes	Yes
60C	N/A	Yes	Yes
61C	N/A	Yes	Yes
63B	N/A	Yes	Yes
64C	Yes	Yes	Yes
65C	N/A	Yes	Yes
67C	N/A	Yes	Yes

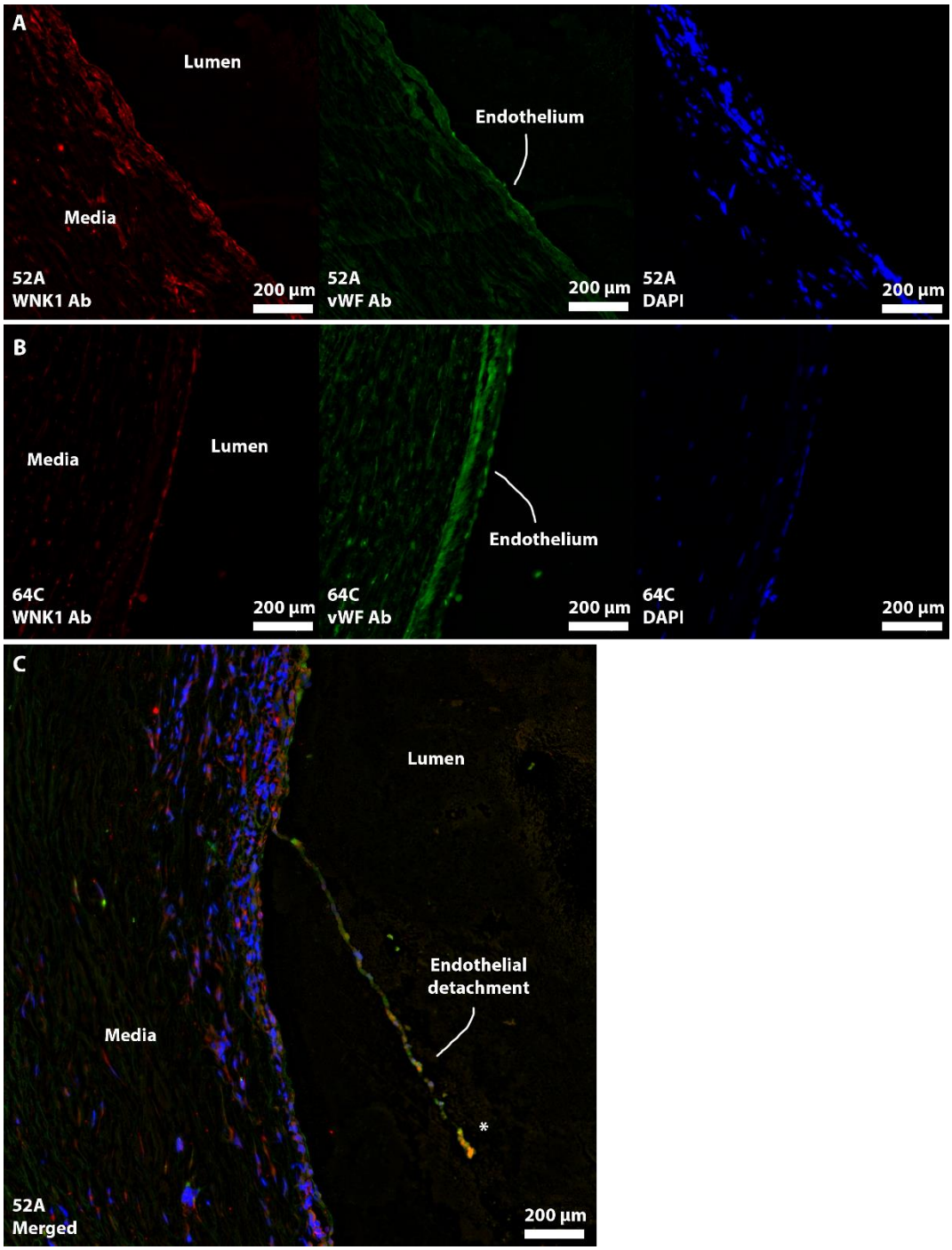

Figure 27: WNK1 was expressed in the endothelium of human plaque sections. Endothelial WNK1 expression was determined by immunolabelling human plaque sections with anti-WNK1 and anti-VWF antibody. Secondary antibodies were applied (WNK1:AF568 – Red. VWF:AF488 – Green) along with a nuclear counterstain (DAPI – Blue), then expression of each marker was studied using confocal microscopy. Strong WNK1 staining was visible in regions positive for vWF, these were characterised as endothelium positive for WNK1 (A, B). (C) – Representative image of endothelial detachment. (*) WNK1 positive endothelium was also visible in detached endothelium.

WNK1 was observed in all sections, and in samples where endothelium was detected WNK1 expression was colocalised with endothelial marker. Further work on quantifying *WNK1* expression in carotid plaque endothelium is ongoing pending delivery of additional AtheroExpress Biobank tissues which are believed to better preserve endothelial tissue.

6.3 Discussion

My observation that WNK1 is upregulated in endothelial cells under LSS is consistent with a role in vascular responses to flow. Hence considering that WNK1 orthologues regulate angiogenesis and proliferation in response to blood flow, I hypothesize that WNK1 is a novel mechanosensory protein involved in regulating endothelial proliferation in response to flow.

6.3.1 WNK1 as a Shear Regulated Protein

WNK1 is a serine/threonine kinase which has a role in regulation of electrolyte homeostasis, cell signalling, survival, and proliferation. WNK1 regulates the activity of sodium and potassium coupled chloride cotransporters and is thought to play a role in organisation of the actin cytoskeleton (Moore et al., 2000).

It is therefore interesting to consider possible mechanisms of shear stress regulation of WNK1. The activity of WNK1 is regulated by phosphorylation of Ser382, which is in turn regulated by the osmotic balance of the cytoplasm (Zagórska et al., 2007). Thus, it is plausible that the effect of shear stress on endothelial cell osmolarity modulates phosphorylation and activation of WNK1. Indeed, there are well described mechanisms for shear responsive control of cellular ion content. For example, *Piezo1* is a mechanically activated cation channel which is critical for vascular development and EC alignment under flow (Beech & Kalli, 2019; Ranade et al., 2014), it could be that *Piezo1*, or other mechanically activated ion channels, regulate changes in cell osmolarity that affect phosphorylation of WNK1 and therefore modulate its activity.

This hypothesis could be tested *in vitro* by studying the presence of WNK1 and phospho-WNK1 in cells under high and low osmolarity, and *in vivo* by studying the expression of phosphorylated WNK1 in a murine *en face* model, if phospho-WNK1 (active WNK1) is affected by shear stress, this would support the shear-osmolarity link. There is also evidence for shear regulation of WNK1 localisation within the cell, indeed shear stress drives apical WNK1 localisation in the kidney (Carrisoza-Gaytan et al., 2020). However, considering kidney epithelial cells control and respond to osmolarity, it is possible that this response is driven by osmolarity rather than shear *per se*. This is supported by data which show that phospho-WNK1 (which becomes phosphorylated after changes in osmolarity) undergoes colocalization with clathrin and AP-1 (Zagórska et al., 2007).

In addition to shear regulated modulation of WNK1 protein function, there is evidence that LSS increases WNK1 expression at the protein level (Fig. 26). This may result from increased transcription or post-transcriptional stability of WNK1 however no data on the effect of shear stress on WNK1 expression is currently available for any other cell types.

6.3.2 WNK1 as a Regulator of Proliferation and Potential Role in Atherosclerosis

In zebrafish with no blood flow, *wnk1a* knockdown led to proliferation returning to a level seen in controls, this suggests that *wnk1a* supresses proliferation in the absence of flow, and loss of *wnk1a* rescues this effect. I then studied the orthologue WNK1 in mouse endothelium and confirmed that WNK1 expression is shear regulated. Hence zebrafish screening was successful in identifying WNK1 as a shear regulated gene that controls arterial EC function.

Investigations of WNK1 function in mammalian cells demonstrate a cell and context dependent role for WNK1 in cell proliferation. In HUVEC (Dbouk et al., 2014), mouse neural cells (Sun et al., 2006), and rat vascular smooth muscle cells (Zhang et al., 2018) knockdown of WNK1 orthologues led to reduced proliferation. Whereas in adipocytes, and mouse and human endometrium WNK1 negatively regulates proliferation by stabilising the alpha form of protein phosphatase 2A (PP2A), leading to Akt dephosphorylation (Chi et al., 2020; Jiang et al., 2005). Interestingly, endothelial PP2A is required for Akt/ERK mediated proliferation and angiogenesis (Xie et al., 2015), and promotes HIF dependent EC survival by supressing PHD2 in complex with B55α (Ehling et al., 2020). Thus, endothelial WNK1 may be anti-atherogenic by stabilising PP2A under LSS/static conditions. Loss of WNK1 would therefore be atherogenic through de-repression of Akt and increased EC proliferation, which was supported by my findings in zebrafish.

WNK kinases are known to affect cell proliferation and survival via various mitogen activated protein kinase (MAPK) cascades. For example, WNK1 knockdown attenuates stimulation of ERK5 by epidermal growth factor (Xu et al., 2004). Since ERK5 exerts endothelial protective effects (Akaike et al., 2004), it is also possible that upregulation of WNK1 under LSS increases the sensitivity of ERK5 to local atherogenic stimuli (Fig. 28).

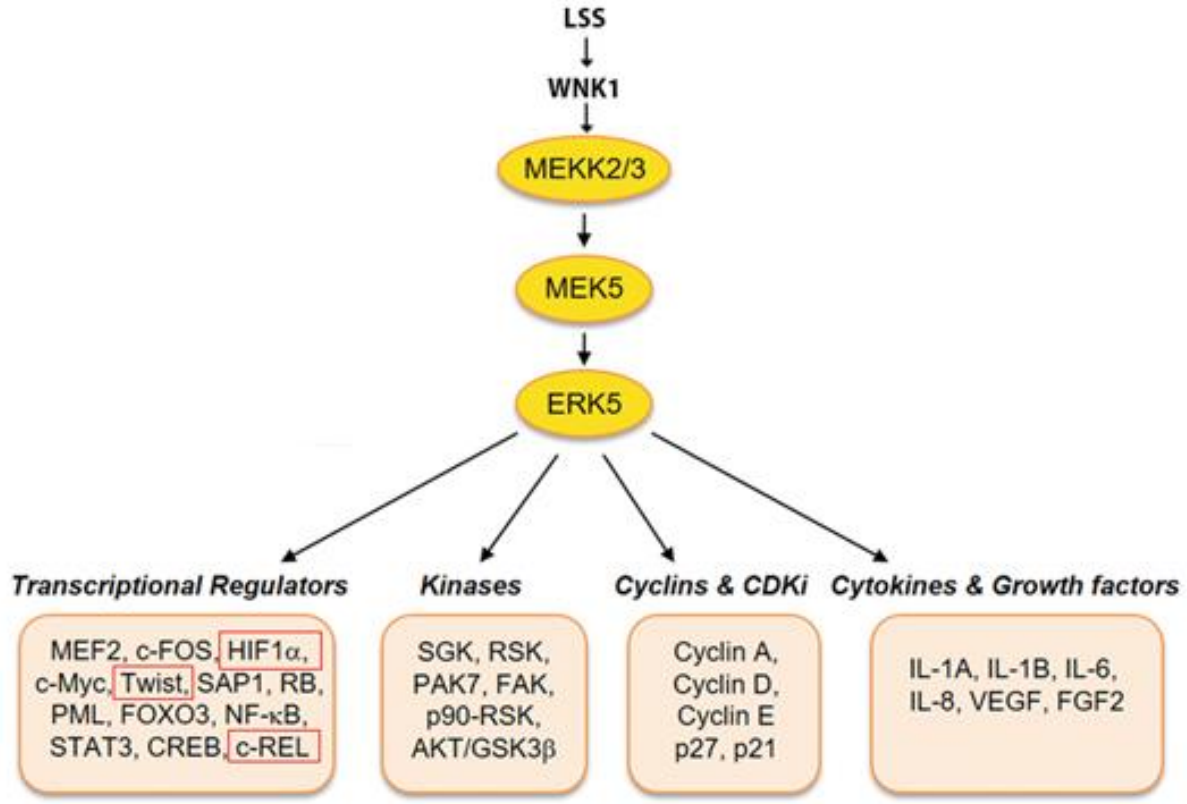

Figure 29: Diagram illustrating the hypothesised shear regulation of WNK1 on the MEK5/ERK5 cascade. Highlighted genes are studied within the group for their roles in atherosclerosis.

Given the apparent differences in WNK1 function across different cell types, and between *in vitro* and *in vivo* models, elucidating the role of WNK1 in arterial EC proliferation requires investigation of arterial EC's. Differences in function could be partially explained by shear and/or osmolarity driven regulation of WNK1 or by changes in the cell microenvironment. I suggest that *in vivo* study of the role of WNK1 in mammalian EC proliferation and development of atherosclerosis would best elucidate the role of the gene in proliferation and disease.

In detail, future work could further characterise the role of WNK1 in atherosclerosis by examining the effect of *Wnk1* knockout on EC proliferation and plaque formation in Tg (*Wnk1*^{ECKO} *ApoE*$^{-/-}$) and wildtype mice. Based on my mouse and zebrafish data, I hypothesize that WNK1 is upregulated under LSS, where it supresses EC proliferation (thus protecting from atherosclerosis), therefore I hypothesise that WNK1 knockout mice would have increased proliferation at LSS sites, leading to increased plaque formation. However, given the pro and anti-proliferative effects of WNK1 described in mammals, and the multiple roles of proliferation in vascular physiology, the effects of WNK1 deletion of vascular development and disease is difficult to predict.

These experiments would inform whether therapeutic targeting of WNK1 could be beneficial in atherosclerosis: if WNK1 is pro-proliferative and pathogenic in atherosclerosis then a pharmacological inhibitor is logical.

6.3.3 Determining the Role of WNK1 in Atherosclerosis by Studying Expression in Human Plaque Sections

A complementary method for studying the role of WNK1 in atherosclerosis is to quantify expression of WNK1 in human plaque sections of varied severity, then calculate whether expression of WNK1 is associated with plaque severity. If expression is associated with plaque severity, that would provide more direct evidence linking WNK1 to atherosclerosis than simply demonstrating that the gene is a shear regulated mediator of EC proliferation.

We examined WNK1 expression in human carotid endarterectomy sections and found strong expression throughout the tissue (Fig. 27). WNK1 was strongly expressed in the endothelium, however difficulty optimizing the endothelial co-stain led to exhaustion of tissue sections prior to completion of the work. Completion of this experiment will allow us to determine whether WNK1 is expressed in association with disease severity in atherosclerosis and thus provide an additional piece of evidence linking WNK1 with disease.

6.4 Conclusions and Future Work

Wnk1 and its orthologues are upregulated under low shear stress, and strongly expressed in human carotid endarterectomy tissue, including in endothelium. Ongoing work will seek to determine whether expression in human plaque endothelium is associated with plaque severity.

I hypothesise that WNK1 is atheroprotective by limiting increased proliferation induced by LSS, therefore WNK1 knockout mice would have increased EC proliferation at LSS sites and increased atherosclerosis. However, due to the dual roles of EC proliferation in disease and

development, and the pro and anti-proliferative effects of WNK1 described in mammals, the outcome of these experiments may be different to the one hypothesised.

If this hypothesis is substantiated, pharmacological activation of WNK1 may supress development of cardiovascular disease. For example, a small molecule to activate WNK1 might confer increased protection from disease. Given the variation seen in WNK1 function across different cell types, and the ubiquity of WNK1 expression, therapies targeting WNK1 would need to be applied cautiously as they could cause pathogenic changes in other cell types such as angiogenesis, tumorigenesis, and kidney function (Sie et al., 2020).

7.0 Overall Discussion: Validating a 3Rs Approach to Studying Vascular Responses to Flow

I hypothesised that zebrafish embryos could be used to screen for genes involved in endothelial responses to flow. The data presented in this thesis show that time-lapse imaging of EC nuclei can be used in conjunction with microinjection of morpholinos targeting putative proliferation linked genes to identify genes which were involved in EC proliferation in response to flow. Data from mice confirmed that a flow-responsive gene identified in zebrafish was flow-associated in mammalian endothelium thus supporting the hypothesis.

I identified a link between shear stress and endothelial expression of WNK1 and propose further studies to elucidate the role of WNK1 on endothelial proliferation and atherosclerosis – summarised below (Fig. 29).

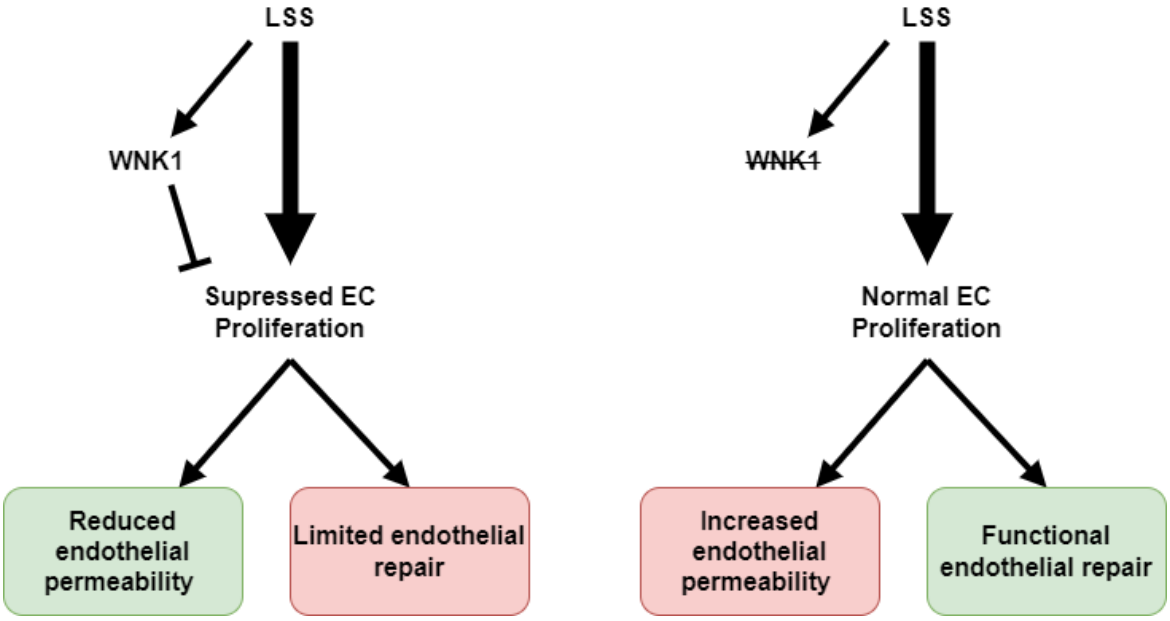

Figure 29: Hypothesized WNK1 function in atherosclerosis. WNK1 expression is increased under LSS (mouse data). Knock-down of WNK1 leads to abolished suppression of EC proliferation in response to absent blood flow (zebrafish data). I hypothesise that suppression of WNK1 would be anti-atherogenic by promoting endothelial barrier repair under LSS, and pro-atherogenic by increasing endothelial permeability under LSS.

7.1 Hypothesised Dual Roles of WNK1 in Atherosclerosis and Impact in the Field

Taking together results from zebrafish and mouse data (Fig 27, Fig 28) show that WNK1 is required for suppression of proliferation under no-flow conditions and is itself upregulated under LSS. Hence, I hypothesise that WNK1 is upregulated under LSS, leading to suppression of EC proliferation. The impact of this in atherosclerosis is twofold. In healthy vasculature suppression of proliferation under LSS maintains tighter cell junctions and thus improves endothelial resistance to lipoprotein accumulation (Morita-Takemura et al., 2016). Thus, we might expect to find abolition of WNK1 is pro-atherogenic by de-restricting proliferation under LSS leading to increased endothelial permeability. However, LSS also increases EC apoptosis which invariably leads to gaps in endothelium if not repaired by fresh EC growth. Hence suppression of EC proliferation may be pro-atherogenic by restricting endothelial repair. In brief, the beneficial effect of reduced EC permeability granted by WNK1 may be outweighed by the limits placed on endothelial repair.

Aberrant EC repair is a known contributor to atherosclerosis (Mak & Kow, 2014) and inability of endothelium to repair damage caused by LSS, ROS, lipids, cigarette smoke, and other factors contribute to initiation of disease (Meng et al., 2018). Given the known roles of WNK1 in EC proliferation and angiogenesis the above hypothesis is plausible. To test it one could create mice with an endothelial specific conditional knockout of WNK1, then study plaque burden in these mice compared to controls. If WNK1 knockout reduced plaque burden, then the hypothesis would be supported.

The major problem for WNK1 is an issue of translating these findings to medical benefits. Should the proposed experiments find that WNK1 knockout reduced plaque formation, it would then be necessary to generate a pharmacological WNK1 inhibitor. However due to the ubiquity of WNK1 expression, including high levels of WNK1 protein and RNA in the male and female reproductive system and brain the likelihood of adverse effects is high (Karlsson et al., 2021; Uhlén et al., 2015). These factors could be somewhat minimized by using tissue targeting drug design approaches which have previously been used to produce vascular targeting agents for anti-cancer medication (Thorpe, 2004), an novel nanoparticle approaches for targeting endothelium exist (Voigt et al., 2014). Thus, it may be possible to achieve endothelium focussed targeting of WNK1 and overcome likely systemic side effects.

Further barriers are the issue of when to begin treatment. Based on the hypothesis one would expect treatment to be most effective prior to development of the fatty streak and onset of disease, as hypothesised WNK1 suppression would increase endothelial repair under LSS, limiting initiation and development of disease. As atherosclerosis is asymptomatic until later stages, this approach would rely on the costly and blanket approach of treating everyone classed as vulnerable by their healthcare system. The alternative, treating symptomatic disease would not result in reversal of disease progression as a complex array of lipid clearing, fibrin degradation and in some cases decalcification would need to occur to reverse the formation of atherosclerotic plaques.

Whilst overall these findings present a well-supported case for further investigation and potential targeting of a powerful upstream shear responsive regulator of EC proliferation, it

may be more fruitful to first investigate the existence of EC specific isoforms of WNK1 as tissue specific isoforms with different functions have been identified in the kidney (Argaiz et al., 2018; Wade et al., 2006). Should similar tissue specific WNK1 isoforms exist in the endothelium they may explain the different effects of on proliferation seen across different cell types (see 6.3.2), and also offer an alternative mechanism for WNK1 targeting treatment either by isoform specific pharmacological targeting or targeting the pathway which produces said theoretical WNK1 isoform (Ma et al., 2019).

7.2 A Novel, Simple Approach for Quantifying EC Proliferation

This work identified a novel, simplified approach for quantifying EC proliferation in the zebrafish embryo. Prior to this thesis, the most widely used methods for studying EC proliferation in zebrafish were counting the number of EC nuclei, which is an indirect approach that ignores EC apoptosis and migration and thus does not truly indicate the rate of proliferation. Or EdU labelling, which detects very few proliferating nuclei during a typical incubation of one hour and is not adaptable to longer detection periods due to the cytotoxicity of EdU and DMSO. Whilst transgenic lines which label the cell cycle in zebrafish ECs exist (Fukuhara et al., 2014), they are not open access, thus there are challenges in their wider use for studying vascular proliferation. I addressed this by describing, and publishing in open access format (Bowley et al., 2021), a method for quantifying EC proliferation using time-lapse confocal imaging of a single fluorophore (*Tg fli1a:nlsmCherry*). The components for generating a transgenic construct for labelling zEC nuclei are open access, and a researcher could produce such a construct in a matter of weeks, which is not the case for EC-fucci. Additionally, the single fluorophore approach allows greater flexibility when imaging, as the user can image at higher speed or reduced laser dosage compared to a two-fluorophore system. Use of a single fluorophore for study of proliferation also permits study of two additional markers (for a three-laser microscope system), whereas a two-fluorophore approach would only leave one 'spare' channel. Consequently, this work offers a novel, accessible, and flexible approach for studying EC proliferation.

7.3 A Novel Approach for Screening Genes for Effects on EC Proliferation, and EC Proliferation in Response to Flow

This work also demonstrated that zebrafish embryos are an efficient *in vivo* tool for screening genes for effects on EC proliferation. No prior approach for screening genes for effects on EC proliferation had been shown, likely because of limited availability of methods for specifically quantifying this process in zebrafish. Here I showed that by utilizing the novel analysis method I described, a targeted, small scale morpholino screen can be used to identify proliferation linked targets from a set of genes identified in existing data. Crucially, genes identified using this screening approach (*wnk1a*) remain flow regulated in mammals. Historically, the most well-known applications of zebrafish for genetic screening were for forward genetics (Knoll et al., 2007), and it is only more recently that application of zebrafish for small molecule and reverse genetic screening has been described (Pott et al., 2018; Serbanovic-Canic et al., 2017).

This study builds on previous work within the group, namely application of zebrafish for screening genes for shear regulation of apoptosis (Serbanovic-Canic et al., 2017). These data support the titular conclusion of this paper, that 'Zebrafish [are a] functional model for screening flow responsive genes', and thus enhance the validity of use of zebrafish as a system to screen for genes involved in EC activation. By demonstrating zebrafish methods for studying apoptosis and proliferation, our work will enhance confidence in zebrafish models and encourage further zebrafish studies which use reverse genetics to screen genes involved in EC activation.

7.4 Potential to Significantly Reduce use of Mice in Vascular Biology Research

The primary model organism for study of EC activation is the mouse. Indeed, internationally, PubMed searches for journal articles (terms [mouse OR mice OR murine] AND endothelial) reveal that from 2011, 56,163 studies used mice to assess endothelial responses to shear stress. Hence with an average group size of eight, and four experimental groups, approximately 1.8 million experimental animals have been used in the past ten years. One aim of this thesis was to show that zebrafish embryos can reduce the use of mice in CVD research. Within the group, successful use of zebrafish for screening of proliferation, and previously apoptosis linked genes (Serbanovic-Canic et al., 2017) has led to internal adoption of zebrafish as a system for pre-screening genes identified in our wider omics studies. By pre-screening candidate genes in zebrafish, we can identify genes which directly affect EC proliferation or apoptosis, and thus reduce the total number of genes taken forward to studies in mice. We calculate that adoption of zebrafish pre-screening within the group will reduce use of mice by 5000 over the next three years, this represents a 50% reduction in mouse usage and meets the aims of this work.

Reduced mouse use confers 3R's benefits, including increased public acceptance of our work – 25% of people don't accept animal research for any reason (Williams, 2020). Additionally, whilst use of zebrafish embryos does not eliminate the use of animals, it uses animals with reduced sentience, which is an improvement. Another consequence of reduced mouse usage is reduced animal costs, which allows allocation of funds to other program components. Wider adoption of zebrafish pre-screening would significantly amplify the impact on animal use, this has been partly facilitated by publication of the methods used, however more could be done to enhance the adoptability of my approach, such as development of an automated system for quantifying EC proliferation, and development of an open access version of the transgenic used.

7.5 Future Work

There are several routes that could be expanded in future work:

7.5.1 Zebrafish Transgenesis and Super Resolution Imaging to Determine the Function of Genes of Interest *In Vivo*

Whilst the approach described in chapter five allowed us to identify genes with roles in EC proliferation in response to flow, it did not allow us to investigate their precise localisation and interaction within the endothelium when subject to varying wall shear stress. Given

what is known about the effect of shear stress on WNK1 localisation and expression (for example), further investigation could uncover more of the mechanism of action for WNK1 in response to flow.

Typically, mechanistic studies of genes emerging from zebrafish screens use cell culture and mice experiments to identify a mechanism of action for the gene of interest in disease (Serbanovic-Canic et al., 2017). Whilst zebrafish cannot yet be used to study the role of genes in plaque formation, their functionally complete vasculature presents an opportunity to study gene function in response to flow *in vivo.* By using the LSM880 in super resolution mode, rather than fast mode, which was used in chapter five, it is possible to image at ~115 nm resolution, which would be sufficient to visualise cytoskeletal conformation and protein localisation within the cell. This approach could be combined with transgenesis techniques such as CRISPR homology directed recombination, to study the movement and localisation of *wnk1a* or other proteins of interest within ECs. If validated, this approach would increase the utility of zebrafish functional studies and would likely produce more biologically relevant data relative to reductionist cell culture approaches.

7.5.2 Zebrafish Embryos for Cardiotoxicity Screening of Pharmacological Modulators of EC Activation

Aside from their use in atherosclerosis research, zebrafish embryos have also been used to screen genes and drugs for effects on cardiac function. Drugs showing pre-clinical efficacy are subsequently analysed for cardiotoxicity in rodents and dogs and discarded if they are deleterious. Hence many drugs are abandoned at a relatively late stage which represents poor value from animal experiments and a waste of resources. Because of this, several groups are screening drug libraries for cardiotoxicity using zebrafish models (G. Bowley, E. Kugler, et al., 2021). For example, the NC3Rs CRACK-IT solution ZeGlobalTox used software to extract beats per minute, QTc, ejection fraction and longest arrest information from high-speed images of the zebrafish heart (Cornet et al., 2017). This technology could be used to study the cardiotoxicity of drugs targeting genes involved in EC activation in zebrafish embryos, prior to use in mammals.

7.5.3 Driving Wider Adoption of Zebrafish Models

Dissemination and uptake of non-mammalian models in the wider scientific community is now recognised as a major challenge in the 3Rs community (termed the ‘valley of death’; NC3Rs Strategy summary 2017-2019). Whilst zebrafish models have clear benefits in terms of both cardiovascular science and 3Rs, their positive impact on animal use requires other research groups in the cardiovascular field to adopt them. However, there are several challenges to the implementation of zebrafish models including: (1) lack of awareness, (2) lack of confidence, (3) practical barriers including access to aquarium facilities and lack of training in specialised protocols. These obstacles are not insurmountable, however establishing zebrafish as a model requires specialised techniques which may be a deterrent. Therefore, to improve adoption, we must educate researchers on the benefits offered by zebrafish models of atherosclerosis, provide detailed protocols on their use, reduce practical barriers, and generate models with greater utility and lower cost than those currently

available. During this project I addressed these challenges by conducting public engagement work with academics (through conference presentations), schools, and by writing detailed methods for my model for F1000 (Bowley et al., 2021).

Future work could greatly shift the balance towards zebrafish adoption by developing and disseminating widely a transgenic line that integrates multiple markers of EC activation (apoptosis, proliferation, inflammation) and cardiac function into a single zebrafish line. If developed from scratch, transgenes could be made as a single insert and full distribution rights would be available, thus greatly simplifying the process of open sourcing the line. Open sourcing this line/plasmid would make it much easier for researchers without prior expertise to establish a zebrafish model for cardiovascular research and will increase visibility and confidence in zebrafish models throughout the field. This would shift the cost/benefit equation in favour of adoption both for academic research groups and industry (for whom rights to transgenics, or plasmids produced in academia are typically restricted), who could use the line to screen novel therapeutics for effects on EC processes and cardiotoxicity thus reducing the number of drugs that go on to mammalian safety studies.

8.0 Bibliography

Agmon, Y., Khandheria, B. K., Meissner, I., Schwartz, G. L., Petterson, T. M., O'Fallon, W. M., . . . Seward, J. B. (2000). Independent association of high blood pressure and aortic atherosclerosis: A population-based study. *Circulation*, *102*(17), 2087-2093. https://doi.org/10.1161/01.cir.102.17.2087

Akaike, M., Che, W., Marmarosh, N. L., Ohta, S., Osawa, M., Ding, B., . . . Abe, J. (2004). The hinge-helix 1 region of peroxisome proliferator-activated receptor gamma1 (PPARgamma1) mediates interaction with extracellular signal-regulated kinase 5 and PPARgamma1 transcriptional activation: involvement in flow-induced PPARgamma activation in endothelial cells. *Mol Cell Biol*, *24*(19), 8691-8704. https://doi.org/10.1128/MCB.24.19.8691-8704.2004

Akimoto, S., Mitsumata, M., Sasaguri, T., & Yoshida, Y. (2000). Laminar shear stress inhibits vascular endothelial cell proliferation by inducing cyclin-dependent kinase inhibitor p21(Sdi1/Cip1/Waf1). *Circ Res*, *86*(2), 185-190. https://doi.org/10.1161/01.res.86.2.185

Allender, S., & Rayner, M. (2007). The burden of overweight and obesity-related ill health in the UK. *Obes Rev*, *8*(5), 467-473. https://doi.org/10.1111/j.1467-789X.2007.00394.x

Amini, N., Boyle, J. J., Moers, B., Warboys, C. M., Malik, T. H., Zakkar, M., . . . Evans, P. C. (2014). Requirement of JNK1 for endothelial cell injury in atherogenesis. *Atherosclerosis*, *235*(2), 613-618. https://doi.org/10.1016/j.atherosclerosis.2014.05.950

Argaiz, E. R., Chavez-Canales, M., Ostrosky-Frid, M., Rodríguez-Gama, A., Vázquez, N., Gonzalez-Rodriguez, X., . . . Gamba, G. (2018). Kidney-specific WNK1 isoform (KS-WNK1) is a potent activator of WNK4 and NCC. *Am J Physiol Renal Physiol*, *315*(3), F734-F745. https://doi.org/10.1152/ajprenal.00145.2018

Arrenberg, A. B., Stainier, D. Y., Baier, H., & Huisken, J. (2010). Optogenetic control of cardiac function. *Science*, *330*(6006), 971-974. https://doi.org/10.1126/science.1195929

Back, M. R., Carew, T. E., & Schmid-Schoenbein, G. W. (1995). Deposition pattern of monocytes and fatty streak development in hypercholesterolemic rabbits. *Atherosclerosis*, *116*(1), 103-115. https://doi.org/10.1016/0021-9150(95)05533-3

Ballermann, B. J., Dardik, A., Eng, E., & Liu, A. (1998). Shear stress and the endothelium. *Kidney Int Suppl*, *67*, S100-108. https://doi.org/10.1046/j.1523-1755.1998.06720.x

Barter, P. (2005). The role of HDL-cholesterol in preventing atherosclerotic disease. *European Heart Journal Supplements*, *7*. https://doi.org/doi:10.1093/eurheartj/sui036

Bartling, B., Tostlebe, H., Darmer, D., Holtz, J., Silber, R. E., & Morawietz, H. (2000). Shear stress-dependent expression of apoptosis-regulating genes in endothelial cells. *Biochem Biophys Res Commun*, *278*(3), 740-746. https://doi.org/10.1006/bbrc.2000.3873

Beech, D. J., & Kalli, A. C. (2019). Force Sensing by Piezo Channels in Cardiovascular Health and Disease. *Arterioscler Thromb Vasc Biol*, *39*(11), 2228-2239. https://doi.org/10.1161/ATVBAHA.119.313348

Bergaya, S., Faure, S., Baudrie, V., Rio, M., Escoubet, B., Bonnin, P., . . . Hadchouel, J. (2011). WNK1 Regulates Vasoconstriction and Blood Pressure Response to α1-Adrenergic Stimulation in Mice. *Hypertension*, *58*(3), 439-445. https://doi.org/10.1161/HYPERTENSIONAHA.111.172429

Bhopal, R., Vettini, A., Hunt, S., Wiebe, S., Hanna, L., & Amos, A. (2004). Review of prevalence data in, and evaluation of methods for cross cultural adaptation of, UK surveys on tobacco and alcohol in ethnic minority groups. *BMJ*, *328*(7431), 76. https://doi.org/10.1136/bmj.37963.426308.9A

Borén, J., Chapman, M. J., Krauss, R. M., Packard, C. J., Bentzon, J. F., Binder, C. J., . . . Ginsberg, H. N. (2020). Low-density lipoproteins cause atherosclerotic cardiovascular disease: pathophysiological, genetic, and therapeutic insights: a consensus statement from the European Atherosclerosis Society Consensus Panel. *European Heart Journal*, *41*(24), 2313-2330. https://doi.org/10.1093/eurheartj/ehz962

Bouldin, C. M., & Kimelman, D. (2014). Dual fucci: a new transgenic line for studying the cell cycle from embryos to adults. *Zebrafish*, *11*(2), 182-183. https://doi.org/10.1089/zeb.2014.0986
Bowley, TJ. Chico, J. Serbanovic-Canic, & Evans, P. (2021). Quantifying endothelial cell proliferation in the zebrafish embryo [version 1; peer review: awaiting peer review]. *F1000Research*, *10*(1032). https://doi.org/10.12688/f1000research.73130.1
Bowley, G., Chico, T., Serbanovic-Canic, J., & Evans, P. (2021). Quantifying endothelial cell proliferation in the zebrafish embryo [version 1; peer review: awaiting peer review]. *F1000Research*, *10*(1032). https://doi.org/10.12688/f1000research.73130.1
Bowley, G., Kugler, E., Wilkinson, R., Lawrie, A., van Eeden, F., Chico, T. J. A., . . . Serbanovic-Canic, J. (2021). Zebrafish as a tractable model of human cardiovascular disease. *Br J Pharmacol*. https://doi.org/10.1111/bph.15473
Braam, B., de Roos, R., Bluyssen, H., Kemmeren, P., Holstege, F., Joles, J. A., & Koomans, H. (2005). Nitric oxide-dependent and nitric oxide-independent transcriptional responses to high shear stress in endothelial cells. *Hypertension*, *45*(4), 672-680. https://doi.org/10.1161/01.HYP.0000154683.33414.94
Brissette, M. J., Lepage, S., Lamonde, A. S., Sirois, I., Groleau, J., Laurin, L. P., & Cailhier, J. F. (2012). MFG-E8 released by apoptotic endothelial cells triggers anti-inflammatory macrophage reprogramming. *PLoS One*, *7*(4), e36368. https://doi.org/10.1371/journal.pone.0036368
Buchanan, C. F., Verbridge, S. S., Vlachos, P. P., & Rylander, M. N. (2014). Flow shear stress regulates endothelial barrier function and expression of angiogenic factors in a 3D microfluidic tumor vascular model. *Cell Adh Migr*, *8*(5), 517-524. https://doi.org/10.4161/19336918.2014.970001
Camacho, P., Fan, H., Liu, Z., & He, J.-Q. (2016). Large Mammalian Animal Models of Heart Disease. *Journal of cardiovascular development and disease*, *3*(4), 30. https://doi.org/10.3390/jcdd3040030
Campinho, P., Vilfan, A., & Vermot, J. (2020). Blood Flow Forces in Shaping the Vascular System: A Focus on Endothelial Cell Behavior. *Front Physiol*, *11*, 552. https://doi.org/10.3389/fphys.2020.00552
Cancel, L. M., & Tarbell, J. M. (2010). The role of apoptosis in LDL transport through cultured endothelial cell monolayers. *Atherosclerosis*, *208*(2), 335-341. https://doi.org/10.1016/j.atherosclerosis.2009.07.051
Cancel, L. M., & Tarbell, J. M. (2011). The role of mitosis in LDL transport through cultured endothelial cell monolayers. *Am J Physiol Heart Circ Physiol*, *300*(3), H769-776. https://doi.org/10.1152/ajpheart.00445.2010
Caplan, B. A., & Schwartz, C. J. (1973). Increased endothelial cell turnover in areas of in vivo Evans Blue uptake in the pig aorta. *Atherosclerosis*, *17*(3), 401-417. https://doi.org/10.1016/0021-9150(73)90031-2
Caro, C. G., Fitz-Gerald, J. M., & Schroter, R. C. (1969). Arterial wall shear and distribution of early atheroma in man. *Nature*, *223*(5211), 1159-1160. https://doi.org/10.1038/2231159a0
Carrisoza-Gaytan, R., Subramanya, A. R., Ray, E. C., Kleyman, T. R., & Satlin, L. M. (2020). Flow regulation of WNK1 localization in the cortical collecting duct (CCD). *The FASEB Journal*, *34*(S1), 1-1. https://doi.org/https://doi.org/10.1096/fasebj.2020.34.s1.05332
Carroll, K. J., & North, T. E. (2014). Oceans of opportunity: exploring vertebrate hematopoiesis in zebrafish. *Exp Hematol*, *42*(8), 684-696. https://doi.org/10.1016/j.exphem.2014.05.002
Cavodeassi, F., Carreira-Barbosa, F., Young, R. M., Concha, M. L., Allende, M. L., Houart, C., . . . Wilson, S. W. (2005). Early stages of zebrafish eye formation require the coordinated activity of Wnt11, Fz5, and the Wnt/beta-catenin pathway. *Neuron*, *47*(1), 43-56. https://doi.org/10.1016/j.neuron.2005.05.026
Chakraborty, A., Chakraborty, S., Jala, V. R., Haribabu, B., Sharp, M. K., & Berson, R. E. (2012). Effects of biaxial oscillatory shear stress on endothelial cell proliferation and morphology. *Biotechnol Bioeng*, *109*(3), 695-707. https://doi.org/10.1002/bit.24352

Chaudhury, H., Zakkar, M., Boyle, J., Cuhlmann, S., van der Heiden, K., Luong, l. A., . . . Evans, P. C. (2010). c-Jun N-terminal kinase primes endothelial cells at atheroprone sites for apoptosis. *Arterioscler Thromb Vasc Biol*, *30*(3), 546-553. https://doi.org/10.1161/ATVBAHA.109.201368

Chen, Y., Jiang, Z., Fisher, K. H., Kim, H. R., Evans, P. C., & Wilkinson, R. N. (2021). Blood flow coordinates collective endothelial cell migration during vascular plexus formation and promotes angiogenic sprout regression via vegfr3/flt4. *bioRxiv*, 2021.2007.2023.453496. https://doi.org/10.1101/2021.07.23.453496

Chen, Y. C., Bui, A. V., Diesch, J., Manasseh, R., Hausding, C., Rivera, J., . . . Peter, K. (2013). A novel mouse model of atherosclerotic plaque instability for drug testing and mechanistic/therapeutic discoveries using gene and microRNA expression profiling. *Circ Res*, *113*(3), 252-265. https://doi.org/10.1161/CIRCRESAHA.113.301562

Chi, R. A., Wang, T., Huang, C. L., Wu, S. P., Young, S. L., Lydon, J. P., & DeMayo, F. J. (2020). WNK1 regulates uterine homeostasis and its ability to support pregnancy. *JCI Insight*, *5*(22). https://doi.org/10.1172/jci.insight.141832

Chistiakov, D. A., Bobryshev, Y. V., & Orekhov, A. N. (2016). Macrophage-mediated cholesterol handling in atherosclerosis. *J Cell Mol Med*, *20*(1), 17-28. https://doi.org/10.1111/jcmm.12689

Chu, J., Mir, A., Gao, N., Rosa, S., Monson, C., Sharma, V., . . . Sadler, K. C. (2013). A zebrafish model of congenital disorders of glycosylation with phosphomannose isomerase deficiency reveals an early opportunity for corrective mannose supplementation. *Dis Model Mech*, *6*(1), 95-105. https://doi.org/10.1242/dmm.010116

Chávez-Canales, M., Zhang, C., Soukaseum, C., Moreno, E., Pacheco-Alvarez, D., Vidal-Petiot, E., . . . Hadchouel, J. (2014). WNK-SPAK-NCC cascade revisited: WNK1 stimulates the activity of the Na-Cl cotransporter via SPAK, an effect antagonized by WNK4. *Hypertension*, *64*(5), 1047-1053. https://doi.org/10.1161/HYPERTENSIONAHA.114.04036

Cornet, C., Calzolari, S., Miñana-Prieto, R., Dyballa, S., van Doornmalen, E., Rutjes, H., . . . Terriente, J. (2017). ZeGlobalTox: An Innovative Approach to Address Organ Drug Toxicity Using Zebrafish. *Int J Mol Sci*, *18*(4). https://doi.org/10.3390/ijms18040864

Dardik, A., Chen, L., Frattini, J., Asada, H., Aziz, F., Kudo, F. A., & Sumpio, B. E. (2005). Differential effects of orbital and laminar shear stress on endothelial cells. *J Vasc Surg*, *41*(5), 869-880. https://doi.org/10.1016/j.jvs.2005.01.020

Dbouk, H. A., Weil, L. M., Perera, G. K., Dellinger, M. T., Pearson, G., Brekken, R. A., & Cobb, M. H. (2014). Actions of the protein kinase WNK1 on endothelial cells are differentially mediated by its substrate kinases OSR1 and SPAK. *Proc Natl Acad Sci U S A*, *111*(45), 15999-16004. https://doi.org/10.1073/pnas.1419057111

DeGraba, T. J. (2004). Immunogenetic susceptibility of atherosclerotic stroke: implications on current and future treatment of vascular inflammation. *Stroke*, *35*(11 Suppl 1), 2712-2719. https://doi.org/10.1161/01.STR.0000143788.87054.85

Dejana, E., & Orsenigo, F. (2013). Endothelial adherens junctions at a glance. *J Cell Sci*, *126*(Pt 12), 2545-2549. https://doi.org/10.1242/jcs.124529

DeStefano, J. G., Williams, A., Wnorowski, A., Yimam, N., Searson, P. C., & Wong, A. D. (2017). Real-time quantification of endothelial response to shear stress and vascular modulators. *Integr Biol (Camb)*, *9*(4), 362-374. https://doi.org/10.1039/c7ib00023e

Dimmeler, S., Fleming, I., Fisslthaler, B., Hermann, C., Busse, R., & Zeiher, A. M. (1999). Activation of nitric oxide synthase in endothelial cells by Akt-dependent phosphorylation. *Nature*, *399*(6736), 601-605. https://doi.org/10.1038/21224

Dimmeler, S., Rippmann, V., Weiland, U., Haendeler, J., & Zeiher, A. M. (1997). Angiotensin II induces apoptosis of human endothelial cells. Protective effect of nitric oxide. *Circ Res*, *81*(6), 970-976. https://doi.org/10.1161/01.res.81.6.970

Dolan, J. M., Meng, H., Singh, S., Paluch, R., & Kolega, J. (2011). High fluid shear stress and spatial shear stress gradients affect endothelial proliferation, survival, and alignment. *Ann Biomed Eng*, *39*(6), 1620-1631. https://doi.org/10.1007/s10439-011-0267-8

Doran, A. C., Meller, N., & McNamara, C. A. (2008). Role of smooth muscle cells in the initiation and early progression of atherosclerosis. *Arterioscler Thromb Vasc Biol*, *28*(5), 812-819. https://doi.org/10.1161/ATVBAHA.107.159327

Doran, S., Arif, M., Lam, S., Bayraktar, A., Turkez, H., Uhlen, M., . . . Mardinoglu, A. (2021). Multi-omics approaches for revealing the complexity of cardiovascular disease. *Brief Bioinform*, *22*(5). https://doi.org/10.1093/bib/bbab061

Douglas, G., & Channon, K. (2010). The pathogenesis of atherosclerosis. *PATHOGENESIS, RISK FACTORS AND PREVENTION*, *38*(8), 397-402. https://doi.org/https://doi.org/10.1016/j.mpmed.2010.05.002

Ebert, A. M., Childs, S. J., Hehr, C. L., Cechmanek, P. B., & McFarlane, S. (2014). Sema6a and Plxna2 mediate spatially regulated repulsion within the developing eye to promote eye vesicle cohesion. *Development*, *141*(12), 2473-2482. https://doi.org/10.1242/dev.103499

Ehling, M., Celus, W., Martín-Pérez, R., Alba-Rovira, R., Willox, S., Ponti, D., . . . Mazzone, M. (2020). B55α/PP2A Limits Endothelial Cell Apoptosis During Vascular Remodeling: A Complementary Approach To Disrupt Pathological Vessels? *Circ Res*, *127*(6), 707-723. https://doi.org/10.1161/CIRCRESAHA.119.316071

Eitzman, D. T., Westrick, R. J., Shen, Y., Bodary, P. F., Gu, S., Manning, S. L., . . . Ginsburg, D. (2005). Homozygosity for factor V Leiden leads to enhanced thrombosis and atherosclerosis in mice. *Circulation*, *111*(14), 1822-1825. https://doi.org/10.1161/01.CIR.0000160854.75779.E8

Ekker, S. C. (2000). Morphants: a new systematic vertebrate functional genomics approach. *Yeast*, *17*(4), 302-306. https://doi.org/10.1002/1097-0061(200012)17:4<302::Aid-yea53>3.0.Co;2-#

El-Brolosy, M. A., Kontarakis, Z., Rossi, A., Kuenne, C., Günther, S., Fukuda, N., . . . Stainier, D. Y. R. (2019). Genetic compensation triggered by mutant mRNA degradation. *Nature*, *568*(7751), 193-197. https://doi.org/10.1038/s41586-019-1064-z

Estruch, M., Sánchez-Quesada, J. L., Ordóñez Llanos, J., & Benítez, S. (2013). Electronegative LDL: a circulating modified LDL with a role in inflammation. *Mediators Inflamm*, *2013*, 181324. https://doi.org/10.1155/2013/181324

Ezaki, T., Baluk, P., Thurston, G., La Barbara, A., Woo, C., & McDonald, D. M. (2001). Time course of endothelial cell proliferation and microvascular remodeling in chronic inflammation. *Am J Pathol*, *158*(6), 2043-2055. https://doi.org/10.1016/S0002-9440(10)64676-7

Fahed, A. C., & Jang, I. K. (2021). Plaque erosion and acute coronary syndromes: phenotype, molecular characteristics and future directions. *Nat Rev Cardiol*, *18*(10), 724-734. https://doi.org/10.1038/s41569-021-00542-3

Fan, J., Shimoyamada, H., Sun, H., Marcovina, S., Honda, K., & Watanabe, T. (2001). Transgenic rabbits expressing human apolipoprotein(a) develop more extensive atherosclerotic lesions in response to a cholesterol-rich diet. *Arterioscler Thromb Vasc Biol*, *21*(1), 88-94. https://doi.org/10.1161/01.atv.21.1.88

Fhayli, W., Boëté, Q., Harki, O., Briançon-Marjollet, A., Jacob, M.-P., & Faury, G. (2019). Rise and fall of elastic fibers from development to aging. Consequences on arterial structure-function and therapeutical perspectives. *Matrix Biology*, *84*, 41-56. https://doi.org/https://doi.org/10.1016/j.matbio.2019.08.005

Fukuchi, M., Watanabe, J., Kumagai, K., Baba, S., Shinozaki, T., Miura, M., . . . Shirato, K. (2002). Normal and oxidized low density lipoproteins accumulate deep in physiologically thickened intima of human coronary arteries. *Lab Invest*, *82*(10), 1437-1447. https://doi.org/10.1097/01.lab.0000032546.01658.5d

Fukuhara, S., Zhang, J., Yuge, S., Ando, K., Wakayama, Y., Sakaue-Sawano, A., . . . Mochizuki, N. (2014). Visualizing the cell-cycle progression of endothelial cells in zebrafish. *Dev Biol*, *393*(1), 10-23. https://doi.org/10.1016/j.ydbio.2014.06.015

Galley, H. F., & Webster, N. R. (2004). Physiology of the endothelium. *Br J Anaesth*, *93*(1), 105-113. https://doi.org/10.1093/bja/aeh163
Gialeli, C., Shami, A., & Gonçalves, I. (2021). Extracellular matrix: paving the way to the newest trends in atherosclerosis. *Current opinion in lipidology*, *32*(5), 277-285. https://doi.org/10.1097/MOL.0000000000000775
Givens, C., & Tzima, E. (2016). Endothelial Mechanosignaling: Does One Sensor Fit All? *Antioxidants & redox signaling*, *25*(7), 373-388. https://doi.org/10.1089/ars.2015.6493
Goettsch, C., Hutcheson, J. D., Hagita, S., Rogers, M. A., Creager, M. D., Pham, T., . . . Aikawa, E. (2016). A single injection of gain-of-function mutant PCSK9 adeno-associated virus vector induces cardiovascular calcification in mice with no genetic modification. *Atherosclerosis*, *251*, 109-118. https://doi.org/10.1016/j.atherosclerosis.2016.06.011
Goetz, J. G., Steed, E., Ferreira, R. R., Roth, S., Ramspacher, C., Boselli, F., . . . Vermot, J. (2014). Endothelial cilia mediate low flow sensing during zebrafish vascular development. *Cell Rep*, *6*(5), 799-808. https://doi.org/10.1016/j.celrep.2014.01.032
Golledge, J., & Norman, P. E. (2010). Atherosclerosis and abdominal aortic aneurysm: cause, response, or common risk factors? *Arterioscler Thromb Vasc Biol*, *30*(6), 1075-1077. https://doi.org/10.1161/ATVBAHA.110.206573
Guo, D., Chien, S., & Shyy, J. Y. (2007). Regulation of endothelial cell cycle by laminar versus oscillatory flow: distinct modes of interactions of AMP-activated protein kinase and Akt pathways. *Circ Res*, *100*(4), 564-571. https://doi.org/10.1161/01.RES.0000259561.23876.c5
Han, K. H., Tangirala, R. K., Green, S. R., & Quehenberger, O. (1998). Chemokine receptor CCR2 expression and monocyte chemoattractant protein-1-mediated chemotaxis in human monocytes. A regulatory role for plasma LDL. *Arterioscler Thromb Vasc Biol*, *18*(12), 1983-1991. https://doi.org/10.1161/01.atv.18.12.1983
Havel, R. J., Yamada, N., & Shames, D. M. (1989). Watanabe heritable hyperlipidemic rabbit. Animal model for familial hypercholesterolemia. *Arteriosclerosis*, *9*(1 Suppl), I33-38.
He, Y., Hara, H., & Núñez, G. (2016). Mechanism and Regulation of NLRP3 Inflammasome Activation. *Trends Biochem Sci*, *41*(12), 1012-1021. https://doi.org/10.1016/j.tibs.2016.09.002
Heo, K. S., Lee, H., Nigro, P., Thomas, T., Le, N. T., Chang, E., . . . Abe, J. (2011). PKCζ mediates disturbed flow-induced endothelial apoptosis via p53 SUMOylation. *J Cell Biol*, *193*(5), 867-884. https://doi.org/10.1083/jcb.201010051
Herbert, S. P., Huisken, J., Kim, T. N., Feldman, M. E., Houseman, B. T., Wang, R. A., . . . Stainier, D. Y. (2009). Arterial-venous segregation by selective cell sprouting: an alternative mode of blood vessel formation. *Science*, *326*(5950), 294-298. https://doi.org/10.1126/science.1178577
Hubbard, A. K., & Rothlein, R. (2000). Intercellular adhesion molecule-1 (ICAM-1) expression and cell signaling cascades. *Free Radic Biol Med*, *28*(9), 1379-1386. https://doi.org/10.1016/s0891-5849(00)00223-9
Hulthe, J., & Fagerberg, B. (2002). Circulating oxidized LDL is associated with subclinical atherosclerosis development and inflammatory cytokines (AIR Study). *Arterioscler Thromb Vasc Biol*, *22*(7), 1162-1167. https://doi.org/10.1161/01.atv.0000021150.63480.cd
Ihle-Hansen, H., Sandset, E. C., & Hagberg, G. (2021). Subclinical Carotid Artery Atherosclerosis and Cognitive Function: A Mini-Review. *Front Neurol*, *12*, 705043. https://doi.org/10.3389/fneur.2021.705043
Ishida, T., Takahashi, M., Corson, M. A., & Berk, B. C. (1997). Fluid shear stress-mediated signal transduction: how do endothelial cells transduce mechanical force into biological responses? *Ann N Y Acad Sci*, *811*, 12-23; discussion 23-14. https://doi.org/10.1111/j.1749-6632.1997.tb51984.x
Ji, D., Zhao, G., Songstad, A., Cui, X., & Weinstein, E. J. (2015). Efficient creation of an APOE knockout rabbit. *Transgenic Res*, *24*(2), 227-235. https://doi.org/10.1007/s11248-014-9834-8
Jiang, Z. Y., Zhou, Q. L., Holik, J., Patel, S., Leszyk, J., Coleman, K., . . . Czech, M. P. (2005). Identification of WNK1 as a substrate of Akt/protein kinase B and a negative regulator of

insulin-stimulated mitogenesis in 3T3-L1 cells. *J Biol Chem*, *280*(22), 21622-21628. https://doi.org/10.1074/jbc.M414464200

Jin, Z. G., Ueba, H., Tanimoto, T., Lungu, A. O., Frame, M. D., & Berk, B. C. (2003). Ligand-independent activation of vascular endothelial growth factor receptor 2 by fluid shear stress regulates activation of endothelial nitric oxide synthase. *Circ Res*, *93*(4), 354-363. https://doi.org/10.1161/01.RES.0000089257.94002.96

Johnson, N. M., Farr, G. H., & Maves, L. (2013). The HDAC Inhibitor TSA Ameliorates a Zebrafish Model of Duchenne Muscular Dystrophy. *PLoS Curr*, *5*. https://doi.org/10.1371/currents.md.8273cf41db10e2d15dd3ab827cb4b027

Johnston, R. D., Gaul, R. T., & Lally, C. (2021). An investigation into the critical role of fibre orientation in the ultimate tensile strength and stiffness of human carotid plaque caps. *Acta Biomaterialia*, *124*, 291-300. https://doi.org/https://doi.org/10.1016/j.actbio.2021.02.008

Kamachi, Y., Okuda, Y., & Kondoh, H. (2008). Quantitative assessment of the knockdown efficiency of morpholino antisense oligonucleotides in zebrafish embryos using a luciferase assay. *Genesis*, *46*(1), 1-7. https://doi.org/10.1002/dvg.20361

Karamanos, N. K., Theocharis, A. D., Piperigkou, Z., Manou, D., Passi, A., Skandalis, S. S., . . . Onisto, M. (2021). A guide to the composition and functions of the extracellular matrix. *FEBS J*, *288*(24), 6850-6912. https://doi.org/10.1111/febs.15776

Karlsson, M., Zhang, C., Méar, L., Zhong, W., Digre, A., Katona, B., . . . Lindskog, C. (2021). A single–cell type transcriptomics map of human tissues. *Science Advances*, *7*(31), eabh2169. https://doi.org/10.1126/sciadv.abh2169

Ketharnathan, S., Labudina, A., & Horsfield, J. A. (2020). Cohesin Components Stag1 and Stag2 Differentially Influence Haematopoietic Mesoderm Development in Zebrafish Embryos. *Front Cell Dev Biol*, *8*, 617545. https://doi.org/10.3389/fcell.2020.617545

Kim, S., & Woo, C. H. (2018). Laminar Flow Inhibits ER Stress-Induced Endothelial Apoptosis through PI3K/Akt-Dependent Signaling Pathway. *Mol Cells*, *41*(11), 964-970. https://doi.org/10.14348/molcells.2018.0111

Knoll, R., Postel, R., Wang, J., Kratzner, R., Hennecke, G., Vacaru, A. M., . . . Bakkers, J. (2007). Laminin-alpha4 and integrin-linked kinase mutations cause human cardiomyopathy via simultaneous defects in cardiomyocytes and endothelial cells. *Circulation*, *116*(5), 515-525. https://doi.org/10.1161/CIRCULATIONAHA.107.689984

Kochhan, E., Lenard, A., Ellertsdottir, E., Herwig, L., Affolter, M., Belting, H. G., & Siekmann, A. F. (2013). Blood flow changes coincide with cellular rearrangements during blood vessel pruning in zebrafish embryos. *PLoS One*, *8*(10), e75060. https://doi.org/10.1371/journal.pone.0075060

Kojda, G., & Harrison, D. (1999). Interactions between NO and reactive oxygen species: pathophysiological importance in atherosclerosis, hypertension, diabetes and heart failure. *Cardiovasc Res*, *43*(3), 562-571. https://doi.org/10.1016/s0008-6363(99)00169-8

Kok, F. O., Shin, M., Ni, C. W., Gupta, A., Grosse, A. S., van Impel, A., . . . Lawson, N. D. (2015). Reverse genetic screening reveals poor correlation between morpholino-induced and mutant phenotypes in zebrafish. *Dev Cell*, *32*(1), 97-108. https://doi.org/10.1016/j.devcel.2014.11.018

Koo, A., Nordsletten, D., Umeton, R., Yankama, B., Ayyadurai, S., García-Cardeña, G., & Dewey, C. F. (2013). In silico modeling of shear-stress-induced nitric oxide production in endothelial cells through systems biology. *Biophys J*, *104*(10), 2295-2306. https://doi.org/10.1016/j.bpj.2013.03.052

Kugler, E., Snodgrass, R., Bowley, G., Plant, K., Serbanovic-Canic, J., Hamilton, N., . . . Armitage, P. (2021). The effect of absent blood flow on the zebrafish cerebral and trunk vasculature. *Vasc Biol*, *3*(1), 1-16. https://doi.org/10.1530/VB-21-0009

Kwak, B. R., Bäck, M., Bochaton-Piallat, M. L., Caligiuri, G., Daemen, M. J., Davies, P. F., . . . Evans, P. C. (2014). Biomechanical factors in atherosclerosis: mechanisms and clinical implications. *Eur Heart J*, *35*(43), 3013-3020, 3020a-3020d. https://doi.org/10.1093/eurheartj/ehu353

Lai, J. G., Tsai, S. M., Tu, H. C., Chen, W. C., Kou, F. J., Lu, J. W., . . . Yuh, C. H. (2014). Zebrafish WNK lysine deficient protein kinase 1 (wnk1) affects angiogenesis associated with VEGF signaling. *PLoS One*, *9*(8), e106129. https://doi.org/10.1371/journal.pone.0106129

Lawson, N. D., & Weinstein, B. M. (2002). In vivo imaging of embryonic vascular development using transgenic zebrafish. *Dev Biol*, *248*(2), 307-318. https://doi.org/10.1006/dbio.2002.0711

Lee, H. C., Tsai, J. N., Liao, P. Y., Tsai, W. Y., Lin, K. Y., Chuang, C. C., . . . Tsai, H. J. (2007). Glycogen synthase kinase 3 alpha and 3 beta have distinct functions during cardiogenesis of zebrafish embryo. *BMC Dev Biol*, *7*, 93. https://doi.org/10.1186/1471-213X-7-93

Lee, J., & Cooke, J. P. (2012). Nicotine and pathological angiogenesis. *Life sciences*, *91*(21-22), 1058-1064. https://doi.org/10.1016/j.lfs.2012.06.032

Leung, A. Y., Leung, J. C., Chan, L. Y., Ma, E. S., Kwan, T. T., Lai, K. N., . . . Liang, R. (2005). Proliferating cell nuclear antigen (PCNA) as a proliferative marker during embryonic and adult zebrafish hematopoiesis. *Histochem Cell Biol*, *124*(2), 105-111. https://doi.org/10.1007/s00418-005-0003-2

Levkau, B., Kenagy, R. D., Karsan, A., Weitkamp, B., Clowes, A. W., Ross, R., & Raines, E. W. (2002). Activation of metalloproteinases and their association with integrins: an auxiliary apoptotic pathway in human endothelial cells. *Cell Death Differ*, *9*(12), 1360-1367. https://doi.org/10.1038/sj.cdd.4401106

Li, X., Wang, L., Fang, P., Sun, Y., Jiang, X., Wang, H., & Yang, X. F. (2018). Lysophospholipids induce innate immune transdifferentiation of endothelial cells, resulting in prolonged endothelial activation. *J Biol Chem*, *293*(28), 11033-11045. https://doi.org/10.1074/jbc.RA118.002752

Lin, K., Hsu, P. P., Chen, B. P., Yuan, S., Usami, S., Shyy, J. Y., . . . Chien, S. (2000). Molecular mechanism of endothelial growth arrest by laminar shear stress. *Proc Natl Acad Sci U S A*, *97*(17), 9385-9389. https://doi.org/10.1073/pnas.170282597

Lister, J. A., Robertson, C. P., Lepage, T., Johnson, S. L., & Raible, D. W. (1999). nacre encodes a zebrafish microphthalmia-related protein that regulates neural-crest-derived pigment cell fate. *Development*, *126*(17), 3757-3767.

Liu, T., Zhang, L., Joo, D., & Sun, S.-C. (2017). NF-κB signaling in inflammation. *Signal Transduction and Targeted Therapy*, *2*(1), 17023. https://doi.org/10.1038/sigtrans.2017.23

Long, L., Guo, H., Yao, D., Xiong, K., Li, Y., Liu, P., . . . Liu, D. (2015). Regulation of transcriptionally active genes via the catalytically inactive Cas9 in C. elegans and D. rerio. *Cell Res*, *25*(5), 638-641. https://doi.org/10.1038/cr.2015.35

Ma, J., Wang, J., Ghoraie, L. S., Men, X., Liu, L., & Dai, P. (2019). Network-based method for drug target discovery at the isoform level. *Sci Rep*, *9*(1), 13868. https://doi.org/10.1038/s41598-019-50224-x

Ma, X. H., Zhao, L., Zhao, Q. M., Feng, T. T., Shang, J. F., & Zhang, Z. Q. (2012). Detection of atherosclerotic plaque progression in the abdominal aorta of rabbits with 3T magnetic resonance imaging. *Chin Med J (Engl)*, *125*(15), 2714-2718.

Mack, J. J., Mosqueiro, T. S., Archer, B. J., Jones, W. M., Sunshine, H., Faas, G. C., . . . Iruela-Arispe, M. L. (2017). NOTCH1 is a mechanosensor in adult arteries. *Nat Commun*, *8*(1), 1620. https://doi.org/10.1038/s41467-017-01741-8

MacLeod, R. S., Cawley, K. M., Gubrij, I., Nookaew, I., Onal, M., & O'Brien, C. A. (2019). Effective CRISPR interference of an endogenous gene via a single transgene in mice. *Sci Rep*, *9*(1), 17312. https://doi.org/10.1038/s41598-019-53611-6

Magid, R., & Davies, P. F. (2005). Endothelial protein kinase C isoform identity and differential activity of PKCzeta in an athero-susceptible region of porcine aorta. *Circ Res*, *97*(5), 443-449. https://doi.org/10.1161/01.RES.0000179767.37838.60

Mahmoud, M., Kim, R., de Luca, A., Gauci, I., Hsiao, S., & Evans, P. (2014). 189 Disturbed Flow Promotes Endothelial Cell Injury Via the Induction of Developmental Genes. *Heart*, *100*(Suppl 3), A105-A105. https://doi.org/10.1136/heartjnl-2014-306118.189

Mak, A., & Kow, N. Y. (2014). Imbalance between endothelial damage and repair: a gateway to cardiovascular disease in systemic lupus erythematosus. *Biomed Res Int*, *2014*, 178721. https://doi.org/10.1155/2014/178721

Mallat, Z., Hugel, B., Ohan, J., Lesèche, G., Freyssinet, J. M., & Tedgui, A. (1999). Shed membrane microparticles with procoagulant potential in human atherosclerotic plaques: a role for apoptosis in plaque thrombogenicity. *Circulation*, *99*(3), 348-353. https://doi.org/10.1161/01.cir.99.3.348

Mallat, Z., & Tedgui, A. (2000). Apoptosis in the vasculature: mechanisms and functional importance. *Br J Pharmacol*, *130*(5), 947-962. https://doi.org/10.1038/sj.bjp.0703407

Mannino, R. G., Myers, D. R., Ahn, B., Wang, Y., Margo Rollins, Gole, H., . . . Lam, W. A. (2015). "Do-it-yourself in vitro vasculature that recapitulates in vivo geometries for investigating endothelial-blood cell interactions". *Sci Rep*, *5*, 12401. https://doi.org/10.1038/srep12401

McCurley, A. T., & Callard, G. V. (2008). Characterization of housekeeping genes in zebrafish: male-female differences and effects of tissue type, developmental stage and chemical treatment. *BMC Mol Biol*, *9*, 102. https://doi.org/10.1186/1471-2199-9-102

Meng, L. B., Chen, K., Zhang, Y. M., & Gong, T. (2018). Common Injuries and Repair Mechanisms in the Endothelial Lining. *Chin Med J (Engl)*, *131*(19), 2338-2345. https://doi.org/10.4103/0366-6999.241805

Mercadante AA, R. A. A. (2021). Anatomy, Arteries. In. Statpearls Publishing. https://doi.org/NBK547743

Meyer, A., & Schartl, M. (1999). Gene and genome duplications in vertebrates: the one-to-four (-to-eight in fish) rule and the evolution of novel gene functions. *Curr Opin Cell Biol*, *11*(6), 699-704. https://doi.org/10.1016/s0955-0674(99)00039-3

Michael Pittilo, R. (2000). Cigarette smoking, endothelial injury and cardiovascular disease. *Int J Exp Pathol*, *81*(4), 219-230. https://doi.org/10.1046/j.1365-2613.2000.00162.x

Moore, J. E., Xu, C., Glagov, S., Zarins, C. K., & Ku, D. N. (1994). Fluid wall shear stress measurements in a model of the human abdominal aorta: oscillatory behavior and relationship to atherosclerosis. *Atherosclerosis*, *110*(2), 225-240. https://doi.org/10.1016/0021-9150(94)90207-0

Moore, T. M., Garg, R., Johnson, C., Coptcoat, M. J., Ridley, A. J., & Morris, J. D. H. (2000). PSK, a Novel STE20-like Kinase Derived from Prostatic Carcinoma That Activates the c-Jun N-terminal Kinase Mitogen-activated Protein Kinase Pathway and Regulates Actin Cytoskeletal Organization*. *Journal of Biological Chemistry*, *275*(6), 4311-4322. https://doi.org/https://doi.org/10.1074/jbc.275.6.4311

Morita-Takemura, S., Nakahara, K., Tatsumi, K., Okuda, H., Tanaka, T., Isonishi, A., & Wanaka, A. (2016). Changes in endothelial cell proliferation and vascular permeability after systemic lipopolysaccharide administration in the subfornical organ. *J Neuroimmunol*, *298*, 132-137. https://doi.org/10.1016/j.jneuroim.2016.06.011

Moro, E., Vettori, A., Porazzi, P., Schiavone, M., Rampazzo, E., Casari, A., . . . Argenton, F. (2013). Generation and application of signaling pathway reporter lines in zebrafish. *Mol Genet Genomics*, *288*(5-6), 231-242. https://doi.org/10.1007/s00438-013-0750-z

Naghavi, M., Libby, P., Falk, E., Casscells, S. W., Litovsky, S., Rumberger, J., . . . Willerson, J. T. (2003). From vulnerable plaque to vulnerable patient: a call for new definitions and risk assessment strategies: Part I. *Circulation*, *108*(14), 1664-1672. https://doi.org/10.1161/01.CIR.0000087480.94275.97

Nam, D., Ni, C. W., Rezvan, A., Suo, J., Budzyn, K., Llanos, A., . . . Jo, H. (2009). Partial carotid ligation is a model of acutely induced disturbed flow, leading to rapid endothelial dysfunction and

atherosclerosis. *Am J Physiol Heart Circ Physiol*, *297*(4), H1535-1543. https://doi.org/10.1152/ajpheart.00510.2009

Navab, M., Berliner, J. A., Watson, A. D., Hama, S. Y., Territo, M. C., Lusis, A. J., . . . Fogelman, A. M. (1996). The Yin and Yang of oxidation in the development of the fatty streak. A review based on the 1994 George Lyman Duff Memorial Lecture. *Arterioscler Thromb Vasc Biol*, *16*(7), 831-842. https://doi.org/10.1161/01.atv.16.7.831

Noseda, M., Chang, L., McLean, G., Grim, J. E., Clurman, B. E., Smith, L. L., & Karsan, A. (2004). Notch activation induces endothelial cell cycle arrest and participates in contact inhibition: role of p21Cip1 repression. *Mol Cell Biol*, *24*(20), 8813-8822. https://doi.org/10.1128/MCB.24.20.8813-8822.2004

Oberoi, R., Vlacil, A.-K., Schuett, J., Schösser, F., Schuett, H., Tietge, U. J. F., . . . Grote, K. (2018). Anti-tumor necrosis factor-α therapy increases plaque burden in a mouse model of experimental atherosclerosis. *Atherosclerosis*, *277*, 80-89. https://doi.org/10.1016/j.atherosclerosis.2018.08.030

Oh, J. G., & Ishikawa, K. (2018). Experimental Models of Cardiovascular Diseases: Overview. *Methods Mol Biol*, *1816*, 3-14. https://doi.org/10.1007/978-1-4939-8597-5_1

Oikonomou, E., Psaltopoulou, T., Georgiopoulos, G., Siasos, G., Kokkou, E., Antonopoulos, A., . . . Tousoulis, D. (2018). Western Dietary Pattern Is Associated With Severe Coronary Artery Disease. *Angiology*, *69*(4), 339-346. https://doi.org/10.1177/0003319717721603

Oppi, S., Lüscher, T. F., & Stein, S. (2019). Mouse Models for Atherosclerosis Research—Which Is My Line? [Mini Review]. *Frontiers in Cardiovascular Medicine*, *6*. https://doi.org/10.3389/fcvm.2019.00046

Osborn, E. A., & Jaffer, F. A. (2013). Imaging atherosclerosis and risk of plaque rupture. *Curr Atheroscler Rep*, *15*(10), 359. https://doi.org/10.1007/s11883-013-0359-z

Packham, I. M., Gray, C., Heath, P. R., Hellewell, P. G., Ingham, P. W., Crossman, D. C., . . . Chico, T. J. (2009). Microarray profiling reveals CXCR4a is downregulated by blood flow in vivo and mediates collateral formation in zebrafish embryos. *Physiol Genomics*, *38*(3), 319-327. https://doi.org/10.1152/physiolgenomics.00049.2009

Parhami, F., Fang, Z. T., Fogelman, A. M., Andalibi, A., Territo, M. C., & Berliner, J. A. (1993). Minimally modified low density lipoprotein-induced inflammatory responses in endothelial cells are mediated by cyclic adenosine monophosphate. *J Clin Invest*, *92*(1), 471-478. https://doi.org/10.1172/JCI116590

Park, S. H. (2021). Regulation of Macrophage Activation and Differentiation in Atherosclerosis. *J Lipid Atheroscler*, *10*(3), 251-267. https://doi.org/10.12997/jla.2021.10.3.251

Parmar, K. M., Larman, H. B., Dai, G., Zhang, Y., Wang, E. T., Moorthy, S. N., . . . García-Cardeña, G. (2006). Integration of flow-dependent endothelial phenotypes by Kruppel-like factor 2. *J Clin Invest*, *116*(1), 49-58. https://doi.org/10.1172/JCI24787

Peiffer, V., Sherwin, S. J., & Weinberg, P. D. (2013). Does low and oscillatory wall shear stress correlate spatially with early atherosclerosis? A systematic review. *Cardiovasc Res*, *99*(2), 242-250. https://doi.org/10.1093/cvr/cvt044

Poduri, A., Chang, A. H., Raftrey, B., Rhee, S., Van, M., & Red-Horse, K. (2017). Endothelial cells respond to the direction of mechanical stimuli through SMAD signaling to regulate coronary artery size. *Development*, *144*(18), 3241-3252. https://doi.org/10.1242/dev.150904

Pott, A., Shahid, M., Kohler, D., Pylatiuk, C., Weinmann, K., Just, S., & Rottbauer, W. (2018). Therapeutic Chemical Screen Identifies Phosphatase Inhibitors to Reconstitute PKB Phosphorylation and Cardiac Contractility in ILK-Deficient Zebrafish. *Biomolecules*, *8*(4). https://doi.org/10.3390/biom8040153

Poulain, F. (2017). *Mutagenesis and Transgenesis in Zebrafish*. Springer, Cham. https://doi.org/https://doi.org/10.1007/978-3-319-33774-6_1

Qi, L. S., Larson, M. H., Gilbert, L. A., Doudna, J. A., Weissman, J. S., Arkin, A. P., & Lim, W. A. (2013). Repurposing CRISPR as an RNA-guided platform for sequence-specific control of gene expression. *Cell*, *152*(5), 1173-1183. https://doi.org/10.1016/j.cell.2013.02.022

Quillien, A., Blanco-Sanchez, B., Halluin, C., Moore, J. C., Lawson, N. D., Blader, P., & Cau, E. (2011). BMP signaling orchestrates photoreceptor specification in the zebrafish pineal gland in collaboration with Notch. *Development*, *138*(11), 2293-2302. https://doi.org/10.1242/dev.060988

Rafieian-Kopaei, M., Setorki, M., Doudi, M., Baradaran, A., & Nasri, H. (2014). Atherosclerosis: process, indicators, risk factors and new hopes. *Int J Prev Med*, *5*(8), 927-946.

Ranade, S. S., Qiu, Z., Woo, S. H., Hur, S. S., Murthy, S. E., Cahalan, S. M., . . . Patapoutian, A. (2014). Piezo1, a mechanically activated ion channel, is required for vascular development in mice. *Proc Natl Acad Sci U S A*, *111*(28), 10347-10352. https://doi.org/10.1073/pnas.1409233111

Renz, M., Otten, C., Faurobert, E., Rudolph, F., Zhu, Y., Boulday, G., . . . Abdelilah-Seyfried, S. (2015). Regulation of β1 integrin-Klf2-mediated angiogenesis by CCM proteins. *Dev Cell*, *32*(2), 181-190. https://doi.org/10.1016/j.devcel.2014.12.016

Ridker, P. M., Libby, P., MacFadyen, J. G., Thuren, T., Ballantyne, C., Fonseca, F., . . . Glynn, R. J. (2018). Modulation of the interleukin-6 signalling pathway and incidence rates of atherosclerotic events and all-cause mortality: analyses from the Canakinumab Anti-Inflammatory Thrombosis Outcomes Study (CANTOS). *Eur Heart J*, *39*(38), 3499-3507. https://doi.org/10.1093/eurheartj/ehy310

Ridker, P. M., Manson, J. E., Buring, J. E., Goldhaber, S. Z., & Hennekens, C. H. (1991). The effect of chronic platelet inhibition with low-dose aspirin on atherosclerotic progression and acute thrombosis: clinical evidence from the Physicians' Health Study. *Am Heart J*, *122*(6), 1588-1592. https://doi.org/10.1016/0002-8703(91)90275-m

Robu, M. E., Larson, J. D., Nasevicius, A., Beiraghi, S., Brenner, C., Farber, S. A., & Ekker, S. C. (2007). p53 activation by knockdown technologies. *PLoS Genet*, *3*(5), e78. https://doi.org/10.1371/journal.pgen.0030078

Rossi, A., Kontarakis, Z., Gerri, C., Nolte, H., Hölper, S., Krüger, M., & Stainier, D. Y. R. (2015). Genetic compensation induced by deleterious mutations but not gene knockdowns. *Nature*, *524*(7564), 230-233. https://doi.org/10.1038/nature14580

Roustaei, M., Baek, K.-I., Wang, Z., Cavallero, S., Satta, S., Lai, A., . . . Hsiai, T. (2021). *Computational Simulation of 4-D Micro-Circular Network in Zebrafish Tail Amputation and Regeneration*. https://doi.org/10.1101/2021.02.10.430654

Roux, E., Bougaran, P., Dufourcq, P., & Couffinhal, T. (2020). Fluid Shear Stress Sensing by the Endothelial Layer. *Front Physiol*, *11*, 861. https://doi.org/10.3389/fphys.2020.00861

Roy, P., Orecchioni, M., & Ley, K. (2022). How the immune system shapes atherosclerosis: roles of innate and adaptive immunity. *Nature Reviews Immunology*, *22*(4), 251-265. https://doi.org/10.1038/s41577-021-00584-1

Sah, R., Mesirca, P., Van den Boogert, M., Rosen, J., Mably, J., Mangoni, M. E., & Clapham, D. E. (2013). Ion channel-kinase TRPM7 is required for maintaining cardiac automaticity. *Proc Natl Acad Sci U S A*, *110*(32), E3037-3046. https://doi.org/10.1073/pnas.1311865110

Salvayre, R., Auge, N., Benoist, H., & Negre-Salvayre, A. (2002). Oxidized low-density lipoprotein-induced apoptosis. *Biochim Biophys Acta*, *1585*(2-3), 213-221. https://doi.org/10.1016/s1388-1981(02)00343-8

Savage, A. M., Kurusamy, S., Chen, Y., Jiang, Z., Chhabria, K., MacDonald, R. B., . . . Wilkinson, R. N. (2019). tmem33 is essential for VEGF-mediated endothelial calcium oscillations and angiogenesis. *Nat Commun*, *10*(1), 732. https://doi.org/10.1038/s41467-019-08590-7

Schrijvers, D. M., De Meyer, G. R., Kockx, M. M., Herman, A. G., & Martinet, W. (2005). Phagocytosis of apoptotic cells by macrophages is impaired in atherosclerosis. *Arterioscler Thromb Vasc Biol*, *25*(6), 1256-1261. https://doi.org/10.1161/01.ATV.0000166517.18801.a7

Schwartz, E. A., Bizios, R., Medow, M. S., & Gerritsen, M. E. (1999). Exposure of human vascular endothelial cells to sustained hydrostatic pressure stimulates proliferation. Involvement of the alphaV integrins. *Circ Res*, *84*(3), 315-322. https://doi.org/10.1161/01.res.84.3.315

Serbanovic-Canic, J., de Luca, A., Warboys, C., Ferreira, P. F., Luong, L. A., Hsiao, S., . . . Evans, P. C. (2017). Zebrafish Model for Functional Screening of Flow-Responsive Genes. *Arterioscler Thromb Vasc Biol*, *37*(1), 130-143. https://doi.org/10.1161/ATVBAHA.116.308502

Sie, Z. L., Li, R. Y., Sampurna, B. P., Hsu, P. J., Liu, S. C., Wang, H. D., . . . Yuh, C. H. (2020). WNK1 Kinase Stimulates Angiogenesis to Promote Tumor Growth and Metastasis. *Cancers (Basel)*, *12*(3). https://doi.org/10.3390/cancers12030575

Spek, C. A., Koster, T., Rosendaal, F. R., Bertina, R. M., & Reitsma, P. H. (1995). Genotypic variation in the promoter region of the protein C gene is associated with plasma protein C levels and thrombotic risk. *Arterioscler Thromb Vasc Biol*, *15*(2), 214-218. https://doi.org/10.1161/01.atv.15.2.214

Stary, H. C., Chandler, A. B., Dinsmore, R. E., Fuster, V., Glagov, S., Insull, W., . . . Wissler, R. W. (1995). A definition of advanced types of atherosclerotic lesions and a histological classification of atherosclerosis. A report from the Committee on Vascular Lesions of the Council on Arteriosclerosis, American Heart Association. *Arterioscler Thromb Vasc Biol*, *15*(9), 1512-1531. https://doi.org/10.1161/01.atv.15.9.1512

Stemme, S., Faber, B., Holm, J., Wiklund, O., Witztum, J. L., & Hansson, G. K. (1995). T lymphocytes from human atherosclerotic plaques recognize oxidized low density lipoprotein. *Proc Natl Acad Sci U S A*, *92*(9), 3893-3897. https://doi.org/10.1073/pnas.92.9.3893

Storey, A. (2018). *Living longer: how our population is changing and why it matters*. Online

Sun, X., Gao, L., Yu, R. K., & Zeng, G. (2006). Down-regulation of WNK1 protein kinase in neural progenitor cells suppresses cell proliferation and migration. *J Neurochem*, *99*(4), 1114-1121. https://doi.org/10.1111/j.1471-4159.2006.04159.x

Tajbakhsh, A., Kovanen, P. T., Rezaee, M., Banach, M., & Sahebkar, A. (2019). Ca2+ Flux: Searching for a Role in Efferocytosis of Apoptotic Cells in Atherosclerosis. *Journal of Clinical Medicine*, *8*(12). https://doi.org/10.3390/jcm8122047

Tang, D., Geng, F., Yu, C., & Zhang, R. (2021). Recent Application of Zebrafish Models in Atherosclerosis Research [Mini Review]. *Frontiers in Cell and Developmental Biology*, *9*. https://doi.org/10.3389/fcell.2021.643697

Taylor, R. G., & Lewis, J. C. (1986). Endothelial cell proliferation and monocyte adhesion to atherosclerotic lesions of white carneau pigeons. *Am J Pathol*, *125*(1), 152-160.

Thorp, E., Subramanian, M., & Tabas, I. (2011). The role of macrophages and dendritic cells in the clearance of apoptotic cells in advanced atherosclerosis. *Eur J Immunol*, *41*(9), 2515-2518. https://doi.org/10.1002/eji.201141719

Thorp, E., & Tabas, I. (2009). Mechanisms and consequences of efferocytosis in advanced atherosclerosis. *J Leukoc Biol*, *86*(5), 1089-1095. https://doi.org/10.1189/jlb.0209115

Thorpe, P. E. (2004). Vascular targeting agents as cancer therapeutics. *Clin Cancer Res*, *10*(2), 415-427. https://doi.org/10.1158/1078-0432.ccr-0642-03

Tinevez, J. Y., Perry, N., Schindelin, J., Hoopes, G. M., Reynolds, G. D., Laplantine, E., . . . Eliceiri, K. W. (2017). TrackMate: An open and extensible platform for single-particle tracking. *Methods*, *115*, 80-90. https://doi.org/10.1016/j.ymeth.2016.09.016

Tokunaga, O., Satoh, T., Yamasaki, F., & Wu, L. (1998). Multinucleated variant endothelial cells (MVECs) in human aorta: chromosomal aneuploidy and elevated uptake of LDL. *Semin Thromb Hemost*, *24*(3), 279-284. https://doi.org/10.1055/s-2007-995855

Traver, D., Paw, B. H., Poss, K. D., Penberthy, W. T., Lin, S., & Zon, L. I. (2003). Transplantation and in vivo imaging of multilineage engraftment in zebrafish bloodless mutants. *Nat Immunol*, *4*(12), 1238-1246. https://doi.org/10.1038/ni1007

Tricot, O., Mallat, Z., Heymes, C., Belmin, J., Lesèche, G., & Tedgui, A. (2000). Relation between endothelial cell apoptosis and blood flow direction in human atherosclerotic plaques. *Circulation*, *101*(21), 2450-2453. https://doi.org/10.1161/01.cir.101.21.2450

Tuinenburg, A., Mauser-Bunschoten, E. P., Verhaar, M. C., Biesma, D. H., & Schutgens, R. E. (2009). Cardiovascular disease in patients with hemophilia. *J Thromb Haemost*, *7*(2), 247-254. https://doi.org/10.1111/j.1538-7836.2008.03201.x

Uhlén, M., Fagerberg, L., Hallström, B. M., Lindskog, C., Oksvold, P., Mardinoglu, A., . . . Pontén, F. (2015). Proteomics. Tissue-based map of the human proteome. *Science*, *347*(6220), 1260419. https://doi.org/10.1126/science.1260419

Vaghela, R., Arkudas, A., Horch, R. E., & Hessenauer, M. (2021). Actually Seeing What Is Going on – Intravital Microscopy in Tissue Engineering [Review]. *Frontiers in Bioengineering and Biotechnology*, *9*. https://doi.org/10.3389/fbioe.2021.627462

Voigt, J., Christensen, J., & Shastri, V. P. (2014). Differential uptake of nanoparticles by endothelial cells through polyelectrolytes with affinity for caveolae. *Proc Natl Acad Sci U S A*, *111*(8), 2942-2947. https://doi.org/10.1073/pnas.1322356111

Vrhovski, B., & Weiss, A. S. (1998). Biochemistry of tropoelastin [https://doi.org/10.1046/j.1432-1327.1998.2580001.x]. *European Journal of Biochemistry*, *258*(1), 1-18. https://doi.org/https://doi.org/10.1046/j.1432-1327.1998.2580001.x

Wade, J. B., Fang, L., Liu, J., Li, D., Yang, C. L., Subramanya, A. R., . . . Welling, P. A. (2006). WNK1 kinase isoform switch regulates renal potassium excretion. *Proc Natl Acad Sci U S A*, *103*(22), 8558-8563. https://doi.org/10.1073/pnas.0603109103

Wang, K. C., Yeh, Y. T., Nguyen, P., Limqueco, E., Lopez, J., Thorossian, S., . . . Chien, S. (2016). Flow-dependent YAP/TAZ activities regulate endothelial phenotypes and atherosclerosis. *Proc Natl Acad Sci U S A*, *113*(41), 11525-11530. https://doi.org/10.1073/pnas.1613121113

Wang, N., Tabas, I., Winchester, R., Ravalli, S., Rabbani, L. E., & Tall, A. (1996). Interleukin 8 is induced by cholesterol loading of macrophages and expressed by macrophage foam cells in human atheroma. *J Biol Chem*, *271*(15), 8837-8842. https://doi.org/10.1074/jbc.271.15.8837

Wang, W. L., Chen, L. J., Wei, S. Y., Shih, Y. T., Huang, Y. H., Lee, P. L., . . . Chiu, J. J. (2021). Mechanoresponsive Smad5 Enhances MiR-487a Processing to Promote Vascular Endothelial Proliferation in Response to Disturbed Flow. *Front Cell Dev Biol*, *9*, 647714. https://doi.org/10.3389/fcell.2021.647714

Wang, X., Fu, Y., Xie, Z., Cao, M., Qu, W., Xi, X., . . . Tian, J. (2021). Establishment of a Novel Mouse Model for Atherosclerotic Vulnerable Plaque. *Front Cardiovasc Med*, *8*, 642751. https://doi.org/10.3389/fcvm.2021.642751

Warboys, C. M., Amini, N., de Luca, A., & Evans, P. C. (2011). The role of blood flow in determining the sites of atherosclerotic plaques. *F1000 Med Rep*, *3*, 5. https://doi.org/10.3410/M3-5

Watson, O., Novodvorsky, P., Gray, C., Rothman, A. M., Lawrie, A., Crossman, D. C., . . . Chico, T. J. (2013). Blood flow suppresses vascular Notch signalling via dll4 and is required for angiogenesis in response to hypoxic signalling. *Cardiovasc Res*, *100*(2), 252-261. https://doi.org/10.1093/cvr/cvt170

Weijts, B., Gutierrez, E., Saikin, S. K., Ablooglu, A. J., Traver, D., Groisman, A., & Tkachenko, E. (2018). Blood flow-induced Notch activation and endothelial migration enable vascular remodeling in zebrafish embryos. *Nat Commun*, *9*(1), 5314. https://doi.org/10.1038/s41467-018-07732-7

White, R. J., Collins, J. E., Sealy, I. M., Wali, N., Dooley, C. M., Digby, Z., . . . Busch-Nentwich, E. M. (2017). A high-resolution mRNA expression time course of embryonic development in zebrafish. *Elife*, *6*. https://doi.org/10.7554/eLife.30860

Williams, B. (2020). *Public attitudes to animal*

research under COVID-19.
https://www.understandinganimalresearch.org.uk/news/communications-media/survey-shows-high-public-acceptance-of-animal-research-to-find-treatments-for-covid-19/

Wolf, D., & Ley, K. (2019). Immunity and Inflammation in Atherosclerosis. *Circ Res*, *124*(2), 315-327. https://doi.org/10.1161/CIRCRESAHA.118.313591
Wu, K. K., & Thiagarajan, P. (1996). Role of endothelium in thrombosis and hemostasis. *Annu Rev Med*, *47*, 315-331. https://doi.org/10.1146/annurev.med.47.1.315
Wu, L., Satoh, T., & Tokunaga, O. (1999). Formation of multinucleated variant endothelial cells in vitro and investigation of MVECs' features. *Fukuoka Igaku Zasshi*, *90*(10), 377-391.
Xie, F., Bao, X., Yu, J., Chen, W., Wang, L., Zhang, Z., & Xu, Q. (2015). Disruption and inactivation of the PP2A complex promotes the proliferation and angiogenesis of hemangioma endothelial cells through activating AKT and ERK. *Oncotarget*, *6*(28), 25660-25676. https://doi.org/10.18632/oncotarget.4705
Xie, J., Farage, E., Sugimoto, M., & Anand-Apte, B. (2010). A novel transgenic zebrafish model for blood-brain and blood-retinal barrier development. *BMC Dev Biol*, *10*, 76. https://doi.org/10.1186/1471-213X-10-76
Xu, B. E., Lee, B. H., Min, X., Lenertz, L., Heise, C. J., Stippec, S., . . . Cobb, M. H. (2005). WNK1: analysis of protein kinase structure, downstream targets, and potential roles in hypertension. *Cell Res*, *15*(1), 6-10. https://doi.org/10.1038/sj.cr.7290256
Xu, B. E., Stippec, S., Lenertz, L., Lee, B. H., Zhang, W., Lee, Y. K., & Cobb, M. H. (2004). WNK1 activates ERK5 by an MEKK2/3-dependent mechanism. *J Biol Chem*, *279*(9), 7826-7831. https://doi.org/10.1074/jbc.M313465200
Xu, J., & Shi, G. P. (2014). Vascular wall extracellular matrix proteins and vascular diseases. *Biochim Biophys Acta*, *1842*(11), 2106-2119. https://doi.org/10.1016/j.bbadis.2014.07.008
Yang, A., Chen, F., He, C., Zhou, J., Lu, Y., Dai, J., . . . Wu, Y. (2017). The Procoagulant Activity of Apoptotic Cells Is Mediated by Interaction with Factor XII. *Frontiers in immunology*, *8*, 1188-1188. https://doi.org/10.3389/fimmu.2017.01188
Yu, H., Fellows, A., Foote, K., Yang, Z., Figg, N., Littlewood, T., & Bennett, M. (2018). FOXO3a (Forkhead Transcription Factor O Subfamily Member 3a) Links Vascular Smooth Muscle Cell Apoptosis, Matrix Breakdown, Atherosclerosis, and Vascular Remodeling Through a Novel Pathway Involving MMP13 (Matrix Metalloproteinase 13). *Arterioscler Thromb Vasc Biol*, *38*(3), 555-565. https://doi.org/10.1161/ATVBAHA.117.310502
Yurdagul, A., Chen, J., Funk, S. D., Albert, P., Kevil, C. G., & Orr, A. W. (2013). Altered nitric oxide production mediates matrix-specific PAK2 and NF-κB activation by flow. *Mol Biol Cell*, *24*(3), 398-408. https://doi.org/10.1091/mbc.E12-07-0513
Zagórska, A., Pozo-Guisado, E., Boudeau, J., Vitari, A. C., Rafiqi, F. H., Thastrup, J., . . . Alessi, D. R. (2007). Regulation of activity and localization of the WNK1 protein kinase by hyperosmotic stress. *J Cell Biol*, *176*(1), 89-100. https://doi.org/10.1083/jcb.200605093
Zakkar, M., Van der Heiden, K., Luong, l. A., Chaudhury, H., Cuhlmann, S., Hamdulay, S. S., . . . Evans, P. C. (2009). Activation of Nrf2 in endothelial cells protects arteries from exhibiting a proinflammatory state. *Arterioscler Thromb Vasc Biol*, *29*(11), 1851-1857. https://doi.org/10.1161/ATVBAHA.109.193375
Zhang, J., Wang, Z., Zuo, G., Li, B., Tian, N., & Chen, S. (2013). Low shear stress induces human vascular endothelial cell apoptosis by activating Akt signal and increasing reactive oxygen species. *Nan Fang Yi Ke Da Xue Xue Bao*, *33*(3), 313-317.
Zhang, S. H., Reddick, R. L., Piedrahita, J. A., & Maeda, N. (1992). Spontaneous hypercholesterolemia and arterial lesions in mice lacking apolipoprotein E. *Science*, *258*(5081), 468-471. https://doi.org/10.1126/science.1411543
Zhang, Y., Song, H., Wu, F., Mu, Q., Jiang, M., Wang, F., . . . Tang, D. (2016). Irisin Inhibits Atherosclerosis by Promoting Endothelial Proliferation Through microRNA126-5p. *J Am Heart Assoc*, *5*(9). https://doi.org/10.1161/JAHA.116.004031
Zhang, Y. J., Zheng, H. Q., Chen, B. Y., Sun, L., Ma, M. M., Wang, G. L., & Guan, Y. Y. (2018). WNK1 is required for proliferation induced by hypotonic challenge in rat vascular smooth muscle cells. *Acta Pharmacol Sin*, *39*(1), 35-47. https://doi.org/10.1038/aps.2017.56

Zhang, Z., Wang, Q., Yao, J., Zhou, X., Zhao, J., Zhang, X., . . . Liao, L. (2020). Chemokine Receptor 5, a Double-Edged Sword in Metabolic Syndrome and Cardiovascular Disease. *Front Pharmacol*, *11*, 146. https://doi.org/10.3389/fphar.2020.00146

Zhou, G., Bao, Z. Q., & Dixon, J. E. (1995). Components of a new human protein kinase signal transduction pathway. *J Biol Chem*, *270*(21), 12665-12669. https://doi.org/10.1074/jbc.270.21.12665